ROUTING OF SUSPENDED SEDIMENT THROUGH GRAVEL BED RIVERS

Ph. D. THESIS

by

NILAV KUMAR KARNA

DEPARTMENT OF CIVIL ENGINEERING
INDIAN INSTITUTE OF TECHNOLOGY ROORKEE
ROORKEE – 247 667 (INDIA)
JANUARY, 2015

ROUTING OF SUSPENDED SEDIMENT THROUGH GRAVEL BED RIVERS

A THESIS

Submitted in partial fulfilment of the requirements for the award of the degree of

DOCTOR OF PHILOSOPHY

in

CIVIL ENGINEERING

by

NILAV KUMAR KARNA

DEPARTMENT OF CIVIL ENGINEERING
INDIAN INSTITUTE OF TECHNOLOGY ROORKEE
ROORKEE – 247 667 (INDIA)
JANUARY, 2015

INDIAN INSTITUTE OF TECHNOLOGY ROORKEE
ROORKEE

CANDIDATE'S DECLARATION

I hereby certify that the work which is being presented in the thesis entitled **"ROUTING OF SUSPENDED SEDIMENT THROUGH GRAVEL BED RIVERS"** in partial fulfilment of the requirements for the award of the degree of Doctor of Philosophy and submitted in the Department of Civil Engineering of the Indian Institute of Technology Roorkee, Roorkee, is an authentic record of my own work carried out during the period from July, 2011 to January, 2015 under the supervision of Dr. K.S. Hari Prasad, Professor, Department of Civil Engineering, Indian Institute of Technology Roorkee, Roorkee and Dr. Sanjay Giri, Research Advisor/ Senior Scientist at Delft The Netherlands.

The matter presented in this thesis has not been submitted by me for the award of any other degree of this or any other Institute.

(NILAV KUMAR KARNA)

This is to certify that the above statement made by the candidate is correct to the best of our knowledge.

(SANJAY GIRI)
Supervisor

(K.S. HARI PRASAD)
Supervisor

Date:……...

The Ph.D. Viva-Voce Examination of **Mr. Nilav Kumar Karna,** Research Scholar, has been held on ……..

Signature of Supervisors **Chairman, SRC** **Signature of External Examiner**

Head of the Department/Chairman, ODC

Abstract

Bed material extraction from bed and banks of channel (erosion) and its subsequent deposition at any other location by the flowing water is an essential part of flow in an alluvial channel. Deforestation and logging are responsible for worsening the disastrous effect of flood generated by extreme rainfall and subsequent sediment discharge (Bathurst 2010). Hence knowledge of sediment entrainment and deposition mechanism and its associated phenomena have become essential for a hydraulic engineer for various purpose as such design of stable channels, design and safety of hydraulic structures, handling soil erosion problem etc.

Out of total load a river carries, there exist two major types of load depending upon the hydraulic condition. They are bed load and suspended load; together called bed material load. Suspended load may further consist of another type of load called wash load, not appreciably available in the channel bed and banks. These types of load join flow from the catchment area and supposed to have no relation with the hydraulics of the flow. It only depends upon the erodibility of catchment area. These types of load join river during periods of heavy rainfall and is believed not to settle on the stream bed.

Several definitions are available for wash load based on different hypotheses. Einstein et al. (1940) introduced the concept of wash load and Einstein (1950) defined wash load as particles of those sizes which correspond to less than 10% of the size of bed material. A high flow can carry large particles whereas low flow can't; i.e., no specific size of wash load can be attributed. This concept was forwarded by Shen (1970) and Woo et al. (1986).

Presence of fine sediment in the flow has several hydraulic and environmental consequences. Vanoni (1946), Vanoni and Nomicos (1960), Cellino and Graf (1999), Samaiya (2009) and many others observed decrease in flow resistance due to presence of fines. Yano and Daido (1964), Taggart et al. (1972), Lyn (1997) and many others reported increase in friction factor

whereas Kikkawa and Fukuoka (1969), Arora et al. (1986) and many others reported conditional increase and decrease.

Presence of suspended sediment in the flow also affects the velocity distribution by affecting the Von Karman constant. Many reporters have reported different opinions about the velocity distribution. Vanoni and Nomicos (1960), Elata and Ippen (1961), Holtrof (1985) and others observed a decrease in Karman constant with an increase in suspended sediment concentration and mentioned that effect of suspended sediment is limited to the near wall region. Lau (1983), Coleman (1986), Parker and Coleman (1986), Vetter (1986), Cioffi and Gallerano (1991) observed a change in wake function due to presence of suspended sediment.

Bed load transport rate also gets affected by the flowing suspended sediment. Very few studies are carried out to study the effect of suspended sediment on the bed load transport. Simons et al. (1963) mentioned a conditional increase or decrease in the bed load transport rate with suspended load. Colby (1964) proposed a graphical solution to the estimation of bed load transport in the presence of suspended load. Wan (1985) observed a decrease in total load transport at low flow intensity and an increase at high flow intensity. From literature review, it was observed that, there is no definite relationship available in literature for bed load transport under the influence of suspended transport.

On the environmental side, suspended sediment has several adverse impacts such as benthic smothering, irritation of fish gills and transport of sorbed contaminants (Davies-Colley and Smith 2007). It reduces or even kills the aquatic biota, macrophytes that form the base of riverine ecology (eg. Cline et al 1982; Lewis 1973a,b). Suspended sediment even harms or kills the animals ranging from microorganism to large fishes (eg. Lemly 1982; Barton 1977). 1987. They reduce the availability of oxygen in water, reduce the space for fish spawning, bury the eggs and fry (eg. Bash et al. 2001).

In order to study the various effects of suspended sediment on hydraulics and sediment transport capacity of flow, an extensive set of experiments were conducted in a tilting flume using 5.2 mm, 2.7 mm and 1.9 mm size uniform gravels as bed material and 0.062mm size uniform sediment as suspended material. Seven series of experiments each having 10-12 individual experiments were conducted. Each series has its own hydraulic properties but each successive run of a series was at an increasing suspended concentration. The first run of each series was a clear water run (water free of suspended sediment). Clear water run facilitated a set of reference

measurements. For all the runs, the flow condition was such that bed material moved purely as bed load only. The flow was steady and uniform. No aggradation or degradation was observed during or after each run. After each run, bed material was sampled from three locations along the flow and over the full depth of bed. The successive runs with increasing concentration in the flow were continued till the fines completely filled the bed pores. At the end of sediment laden run, clear water was allowed so that the fines deposited in the bed get entrained in the main flow.

Point velocity distribution data that corresponds to the near wall region $(y^+ \leq 0.2)$ were picked up and plotted on logarithmic scale to check the variation of Karman constant. It was observed that logarithmic velocity distribution fitted well with the data but the Karman constant were different for runs of different concentrations. Compared to the clear water flow, the Karman constant gradually decreased with increasing suspended sediment concentration. A relationship that fits well the variation of Karman constant with sediment concentration has been proposed and is given as

$$\kappa = 3 \times 10^{-10} C^2 - 5 \times 10^{-6} C + 0.407$$

Where κ is Karman constant and C is suspended sediment concentration in ppm.Arora et al.'s (1986) conditional criteria of increase or decrease of friction factor with the limiting value of $\frac{C\omega}{US}$ are tested with the data of present study. It is found that Arora et al. (1986) criteria doesn't hold good with the present data. It is observed that as the concentration of suspended sediment increases, the friction factor decreases. Apart from the present study data, data of Vanoni (1946), Vanoni and Nomicos (1960), Cellino and Graf (1999) and Khullar (2002) are taken to arrive at a new relationship for change in friction factor due to the presence of suspended load. A new relationship relating the friction factors and the parameter $(s-1)\frac{C\omega}{US}$,is developed as;

$$0.985 - \frac{f}{f_0} = 8 \times 10^{-6} (s-1) \frac{C\omega}{US}$$

Where f and f_0 are respectively friction factors for sediment laden flow and clear water flow. s is relative density, ω is the fall velocity of a sediment, U is the flow velocity and S is the channel slope. The fine sediments completely filled the pores of the gravel bed, specially the pores of the top gravel layer. But, since the gravel on the bed is large enough in size that fine sediments in pores don't hinder the coarse gravel exposure though fines are sheltered by coarser, it is supposed that the bed material properties remained same as that of parent bed materials.

Visual observation showed that fine sediment infiltrated down to the bottom of the bed composed of 5.2 mm and 2.7 mm gravel whereas only half way down infiltration was observed in bed of 1.9 mm gravel. The deposition gradually piled up to the surface. The proportion of fine sediments infiltrated in the bed at the upstream section of the channel was found to be more than that at the downstream section. During entrainment run, at lower discharge, only the top most layer of gravel was cleaned up. The flow entrained deeper and deeper as the discharge was increased. But from visual observation, it is seen that complete entrainment of fines is not possible until and unless the gravels hiding the fines also gets washed away.

The process of infiltration of suspended sediment during its routing was modeled using flow and sediment continuity equations and flow momentum equation. The governing differential equation for the process is

$$\frac{\partial P_G}{\partial t} + a_1 \frac{\partial Q_s}{\partial t} + a_2 \frac{\partial Q_s}{\partial x} = 0$$

Where Q_s is suspended load transport, P_G is porosity of bed material, $a_1 = -1/Ub\Delta z$ and $a_2 = -1/b\Delta z$, b is the width of the channel and Δz is the thickness of active bed layer, x and t are flow direction and time ordinates respectively. Predictor and corrector based finite difference numerical scheme of MacCormack (1969) is used to solve the above equation along with initial and boundary condition. Validation of the above model gave a good agreement between computed and observed porosity.

Some of the well known bed load transport equations (Meyer-Peter and Müller 1948; Misri et al. 1984 and Patel and Ranga Raju 1996) are tested with the present data. None of the relationship found to perform satisfactorily in predicting the bed load in the presence of suspended sediment. Probable reason for the poor performance may be the exclusion of suspended sediment effect on bed load transport. After attempting several other ways to incorporate the suspended sediment effect on the bed load transport, a more fruitful attempt came out as the inclusion of change in hydraulic parameter as a function of change in friction factor. Modified flow velocity and flow depth were obtained from the decreased friction factor. Incorporating these modified parameters in the original relationships gave much better results. The best estimation of bed load transport rate for the present data is by Misri et al. (1984) with incorporation of modified parameters. The result showed just 10% of observed data falling out of range of ±30% error band.

The turbulence characteristics of flow is analyzed with the instantaneous three dimensional velocity components measured by Acoustic Doppler Velocimeter (ADV). The vertical distributions of the streamwise velocity are found to follow the standard velocity distribution pattern. It is observed that streamwise flow velocity slightly gets increased with an increase in concentration. This supports the hypothesis that modified velocity calculated (which comes bit higher) from the reduced friction factor. The streamwise turbulence intensity (TI_u) is found to attain maximum value in the near wall region. Below and above that region, TI_u decreases. It is also observed that TI_u of the successive runs gradually decreases indicating the effect of suspended sediment and bed load transport on the turbulence intensity. It is observed that turbulence intensity decreased with increased concentration supporting the reduction/dampening of turbulence intensity. The rough elements present on the bed are supposed to be responsible for the dampening of intensity. The Reynold shear stress attains maximum value in the wall region and decreases towards bed. The turbulent kinetic energy (TKE) synchronizes well with the turbulence intensity and Reynold stress. Ejection and sweep events dominated the flow structure. They well synchronize each other. In the middle part of flow depth, the ratio of contribution of sweep to ejection is found to be about 0.8.

Acknowledgements

I feel privileged to express my deeps sense of gratitude and sincere regards to **Late Dr. U. C. Kothyari**, Professor of Civil Engineering with whom I started this study. His initial guidance, suggestions and motivations drove me to the completion of this study. I also feel privileged to express deep sense of gratitude to **Dr. K.S. Hari Prasad**, Professor of Civil Engineering IIT Roorkee and **Dr. Sanjay Giri**, Research Advisor at Delft the Netherlands for providing me an opportunity to undergo study under their esteemed guidance. This work is a result of their keen interest, invaluable guidance, fruitful suggestions and motivation throughout the study.

My special thanks goes to **Dr. Narinder Kumar K.**, Professor of Civil Engineering Punjab Agricultural university for his excellent suggestion and guidance during my experimental works. Thanks are due to my research committee members **Dr. S.C. Sharma**, Professor of Mechanical Engineering and **Dr. P.K. Sharma**, Associate professor of Civil engineering for their valuable suggestions. I would also like to say deepest thanks to **Dr. Z. Ahmed**, Professor of Civil Engineering for his suggestions during my experimental works.

I convey with my heartiest feeling, the never ending heartfelt stream of caring and blessings of my father **Mr. Ratneshwor Lal Karna** and mother **Mrs. Sudama Devi**, my brother **Mr. Morish Karna** and my sisters **Nilam, Tanuja and Nutan**. My most special thanks goes to **Madavi Das**, my fiancee for her love and support. I liked her occasional momentarily sadness ☹☹ when I was unable to come to Banglore on time because of my thesis work.

I am extremely thankful to my dear friends **Mr. Ajay Singh Lodhi**, **Mr. Ankit Chakravarti**, **Mr. Umesh Kumar Singh** and **Mr. Himanshu Sharma** Research Scholars of the Hydraulic Engineering Group for their constant support and help in all aspects of my work and life since my day one in this institute. I will always cherish the moments spent with them during my stay at IIT Roorkee.

I wish to convey my sincere thanks to **Mr. Y.S. Pundir**, **Mr. Vinod**, **Mr. Pramod**, **Mr. Rati Ram**, **Mr. Ajay Saini**, **Mr. Nadeem** and all other members of Hydraulic Engineering Laboratory. I acknowledge their assistance in conducting the experiments in lab. Last but not the least, I am extremely thankful to all those whose names have been unknowingly left to be mentioned here.

Date: _____ NILAV KUMAR KARNA

Contents

List of Figures

List of Tables

Nomenclature/Acronyms

Notation	Description	Dimension
b	Flume width	L
c	Concentration	ppm
C_n	Courant Number	-
d_i	Geometric mean diameter of i^{th} grain	L
d_a	Arithmetic mean diameter of grain	L
d_{16}	Grain size for which 16% sediment is finer	L
d_{50}	Median sediment size	L
d_{65}	Grain size for which 65% sediment is finer	L
d_{84}	Grain size for which 84% sediment is finer	L
d_{90}	Grain size for which 90% sediment is finer	L
f	Friction factor for sediment laden flow	-
f_0	Friction factor for clear water flow	-
F_r	Froude number	-
g	Acceleration due to gravity	LT^{-2}
h	Flow depth	L
h_0	Clear water flow depth	L
i_B	Proportion of size fraction d_i in bed load as obtained from sieve analysis	-
i_b	Proportion of size fraction d_i in bed material as obtained from sieve analysis	-
k_s	Equivalent roughness	-
M	Kramer's uniformity coefficient	-
N	Number of modes in x-direction	-
n	Manning's roughness coefficient	$L^{-1/3}T^{-1}$
n'	Manning's roughness coefficient as per Strickler	$L^{-1/3}T^{-1}$
P_G	Porosity of gravel bed	-

Notation	Description	Dimension
P_S	Porosity of suspended sediment	-
P_{max}	Maximum proportion of fine sediment in composite bed	-
P_i^*	Predicted value of porosity at node i^{th}	-
P_i^K	Porosity value at node (i, K)	-
P_i^{**}	Corrected value of porosity at node i^{th}	-
P_i^{K+1}	Final value of porosity at node $(i, K+1)$	-
Q	Discharge	L^3T^{-1}
Q_s	Volume of fines entering control volume per unit time	L^3T^{-1}
${Q_{Si}}^*$	Predicted volume of fines at i^{th} node	L^3T^{-1}
${Q_{Si}}^K$	Volume of fines at node (i, K)	L^3T^{-1}
${Q_{Si-1}}^*$	Predicted volume of fines at $(i-1)^{th}$ node	L^3T^{-1}
${Q_{Si}}^{**}$	Corrected volume of fines at i^{th} node	L^3T^{-1}
${Q_{Si}}^{K+1}$	Final value of suspended load at node $(i, K+1)$	-
${Q_{S0}}^{K+1}$	Final value of suspended load at fictitious node	-
q	Discharge per unit width	L^2T^{-1}
q_B	Bed load transport by weight per unit width	MT^{-3}
q_{Bi}	Bed load transport by weight per unit width of i^{th} size fraction	MT^{-3}
R	Hydraulic radius	L
R_b	hydraulic radius required to overcome form resistance due to undulation	L
R_g	hydraulic radius required to overcome grain resistance	l
S	Channel slope	-
S_b	Slope required to overcome form resistance due to bed undulation	-
S_g	Slope required to overcome grain resistance	-
s	Sediment specific gravity	-
TI_u	Turbulence intensity in flow direction (x)	LT^{-1}
TI_v	Turbulence intensity in across flow direction (y)	LT^{-1}
TI_w	Turbulence intensity in vertical direction (z)	LT^{-1}
u'	Velocity fluctuation in flow direction (x)	LT^{-1}
v'	Velocity fluctuation in across flow direction (y)	LT^{-1}
w'	Velocity fluctuation in vertical direction (z)	LT^{-1}
u_i	Instantaneous velocity component in flow direction (x)	LT^{-1}
v_i	Instantaneous velocity component in across flow direction (y)	LT^{-1}
w_i	Instantaneous velocity component in vertical direction (z)	LT^{-1}

Notation	Description	Dimension
$\overline{u}$	Time averaged velocity of u'	LT^{-1}
$\overline{v}$	Time averaged velocity of v'	LT^{-1}
$\overline{w}$	Time averaged velocity of w'	LT^{-1}
U	Mean/ approach flow velocity	LT^{-1}
U_*	Shear velocity	LT^{-1}
U_c	Critical velocity	LT^{-1}
U_{*c}	Critical shear velocity	LT^{-1}
V	Bulk volume	L^3
V_{SG}	Volume of solid gravels only	L^3
V_{SS}	Volume of solid of suspended sediment only	L^3
V_{PG}	Volume of voids in gravels	L^3
V_{SC}	Volume of solid in composite material	L^3
W_f	Weight of fines in bed due to change in porosity by Δp	MLT^{-2}
W_0	Initial dry weight of active bed layer	MLT^{-2}
y	Depth of point of velocity measurement	L
β	Shape factor of particle	-
γ_f	Specific weight of fluid	$ML^{-2}T^{-2}$
γ_s	Specific weight of sediment	$ML^{-2}T^{-2}$
ρ_f	Fluid density	ML^{-3}
ρ_s	Sediment density	ML^{-3}
σ_g	Standard deviation of sediment	-
τ_0	Total shear stress	$ML^{-1}T^{-2}$
$\tau_0{}'$	Grain shear stress	$ML^{-1}T^{-2}$
τ_{0c}	Critical shear stress	$ML^{-1}T^{-2}$
$\tau_*{}'$	Dimensionless shear stress	-
Φ	Dimensionless bed load transport rate	-
ξ	Exposure cum hiding coefficient	-
ω	Fall velocity	LT^{-1}
ω_*	Dimensionless fall velocity	-
ΔP_i	Percent of size d_i in bed material	-
ΔP	Change in porosity	-
Δx	Length of control volume	L
Δz	Thickness of active bed layer	L

Notation	Description	Dimension
Δt	Time interval used in modeling	T
ΔQ_s	Rate of increase of fines at starting node	L^3T^{-1}
$\Delta\gamma_s$	Difference in specific weights of sediment & fluid	$ML^{-2}T^{-2}$
κ	Von Karman Constant	-
ν	Kinematic viscosity	L^2T^{-1}
ABBREVIATIONS USED		
AVE	Average proportion of fines in bed layer	-
$AVEDEV$	Average deviation of proportion of fines in bed	-
$STDEV$	Standard deviation of proportion of fines	-
L	Large size gravels (5.2 mm)	-
M	Medium size gravels (2.7 mm)	-
S	Small size gravels (1.9 mm)	-

Chapter 1

Introduction

1.1 General

A river passing through an alluvium fan invariably carries sediment along with water. Design of hydraulic structures such as construction/ maintenance of reservoirs, irrigation canals, water supply and navigation channels, flood control measures, river training structures require knowledge of sediment transport. Extracting sediment at some place on the upstream section and depositing at another place somewhere downstream is a natural phenomenon in an alluvial river. Except under some natural calamities, this natural phenomenon attains an equilibrium after sufficient time.

There are two sources of sediment inflow viz. channel and non channel source. Bed and banks of a channel provide sediments to the flow. Such sources are called channel sources. Catchment area provides considerable amount of sediment to the river and is called non channel source. Mostly anthropogenic activities such as unmanaged agricultural practice, overgrazed grassland, construction and mining activities etc. exaggerate the availability of sediment for transportation.

When the shear stress acted by flow on the bed of channel exceeds a certain minimum value called critical shear stress, the bed material comes into motion. The various modes of sediment transport may be sliding, rolling, saltation or suspension (Garde and Ranga Raju 1985). Those sediments which move by rolling, sliding or saltation near the bed are called bed load, while those which move by being in suspension are called suspended load. In many cases, a

significant quantity of suspended loads are migrants, not significantly found in channel bed and bank. Such migrant sediments from the feeding catchment are called wash load. Wash loads are not supposed to settle down practically. The pattern of scouring/ erosion also determines the mode of sediment transport. For example, extraction bed material from the development of vertical dimension of scour changes the mode of transportation to the combination of bed load and suspended load (Verma and Goel 2005; Goel and Pal 2009). A more detailed division of mode of sediment transport is shown in Figure 1.1.

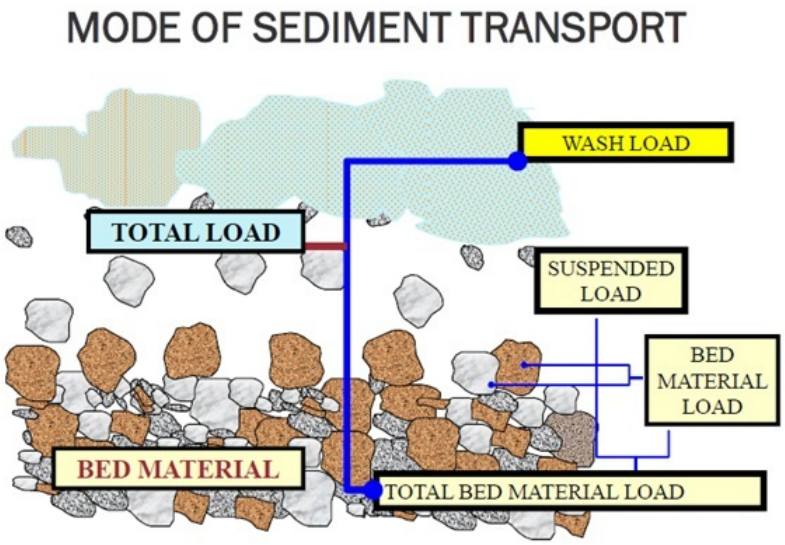

Figure 1.1: Various modes of sediment transport

Fine sediments has both environmental as well as hydraulic significance. Fine sediment in the flow puts an impact on river health and entire riverine ecosystem. Bank Failure induced sediment transport also threatens the local ecological environment (Li 2013). Excessive sediment in the flow has adverse impact on lower order organism, aquatic plants and invertebrates and higher order organism like fishes. Fines in excess in the flow hinder photosynthesis process, reduce oxygen level in water, and abrade leaves and body of organism. Fines deposit into the intra-gravel space and occupy fishes spawning spaces. The consequences may lead up to the fatal death of plants and animals disturbing the entire riverine ecosystem.

Similarly fines in the flow may change fluid and flow properties. Vertical velocity distribution of flow is found to get changed in presence of sediment compared to that of clear water. Bed load transport capacity, resistance to flow and other hydraulic properties are found to get modified due to the presence of suspended sediment in the flow.

1.2 Mechanics of Suspension

Jeffrey (1929) stated that when the hydrodynamic lift force exceeds the submerged weight of a particle, the particle comes into suspension. Laursen (1958) said that bed particles while moving over dunes or some irregularities on bed, sometimes lose its contact with the bed for a moment. At the same moment if gravitational force acting on particle is small and flow pattern and velocity of particle are such that the particle can be driven up in suspension, it moves up and joins the main flow. Number of moving particles, size and velocity of each individual particle governs the amount of material that may be lifted up in suspension.

Sutherland (1967) proposed a different mechanism of suspension. According to him, turbulent flow generates round and oval shaped eddies. These eddies, when approach bed, get distorted and the velocity of fluid within the eddies increases. Such eddies impinge into the laminar sub layer and increases the local (on spot) shear stress causing motion of particle at incipient motion condition. Obviously size of eddies are more than the size of individual particle; hence more than one number of particle move on each strike and comes at rest beyond the area of influence of eddy. At the stage of incipient motion, the phenomena is only intermittent as the eddies strike only few spots but when eddies strikes at many number of spots, sufficient drag force is applied on the particles and hence particles gain acceleration. On the course of their motion, may be due to position or due to rolling over neighboring particles, some particles may come into a situation when they can be entrained in the main flow by the vertical velocity component of eddy and the particle comes in suspension.

1.3 Resistance to Flow

Knowledge of resistance to flow is almost invariably required in any hydraulic computation in rigid boundary or alluvial channels. Despite numerous investigations, during last several decades, estimation of friction factor in open channel in presence of suspended load remained unresolved (Khullar 2002). The problem even gets worse in case of alluvial channels with geometric irregularities and changing bed configuration. Huge quantity of suspended load enters the channel especially during the rainy season. They flow through channel keeping part of them in suspension and remaining depositing in the bed pores and on the surface. The suspension

and deposition of suspended load affects the resistance to flow.

Numerous studies have been done on this subject but there are different opinions. Vanoni (1946), Einstein and Chien (1955), Vanoni and Nomicos (1960), Cellino and Graf (1999) etc. observed a decrease in resistance to flow due to the presence of suspended load. However, Yano and Daido (1964), Taggert et al. (1972) have shown thats the friction factor in rigid boundary increases with an increase in suspended load concentration. Few researchers had proposed conditional criteria for decrease and increase of friction factor with sediment concentration (Simons et al. 1963, Kikkawa and Fukuoka 1969, Arora et al. 1986). Hence there is a need for further studies on the effect of presence of suspended sediment on resistance to flow.

1.4 Infiltration and Deposition of Fines into Gravel Bed

Einstein (1968) studied the process of fine sediment infiltration and deposition into the pores of the gravel bed for the purpose of designing spawning ground for Salmonid fishes. He observed this interesting behavior of sediment on how and where the sediment infiltrates and deposits. It has been observed by many that due to the suspended sediment in the flow, the natural spawning ground is increasingly becoming unsuitable for these fishes. The adverse impact of excessive fines in the bed has also been recognized by Diplas and Parker (1992) including many others.

Deposition of fines in the reservoir has been recognized as a universal problem (Vorosmarty et al. 2003). Clay, silt and sand are the main constituents of the materials deposited in the reservoir. The reservoir capacity drastically reduces over a period of time. When these sediments are flushed, it interacts with the downstream bed and bank of channel and puts adverse impact on riverine system as discussed earlier. The adverse impact of fines in the flow ranges from microorganism and macrophytes to large animals like fishes. Not many studies have been done on the infiltration of fines in coarse alluvial bed. A common belief that *"wash load doesn't deposit"* was contradicted by Einstein and Chien (1955). Rate of deposition of fines was linked to its concentration in the flow by Einstein (1968) and Diplas and Parker (1992). Huang and Garcia (2000) proposed an analytical model for predicting concentration profile and transport of fine sediment over gravel bed under uniform steady state condition. However, it may be noted that the process and amount of fines extracted from the flow also depends on bed material composition besides others.

1.5 Bed Load

It is believed that the estimation of bed load transport rate actually started by Du Boys in 1879. Since then Gilbert and many others investigated the bed load transport of uniform sediment. The phenomena, influencing factors and methods of estimations are reasonable well understood (Garde and Ranga Raju 1985). Recently in last four decades, attempts have been made to understand the bed load transport of non uniform sediment. The bed load transport equations are either of empirical nature, based on dimensional consideration or based on semi-theoretical approach. One of the oldest, yet widely used empirical method of bed load transport estimation is due to Meyer-Peter and Müller (1948).

Many investigations have been done on the transport of bed load and suspended load as individual components. Some investigations have also been done to estimate the total load. But only few investigations have been done on the bed load transport taking into effect of suspended sediment.

Simons et al. (1963) experimentally studied the transport of sand in the bentonite and clay suspension. They arrived at varying conclusions for various conditions. Colby (1964) proposed graphical approach for estimation of bed load transport. Similarly Wan (1985) experimentally concluded the conditional increase or decrease of bed load transport. Khullar (2002) modified Patel and Ranga Raju (1996) formulation and made it applicable for bed load estimation considering the effect of suspended load. In actual field situation, fine materials may also flow through channel, hence there is a need for the study of effect of suspended load on the bed load transport.

1.6 Objectives

Detailed review of the literature (briefly explained from section 1.3 to 1.5 and explained in detail in Chapter 2) brought out the fact that resistance to flow and bed load transport in alluvial channels are likely to be affected by the presence of suspended sediment in the flow. But there is no definite and unanimously accepted conclusion and relationship for these scenarios. Hence there is a need for such study. Apart from these, there is also a need to study the fines infiltration in the coarse alluvial bed and its consequences on bed material characteristics. There is also a need

to understand the coherent structures of flow through gravel bed carrying suspended sediment. Keeping in view these issues, the present study is undertaken with following objectives.

- To study the effect of fine sediment on the velocity distribution
- To study the effect of fine sediment on resistance to flow
- To study the process of fine sediment infiltration into the bed
- To model the sediment infiltration process
- To study the effect of fine sediment on the bed load transport rate
- To study the turbulence characteristics of mobile bed under sediment laden flow

This study was undertaken by the investigators through experiments conducted in the Hydraulics laboratory of Indian Institute of Technology Roorkee, India.

1.7 Organization of the Thesis

The complete thesis is divided into eight chapters. The first chapter is the introduction that explains the basics of the whole study. It includes the brief introductions and findings about the various terminologies and activities occurred in the thesis. Chapter two is the literature review that includes the detailed review of various aspects of the study. Mainly, the previous findings on effect of presence of suspended sediment on various hydraulics and its associated parameters such as friction, bed load, turbulence etc. are discussed. The third chapter discusses in detail about the experimental setup, various equipments and materials used for the entire experiments. It also explains in detail the experimental procedure followed during all the runs. From fourth to seventh chapter is the data analysis and its results. The fourth chapter is devoted to the analysis of change in Karman constant and resistance to flow due to the presence of suspended sediment in the flow. The fifth chapter includes the various visual analysis and results. It also includes the mathematical modeling for change in porosity of the bed due to the routing of suspended sediment. The sixth chapter presents the analysis of the effect of suspended sediment on the bed load transport. Various existing methodologies have been checked for their utility with the present data and a modification is proposed. The seventh chapter examines the turbulence

characteristics of the flow carrying suspended sediment over mobile gravel bed. The eighth and the last chapter summarizes the general and specific conclusions of the present study.

Chapter 2

Literature Review

2.1 General

Problems related to hydraulic engineering have been of great concern to scientist and engineers since several centuries. Well before the Renaissance, many huge and marvelous hydraulic works such as dams, weirs, and water supply and irrigation networks have been constructed.

Sediment transport through rivers and open channel play a significant role in several hydraulics related problems. It has been observed in literature that presence of suspended sediment (fines) in flow has broadly two consequences viz. hydraulics and environmental. The presence of suspended sediment in the flow affects the flow resistance, bed load transport, turbulence characteristics etc. The environmental issues consists of effects on aquatic lives such as microorganism, macrophytes and fishes etc. The present chapter presents a comprehensive review on both hydraulics and environmental aspects in the flows containing suspended sediments.

2.2 Wash Load

The sediments which essentially move by being in touch with the bed of the channel are called the bed load; those which move by keeping themselves in suspension are suspended load. A part of the suspended load constitutes of such particles that are migrated from the catchment. Those suspended materials are called wash load. Wash load is defined in several ways by several researchers. Probably Einstein et al. (1940) was the first to write about the wash load.

They mentioned that those fine sediments in suspension which are not appreciably available in the channel bed material and get washed away with flow is called wash load. But they didn't delineate any specific size of the sediment. Lane (1947) proposed almost a similar definition of wash load. He said that wash load is composed of smaller sized particles than those found in channel bed in appreciable quantity. In 1950, Einstein mentioned that the maximum size of wash load can be arbitrarily chosen as d_{10} of the channel bed material, where d_{10} represent the particle diameter for which 10% of the particles are finer than that size. Shen (1970) didn't specify any specific size of wash load, rather proposed a criterion based on supply and demand of sediment. That sediment size for which the supply rate of sediment is less than the sediment carrying capacity of channel is called wash load. According to this definition wash load size may vary depending on the hydraulic condition of flow. Woo et al. (1986) distinctly mentioned that fine sediment load and wash load are not synonymous. According to them, fine sediments are of the order of silt size and wash loads are part of suspended load that is washed away without leaving its trace.

2.3 Hydraulic Significance of Fine Sediment in River Flow

It has been observed that the fine sediments present in the flow considerably affect the velocity distribution, flow resistance, bed load transport and turbulence characteristics. In the following sections, a brief review of all these aspects have been discussed.

2.3.1 Effects on vertical velocity distribution and resistance to flow

Velocity of flow at a section varies both vertically and transversely. Hence mean velocity of a flow in the channel is derived by integrating the velocity profile over the channel section. The problems of resistance to the flow and velocity distribution are interrelated and hence generally studied together (Garde and Ranga Raju 1985).

Irrespective of channel type (rigid or alluvial), there exists a unique relationship between the velocity and channel characteristics such as slope of channel, hydraulic radius of flow, and its boundary roughness. This relationship is called the resistance equation. The knowledge of velocity distribution in a rigid bed channel is almost well understood. The coefficients and

constants involved in the governing equations of velocity distribution for subcritical flow in rigid bed channels are almost well known (Garde and Ranga Raju 1985).

The presence of suspended sediment in the flow adds difficulty in understanding and predicting the resistance to flow and velocity distribution. Study by Buckley (1922) on the river Nile showed an increase in flow velocity during rising stage as compared to falling stage for given stage and slope as seen in Table 2.1 . This shows the effects of presence of fines in suspension on flow velocity.

Table 2.1: Resistance data of river Nile (Garde and Ranga Raju 1985)

Date	**Stage** (m)	**Hydraulic Radius** (m)	**Slope**	**Condition**	**Discharge** (m^3)	**Sediment load** (N/m^3)	**Mean Velocity** (m/s)	**n**
16.08.1920	87.54	8.60	7.2x10^{-5}	Rising	7200	18	1.48	0.024
16.09.1920	87.54	8.60‘	7.2x10^{-5}	Falling	6400	10	1.32	0.027

Table 2.1 shows that during rising stage the flow was almost doubly loaded with fine sediment. The Manning's coefficient was low during rising stage resulting in an increase in the mean flow velocity. The possible reason for this was attributed to the presence of suspended sediment in flow. It is agreed by several researchers that presence of fine sediments in the flow has significant impact on velocity distribution (eg. Vanoni 1946; Einstein and Chien 1955; Elatta and Ippen 1961; Coleman 1986; Gua and Julien 2001).

The presence of suspended sediment in channel affects either Chezy's or Manning's coefficients or the equivalent roughness (k_s), therefore affects the velocity distribution and finally gets reflected on resistance to flow. The equation that defines vertical velocity distribution in open channel is the logarithmic law given by equation (2.1).

$$\frac{U}{U_*} = \frac{1}{\kappa} ln\left(\frac{y}{y'}\right) + \text{Constant} \tag{2.1}$$

Where U is the velocity of flow at height y from the boundary wall, U_* is the shear velocity derived from hydraulic radius and slope, κ is the Von Karman constant usually taken as 0.41 for clear water flow y' is the distance from boundary wall where $U = 0$. Constant term in equation (2.1) varies for smooth and rough boundary flow. Keulegan (1938) recommended equation (2.1) to be applied for the whole flow depth. But specific studies on turbulence later on showed that log law (equation 2.1) is only applicable to a certain region of flow depth called the wall region $(y/h \leq 0.2)$; where h is the whole flow depth. The region beyond the wall region is called the outer region. A more detailed division of flow region is shown in Figure 2.1 .

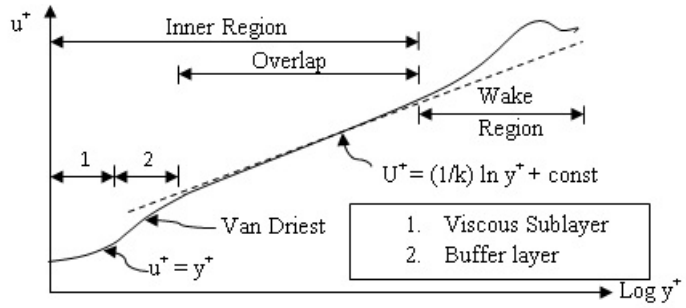

Figure 2.1: Representative sketch of velocity profile in open channel

As per Nezu and Nakagawa (1993), various regions in Figure 2.1 are delineated as viscous layer y^+<5, buffer layer 5<y^+<30, overlap layer 30<y^+<0.2R_* and beyond 0.2R_* is the wake region; where y^+ is the dimensionless length given as $(U_* y/\nu)$, and R_* is the Reynold number given as (hU_*/ν), ν is the kinematic viscosity.

The velocity distribution in the viscous layer is governed by the linear law as given in equation (2.2). This equation is also called the "law of wall".

$$\frac{U}{U_*} = \frac{U_* y}{\nu} \tag{2.2}$$

The buffer layer is governed by the Van Driest function. Unlike other region, no simple expression is available for buffer layer (Nezu and Nakagawa 1993). The velocity distribution in buffer layer is governed by following Van Driest expression given in equations (2.3) and (2.4) as.

$$dU^+ = \frac{2(1 - y/h)}{1 + \sqrt{1 + 4l^{+2}(1 - y/h)}} dy^+ \tag{2.3}$$

$$l^{+2} = ky^+[1 - exp(-y^+/B) \tag{2.4}$$

The velocity distribution in the overlap region is well governed by the well known log law given in equation (2.5).

$$\frac{U}{U_*} = \frac{1}{\kappa} ln\left(\frac{U_* y}{\nu}\right) + \text{Constant} \tag{2.5}$$

Nezu and Nakagawa (1993) mentioned that values of κ and Constant are universal constants and taken as 0.41 and 5.29 respectively.

The effects of sediment in suspension on velocity distribution and flow resistance have been studied by several researchers. Some notable contributions are given below. Vanoni's (1946) experiments showed the effect of presence of sediment in the flow on the Karman constant and hence resistance to flow. The same result was later supported by Vanoni and Nomicos

(1960). They found a decrease in Karman constant and hence a decrease in resistance to flow. They attributed the above result to the dampening of flow due to the presence of suspended sediment. Einstein and Chien (1955) used energy concept and proposed a graphical method of estimating the Karman constant. They mentioned that sediment in suspension dampens the turbulence and hence reduces the resistance to flow. Barton and Lin (1955) argued the change in Karman constant from the point of view of density gradient of suspended sediment in flow. Elata and Ippen (1961) also accepted the views of earlier researchers. Measuring the velocity fluctuation of a neutrally buoyant particle, they also observed a decrease in Karman constant. Yano and Daido (1964) observed an increase in friction factor with an increase in concentration of suspended sediment in supercritical flow. Kikkawa and Fukuoka (1969) observed conditional change in resistance. A decrease in resistance with an increase in sediment concentration of size 0.015mm was observed in a flow with Froude number 0.58; while no change was observed for flat and antidune beds at Froude number 1.05 and 1.34 respectively. Ippen (1971) mentioned that presence of suspended sediment in the flow changes the water viscosity and hence affects the velocity profile. Imamoto et al. (1977) observed 13% increases in the resistance coefficient in a supercritical flow of 10000 ppm concentration of sediment size 0.152 mm and specific gravity 2.65.

Experimental results of Pullaiah (1978) also showed conditional increase or decrease in friction factor. He observed an increase in friction factor with increased suspended sediment when $\sqrt{v'^2}/\omega < 100$ and decrease in friction factor with increasing concentration when $\sqrt{v'^2}/\omega > 200$; where v' is vertical velocity fluctuation component and ω is fall velocity of suspended sediment. Effect on friction factor for values of $\sqrt{v'^2}/\omega$ between 100 and 200 was not mentioned. Holtroff (1985) mentioned that energy is required to keep the fine sediment in suspension. He hypothesized that energy is extracted from main flow, thus reducing the energy available to sustain turbulence and hence the Karman constant decreases. Arora et al. (1986) mentioned the change in friction factor due to presence of suspended load in the flow.According to them, compared to the friction factor in clear water flow, friction factor for sediment laden flow increases with an increase in sediment concentration if $\frac{C\omega}{US} \geq 1200$ and friction factor decreases with increase in concentration if $\frac{C\omega}{US} < 1200$. Here C is volumetric sediment concentration in ppm and S is the slope of channel. Barenblatt (1996) analyzed the effect of suspended sediment on the log law of velocity distribution and concluded that log law is valid in sediment laden flow with smaller Karman constant. Muste and Patel (1997) analysed the effect of sus-

pended sediment on log law and reported little effect on log law near bed at lower concentration of sediment. Khullar et al. (2002) observed a decrease in friction factor with an increase in sediment concentration in closely packed non alluvial channel and alluvial channel.

As seen in Figure 2.1, beyond the overlap region, the velocity profile slightly deviates from the log law. (Nezu and Nakagawa 1993) suggested the addition of Cole's strength parameter to account for the deviation. Although several empirical relations (eg. Sarma et al. 1983, Coleman and Alonso 1983) have been developed for the velocity distribution in outer region; the most acceptable is the Cole's wake function. The log law in velocity defect form with Cole's wake strength parameter can be written as;

$$U_{max}{}^{+} - U^{+} = \frac{1}{\kappa} ln\left(\frac{y}{h}\right) + \frac{2\Pi}{\kappa} cos^2\left(\frac{\pi y}{2h}\right) \tag{2.6}$$

Where $U_{max}{}^{+} = \frac{U_{max}}{U_*}$ and U_{max} is the velocity at $y = h$ (free surface), Π is Cole's wake strength parameter that varies with pressure gradient in the boundary layer. Equation (2.6) is called the log-wake law. The value of Π as obtained by some researchers are 0.2 (Nezu and Rodi 1986), 0.1 (Kirkoz 1989), -0.077 for flow over smooth bed (Cardoso et al. 1989), -0.08 - 0.04 for flows over gravel bed (Kironoto and Graf 1994).

Some researchers have analyzed the change in velocity distribution and resistance to flow with respect to effect in log-wake law. Karman constant is independent of sediment concentration but the mean velocity profile shows the effect by changing its shape (Coleman 1981). Coleman (1981) also pointed out that Vanoni (1946), Einstein and Chien (1955), Elata and Ippen (1961) determined κ from the central part of velocity distribution not from the overlap region where the log law is actually valid, therefore wrongly concluded the decrease in Karman constant. He also pointed out that there were very small or no wake region in the data considered. Coleman (1981) based on his own experimental data found that sediment effect is limited to the wake region only as turbulence is reduced only in outer region. He found that Karman constant remained constant and observed an increase in wake strength parameter only compared to that of clear water flow. Later Parker and Coleman (1986), Coleman (1986), Cioffi and Gallerano (1991) supported his observations. Lau (1983) also observed that wake strength coefficient increases with an increase in sediment load. Using the data from laboratory and field, Vetter (1986) demonstrated no change in κ with suspended sediment concentration; instead wake component accounted the effect of sediment concentration. Parker and Coleman (1986) observed a reduction in flow resistance and increase in wake strength parameter due to increase

in sediment concentration. Lyn (1992) contradicted the finding of Coleman (1981) saying that effect of suspended sediment can be felt only in near bed region, hence Karman constant may decrease. He also mentioned that the wake strength parameter for sediment laden flow may be taken that of clear water flow equal to 0.2. Guo (1998) proposed a modified log-wake law for clear water. Stepping on to the modified log-wake law, Guo and Julien (2001) studied the velocity profile in sediment laden flow. Compared to the clear water flow, they observed a decrease in Karman constant and a fixed value of $\Pi = 0.3$ for sediment laden flow. They related the change in Karman constant with the local concentration of sediment as

$$\frac{\kappa}{\kappa_0} = 1 - 0.92\bar{C} \tag{2.7}$$

Where κ_0 is Karman constant for clear water flow taken as 0.41 and $\bar{C}$ is local time averaged volumetric sediment concentration.

2.3.2 Effect of fine sediment on bed load transport

Many investigations have been done considering the transport of bed load and suspended load as individual components. Some investigations have also been done to estimate the total load. But only few investigations have been done on the bed load transport taking into account the effect of suspended sediment (eg. Colby 1964; Kikkawa and Fukuoka 1969; Wan 1985 etc). This section reviews the effect of suspended load on bed load transport.

Simons et al. (1963) experimentally studied the transport of sand in the suspension of bentonite and clay. The fines concentration in the flow reached as high as around 59000 ppm and flow condition varied from lower flow regime with ripple to upper flow regime with antidunes. Bed load transport rate was observed to decrease in lower flow regime and increase in upper flow regime. Concentration below 10000 ppm was not reported to have much effect on bed load transport. Flow even at moderate concentrations passing through ripple bed, stabilized the bed, streamlined the bed form and reduced the resistance, and hence reduced the bed load transport. Same phenomenon was observed when relatively higher concentration of fines in the flow passed through dune bed. At very large concentration, the decrease in bed load transport was attributed to the decrease in resistance to flow and decrease in shear stress that resulted due to change in depth and slope to adjust smaller resistance. Large concentration of fine in flow passing through bed form of upper regime showed increase in bed load transport and the

reason attributed was increased viscosity and specific weight of fluid, decrease fall velocity of bed material and increased resistance to flow and shear stress.

Since many factors were involved in controlling sand discharge in sand bed streams, Colby (1964) provided a graphical solution for the estimation of bed load transport in presence of suspended sediment in the flow. Hence he proposed several graphs showing relation between sand discharge and its influencing factors. He prepared a graph of discharge per unit width versus mean velocity, a graph to obtain approximate effect of water temperature and fines in suspension on relationship of sand discharge and velocity. Another plot was between flow depth and sand discharge of various sizes. The procedure of graphical analysis consists of progressively eliminating the approximate effect of one variable after another. The estimation of sand discharge using one or more of the above graphs depends on the number of variables need to be considered in computation. All the graphs can be seen in Colby (1964).

Wan (1985) studied the effect of bentonite suspension on the transport of plastic beeds of specific gravity 1.29 and diameter 3.45 mm. Reduced fall velocity, incipient conditions occurring at higher discharge were observed due to presence of bentonite clay. Relatively flat dune bed formation was observed compared to clear water flow. The bed became flatter with increasing concentration of fines. He observed reduced bed load transport since the incipient motion required higher shear stress in the presence of suspended sediment in flow compared to that in clear water. In addition, due to reduction in settling velocity, more suspended sediments were observed to be transported. Hence at low flow intensities the total load was observed to decrease and at high flow intensities, total load increased.

Using the data of Simons et al. (1963), Woo et al. (1987) performed test on the applicability of Einstein (1950) and Colby (1964) relationships for bed load transport. Simons et al. (1963), in some of their experiments had observed huge change in fluid viscosity and density compared to those of clear water. Einstein (1950) relationship was tested with both corrected and uncorrected fluid viscosity and density. The total load showed an increase with increasing concentration when corrected viscosities and densities were used. That is, at higher concentration, use of corrected fluid properties showed better agreement with measure transport rate than without using corrected values of fluid properties. Though total load increased, the bed load component remained practically unchanged indicating only increase in suspended load due to fines in the flow. Colby (1964) approach provided almost similar result as that of Einstein

(1950) without using corrected values of fluid properties. Hence it was concluded by Woo et al. (1987) that Colby (1964) doesn't yield a better total load transport rate than Einstein (1950).

Khullar et al. (2007) observed increase in bed load transport with increase in wash load concentration in flow. They mentioned that though wash load infiltrates and deposits in the pores of gravel bed, the gravel properties remains unchanged; instead flow properties get changed due to wash load in the flow. In the case of non uniform sediment, smaller particles are sheltered by coarser and hence coarser particles are exposed to additional shear stress; thus introducing shelter-cum-exposure effect. Khullar et al. (2007) followed the same dimensionless bed load transport parameter for uniform sediment as followed by Meyer-Peter and Müller (1948), Misri et al (1984), Patel and Ranga Raju (1996).

$$\phi = \frac{q_B}{\gamma_s}\sqrt{\frac{\gamma_f}{(\gamma_s - \gamma_f)gd^3}} \tag{2.8}$$

For non uniform sediment equation (2.8) can be written as

$$\phi_i = \frac{i_B q_{Bi}}{i_b \gamma_s}\sqrt{\frac{\gamma_f}{(\gamma_s - \gamma_f)g{d_i}^3}} \tag{2.9}$$

where i_B and i_b are proportions of particle size fraction d_i in bed load and parent bed, d_i is geometric mean diameter obtained as $\sqrt{d_1 d_2}$. q_B is the bed load transport by weight per unit width, q_{Bi} is bed load transport by weight per unit width of i^{th} size fraction, g is acceleration due to gravity and γ_s and γ_f are specific weights of sediment and fluid respectively. Using dimensional analysis and logical reasoning, Patel and Ranga Raju (1996) and others deduced following functional relation for shelter-cum-exposure coefficient (ξ).

$$\xi = f\left[{\tau_{*i}}', \frac{{\tau_0}'}{\tau_{0C}}, M\right] \tag{2.10}$$

Here ${\tau_0}'$ is grain shear stress, τ_{0c} is critical shear stress, M is Kramers uniformity coefficient and ${\tau_{*i}}' = \frac{{\tau_0}'}{\Delta\gamma_s d_i}$.

$$M = \frac{\sum \Delta p_i d_i .....for d_i < d_{50}}{\sum \Delta p_i d_i .....for d_i > d_{50}} \tag{2.11}$$

Here Δp_i is percent of d_i in bed material and is equal to the difference in percent of d_1 and d_2. ${\tau_0}'$ is obtained using $n' = \frac{{d_{65}}^{(1/6)}}{25.4}$. d_{65} (in meter) is particle size such that 65% of particles are finer than this size. Analyzing own data and using the results of Misri et al. (1984), Samaga et al. (1986) and Mittal et al. (1990) as guide, Patel and Ranga Raju (1996) found

$$C_m \xi = 0.0713\left(C_s {\tau_{*i}}'\right)^{-0.75144} \tag{2.12}$$

where C_s and C_m are parameters that depend on $\frac{\tau_0{}'}{\tau_0 c}$ and M respectively. C_s and C_m are computed as

$$log(C_s) = -0.1957 - 0.9571\left(log\frac{\tau_0{}'}{\tau_0 c}\right) - 0.1949\left(log\frac{\tau_0{}'}{\tau_0 c}\right)^2 + 0.0644\left(log\frac{\tau_0{}'}{\tau_0 c}\right)^3 \tag{2.13}$$

where $C_m = 1.0$ for $M > 0.38$ and $C_m = 0.7092logM + 1.293$ for $0.05 < M < 0.38$ Khullar (2002) plotted a relationship between and ϕ and $\xi\tau_{*i}{}'$ and obtained the following relations to represent the graph.

For $0.02 \leq \xi\tau_{*i}{}' \leq 0.062$,

$$\phi = 10^8\left(\xi\tau_{*i}{}'\right)^{8.345} \tag{2.14}$$

For $0.062 < \xi\tau_{*i}{}' \leq 0.175$,

$$\phi = -2545.5\left(\xi\tau_{*i}{}'\right)^5 - 412.33\left(\xi\tau_{*i}{}'\right)^4 + 518.81\left(\xi\tau_{*i}{}'\right)^3 - 81.01\left(\xi\tau_{*i}{}'\right)^2 + 6.19\left(\xi\tau_{*i}{}'\right) - 0.178 \tag{2.15}$$

For $0.175 < \xi\tau_{*i}{}' \leq 1.83$,

$$\phi = 13.895\left(\xi\tau_{*i}{}'\right)^{1.9356} \tag{2.16}$$

2.4 Turbulent Analysis

2.4.1 Acoustic Doppler Velocimeter (ADV)

Numerous intrusive and non intrusive techniques and instruments have been developed to study the flow pattern/ turbulent characteristics of an open channel flow. One of the kinds is point or probe measurement in which a sensing instrument is inserted into the flow to measure the flow properties. Reddy et al. (2012) used PIV for turbulence analysis of flow. Another such instrument is the Acoustic Doppler Velocimeter (ADV). As the name itself suggests, it is based on the Doppler shift principal. ADV records very accurate three dimensional instantaneous velocities (Kraus et al. 1994). Voulgais and Trowbridge (1998) evaluation of ADV for its utility in turbulence analysis showed that ADV can measure the velocity and Reynols shear stress within ±1% accuracy of estimated true value. Ali and Lim (1986) and Liriano and Day (2000) studied velocity inside a scour hole using ADV. Dey and Raikar (2007) studied flow through loose gravel bed with ADV. Kumar et al. (2011) studied the flow pattern in the scour hole and wake region using ADV. Ramesh (2012) studied the particle motion over transionally rough bed

Figure 2.2: Acoustic Doppler Velocimeter (ADV)

using ADV. Garcia et al. (2005) article on some instrumental issues gave a very good summary of its working principal and some limitations of digitally averaging the velocity signal. Based on the literature and wide acceptance of ADV, it has been selected to be used for turbulence analysis in this study.

2.4.2 Velocity distribution

In turbulent flows, even though the flow is steady and uniform, slight fluctuations in the velocity components at a particular point are observed. The fluctuations in velocities in the longitudinal (x), lateral (y) and vertical (z) directions of the recorded instantaneous velocity may be u', v', w' respectively. The fluctuations in the respective directions are obtained as

$$u' = \bar{u} - u_i \qquad v' = \bar{v} - v_i \qquad w' = \bar{w} - w_i \tag{2.17}$$

Where, $\bar{u}$, $\bar{v}$ and $\bar{w}$ are the time averaged velocities of instantaneous velocities u_i, v_i and w_i respectively. $\bar{u}$, $\bar{v}$ and $\bar{w}$ are computed from the measured instantaneous velocities as;

$$\bar{u} = \frac{1}{N}\sum_{i=1}^{N} u_i \qquad \bar{v} = \frac{1}{N}\sum_{i=1}^{N} v_i \qquad \bar{w} = \frac{1}{N}\sum_{i=1}^{N} w_i \tag{2.18}$$

Where N is the total number of observations at a point.

2.4.3 Turbulent intensities

The instantaneous flow velocities are actually composed of mean velocities and fluctuations as expressed in equation (2.17). Hence turbulence intensity is defined as the root of mean of

square of the fluctuating velocity components. Mathematically, turbulence intensities in x, y and z directions can be given as

$$TI_u = \sqrt{\overline{u_i{}^2}} = [\frac{1}{N}\sum(u_i - \overline{u})^2]^{0.5} \qquad TI_v = \sqrt{\overline{v_i{}^2}} \qquad TI_w = \sqrt{\overline{w_i{}^2}} \tag{2.19}$$

where TI_u, TI_v and TI_w are respectively stream wise, transverse and vertical direction turbulence intensities. Half of the sum of average of squares of the velocity fluctuations is called turbulence kinetic energy (TKE).

$$TKE = \frac{1}{2}\left[\overline{u'^2} + \overline{v'^2} + \overline{w'^2}\right] \tag{2.20}$$

Numerous turbulence intensity and turbulence kinetic energy equations have been developed. Based on $\kappa - \varepsilon$ turbulence model, the equations developed to describe the TI and TKE distributions are

$$\begin{aligned} TI_u &= au_* exp(-C_k z/h), \\ TI_v &= av_* exp(-C_k z/h), \\ TI_w &= aw_* exp(-C_k z/h), \\ TKE &= du_*^2 exp(-2C_k z/h) \end{aligned} \tag{2.21}$$

Where a, b, c, d and C_k are the empirical constants. C_k is approximately taken as unity in the log-law region. The values of $a = 2.30$, $b = 1.27$, $c = 1.63$ and $d = 1.43$ were suggested by Nezu and Nakagawa (1993) for smooth bed. For gravel bed $a = 2.4$ was suggested by Kironoto and Graf (1994) and Song et al. (1994). Another famous equation for TI and TKE was proposed by Nikora and Goring (2000) as;

$$\begin{aligned} \left(\frac{TI_i}{U_*}\right)^2 &= M_i - N_i ln\frac{z}{h}, \\ TKE &= U_*{}^2\left[1.84 - 1.02 ln\frac{z}{h}\right], \end{aligned} \tag{2.22}$$

Where i is the index of velocity component; $M_u = 1.90$, $M_v = 1.19$ and $M_w = 0.59$ and $N_u = 1.32$, $N_v = 1.39$ and $N_w = 0.22$ were recommended by them.

2.4.4 Quadrant analysis

The total Reynold shear stress $\overline{-u'w'}$ at a particular point in the flow is the combination of contribution from different bursting events. In order to analyze the shear stress produced by coherent structures it may be necessary to arrange streamwise (u') and vertical (w') fluctuations

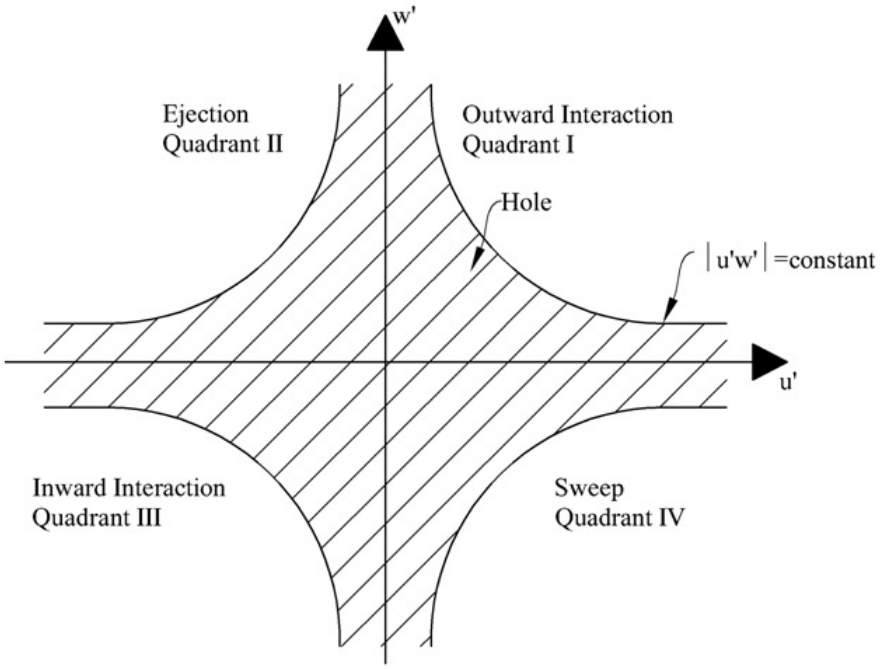

Figure 2.3: Quadrant technique (Lu and Willmarth 1973)

according to the quadrant in $u'w'$ plane as shown in Figure 2.3. This technique to investigate the coherent structure produced shear stress is called quadrant analysis. The shaded hyperbolic zone shown in Figure 2.3 is called hole. The boundary of hyperbolic zone is represented by $|\overline{u'w'}| = constant$ and the hole size H represents the threshold (Nezu and Nakagawa 1993) and is decided by the curve $|u'w'| = H(\overline{u'u'})^{0.5}(\overline{w'w'})^{0.5}$. The four quadrants of $u'w'$ plane are categorized as

- Outward interaction (i = 1, $u' > 0$ and $w' > 0$)
- Ejection (i = 2, $u' < 0$ and $w' > 0$)
- Inward interaction (i = 3, $u' < 0$ and $w' < 0$)
- Sweep (i = 4, $u' > 0$ and $w' < 0$)

The process in which a parcel of low speed fluid lifts away from the wall region and breaks down to mix the outflow is called ejection. And if those ejected fluids due to retardation get washed away by the high speed approaching fluid is called sweep. Kim et al. (1971) emphasized the ejection and sweep as the most important phenomena as they contribute the most to the turbulent energy and Reynold stress.

Lu and Willarth (1973) experimentally studied the Reynold shear stress structure throughout the boundary layer. Burst and sweep durations were also measured. They arrived at a conclusion that burst occurs when streamwise velocity at the edge of viscous sub layer becomes low and decreasing. On the contrary, when the same becomes large and increasing, sweep event occurs. They also concluded that ejection of low momentum fluid from wall dominates all other events within turbulent boundary layer. For smooth surface, they observed 70% contribution from ejection and 55% from sweep. The excess percentage was due to negative contribution from outward and inward interaction.

Bogard and Tiedman (1986) found quadrant technique the best for burst event analysis among some other techniques like VITA, TPAV, UI Level, and Positive Slope. He mentioned that quadrant technique was found to have greatest reliability of high probability of detecting ejection events.

By placing spherical particles of same size and density over a rough bed, Papanicolaous et al. (2001) formed three different regimes to experimentally study the near bed turbulence characteristics. The three regimes were isolated, wake interference and skimming. Based on the quadrant analysis of their results they mentioned that time averaged velocities and Reynold stresses are insufficient to describe the effect of roughness on flow characteristics. They also mentioned that effect of roughness on turbulence structure occurs throughout the boundary layer and frequency of occurrence and magnitude of turbulent event under incipient condition vary significantly with bed roughness.

Balchandar and Bhuiyan (2007) compared the flow over ribs and dunes with that over smooth surface. They investigated the higher order moments, conditional statistics based on the quadrant analysis and relationship of higher order moment to Reynold stress and energy production. Contrary to smooth channel, they observed the effect of roughness throughout the flow depth. Hence they concluded that triple product and second quadrant event were sensitive to wall condition and this effect was prevalent throughout the flow depth.

Thomas (1985) experimentally denied the effect of instantaneous RSS on the bed load transport. Drake et al. (1988), after field investigation mentioned that sweep events are mainly responsible for gravel transport. Nikora and Goring (2000), from field evidences reported that turbulence characteristics over weak mobile bed differ from that of immobile bed and intense mobile bed.

2.5 Environmental Significance of Fines in the Flow

2.5.1 Effect of fine sediment inflow on reservoir capacity

As the natural regime of river is disturbed by dams, aggradation above and degradation below the dam are often observed. Because of construction of barrier, downward flow of sediment with water also gets blocked and hence sediment deposit on the upstream of the dam and it's called reservoir sedimentation. It reduces the designed capacity of the reservoir. Reservoir sedimentation is a worldwide problem (Vorosmarty et al. 2003). But it is more prone in the area/ river which are more susceptible to the erosion of surface material from catchments. Deposition of larger particles generally moving as bed load is almost certain while most of the suspended particles also deposits. Generally coarse sediments get deposited in the head water areas of reservoir whereas fines move closer to the dam and deposited nearby if not passed.

The dead storage in a reservoir is created to store some water all the time which only diminishes due to evaporation. But because of sediments, dead storage is not utilizable and only meant to get gradually filled up during the life of reservoir. Accumulation of sediment reduces the water holding capacity of reservoir and the reservoir gradually loses its purpose for which it was actually constructed.

Some other detrimental effects are eutrophication, effects on biota and hungry water effect on downstream of dam. Eutrophication is the response of an ecosystem due to excessive increase in the artificial or natural substances like phosphates and nitrates brought by the sediments. An excessive increase in phytoplankton due to increase in nutritional level in the water body, decrease in dissolved oxygen content in water are some examples of the eutrophication. Effects on biota and aquatic habitats are applicable for other situations also and hence discussed in detailed in separate sections below. Clear water passing down the reservoir has some sediment holding capacity and hence called hungry water. Such sediment starved water (hungry water) may lead to severe bed and bank erosion, modification of channel morphology, change in particle size distribution, undermining of riverine structures (Kondolf 1997).

It is estimated that reservoirs traps 25-30% of the global sediment discharge into ocean (Vorosmarty et al. 2003). Nizamsagar reservoir constructed for water supply purpose has lost 52% of its live capacity in just 37 years of existence (Mohanakrishna 2001).

2.5.2 Effect of fine sediment on aquatic plants

Excessive sediment in river system affects the growth and survival of plants and animals in the river systems that are the base of food chain. These are the primary producers and any deleterious effects on these are reflected on higher communities (fishes and other invertebrates of water). Periphytons and aquatic macrophytes are the roots of river food chain.

Sediment concentration ranges from its highest level during flood event to the lowest level during base flow. The existence of high concentration of fines may be a short term event but its impact can be observed over long duration. The most deleterious effect is by the human induced long term activities such as mining, deforestation, unmanaged agriculture etc. Wood and Armitage (1997) citing several investigators have proposed four different ways in which producers get affected by fine sediments. First is by reducing photosynthesis process by limiting the light penetration (Van Nieuwenhuyse and LaPerriere 1986). Second is by reducing organic content for periphyton cell (Cline et al 1982; Graham 1990). Third is by damaging leaves of macrophytes by abrasive action of sediment (Lewis 1973a,b) and the fourth is by sweeping away periphyton and aquatic macrophytes in extreme cases (Brookes 1986; Albaster and Llyod 1981). For example a study by Lewis (1973a) showed that at just 100 ppm concentration of coal in a stream damaged leaves of aquatic moss.

2.5.3 Effect of fine sediment on aquatic invertebrates

Effects of fine sediment on aquatic invertebrates vary with the species and the tolerance capacity of individual aquatic invertebrates. The aquatic invertebrates may be herbivorous or carnivorous. Herbivorous invertebrates consume aquatic plants and carnivorous invertebrates make herbivorous invertebrates as food. Aquatic plants are affected by presence of fine sediment in flow, which in turn affect the herbivorous invertebrates. And any effect on herbivorous invertebrates is reflected on the carnivorous invertebrates. Citing several investigators Wood and Armitage (1997) mentioned four different ways in which benthic invertebrates may get affected by fine sediment in flow. First one is by scouring and abrasive action of flow on invertebrates. This can damage the exposed respiratory organs and make it more vulnerable to the predators (Langer 1980). Sediments may harm the gills of invertebrates, impairing the respiratory (Lemly 1982; Newcombe and MacDonald 1991). Second way is that the suspended sediment alters the

channel substrata and makes it unsuitable for invertebrate's habitat (Erman and Ligon 1988; Richards and Bacon 1994). Third is that, some invertebrates are filter feeders but sediment inflow clogs their filter organ reducing their feeding efficiency and hence reducing their growth and sometimes even killing (Aldridge et al. 1987; Hynes 1970). Fourth is the association of sediment with invertebrates drift. Due to sediment deposition and substrate instability, benthic invertebrates migrate up or down of the channel (Culp et al. 1985; Rosenberg and Wiens 1978; Gammon 1970). Gammon (1970) showed 25-90% invertebrates drift with just minor increase in concentration to 40-80 ppm.

Davis- Colley et al. (1992) reported loss in the see through characteristics of water of west coast of south island of New Zealand. They also reported the deposition of fines on or beneath the surface of channel bed due to placer gold mining. Further Quinn et al. (1992) reported that high sediment concentration and associated turbidity in the water resulted in reduced densities of benthic flora and invertebrates.

2.5.4 Effect of fine sediment on fishes

Amongst many Cordone and Kelley (1961), McNeil and Ahnell (1964), Barton (1977), Adams and Beschta (1980), Carling (1984), Berkman and Rabeni (1987), Carling and McCahon (1987), Chapman (1988), Sear (1993), Baxter and Hauer (2000), Harrod and Theurer (2002), Greig et al. (2005) are the few among many investigators who worked on the effect of fine sediment on the fish and its associates. Salmonids including trouts, salmons, and grayling white fishes are valuable game fishes and source of nutrients for human (Cordone and Kelley 1961; Ryan 1991). Since fishes have more economical and commercial values than any other aquatic animals, the studies on effect of fines on fishes are more compared to others. Of all the stages of life cycle of salmon fish, the egg incubation stage is most important. Female salmons deposit their eggs in a pit of 10-40cm depth below the river bed. The salmon separates existing fines in the gravel bed to increase the permeability and inter gravel oxygen flow around incubating location. Eggs are very susceptible to increase in sediment concentration. Studies have shown that even at relatively small increase in sediment concentration results in reduced survival of eggs (Levasseur et al 2006), increase in number of premature alevins (Olsson and Petersen 1986; Reiser and white 1990). Sediment deposition reduces the hyporheic zone that is vital for the survival of eggs. Sometimes excessive deposition of sediment may coat the eggs resulting in

reduced oxygen supply to the eggs. Even if an egg gets critical oxygen supply (16 $g/cm^2/hr$), the non removal of metabolic waste due to blockage of fine sediment may result in fatal increase in Co_2 and ammonia (Bash et al. 2001). Also the alviens may not be able to migrate through gravel bed due to sediment coating of eggs and blockage of interstices of gravel.

A quality habitat of a young fish is pools and interstitial spaces between gravels. But sedimentation fills up those spaces and reduces quality habitat for young fishes. Gills are the very important organ of fishes. If the water is sediment laden, the gills may get clogged. Fishes try to clean up the gills by excessive opening and closing the gills and developing mucus. In some cases fishes may die because of clogging of gills. So the presence of sediment in excess hinders the growth and survival of fishes by damaging their lower order food chain, reducing spawning habitat and physically damaging fishes.

2.5.5 Fine sediment intrusion into river bed

In this section various factors that may affect the fine sediment intrusion and deposition process in river beds are reviewed along with its entrainment process. The possible influential factor of sediment deposition and entrainment in a river system may be the hydraulic properties, fluid properties, channel properties, sediment properties, input rate, and duration of availability of fines in flow.

One of the pioneers to conduct laboratory study to understand the fines intrusion and deposition in the channel was Einstein (1968). Two different gravel mixture; first one ranging from 2.5 cm to 15 cm and second ranging from 6.4 mm to 38 mm were put separately in the two different recirculatory flumes, leveled and clear water passed through it below incipient condition. Silica flour (0.0035 mm to 0.03 mm) was fed into the flow at predetermined quantity. Einstein (1968) observed water becoming cloudy at the beginning after adding silica but by the end of each experiment, the water again gained clarity indicating release of fines into the interstices of gravel bed. Einstein (1968) observed that fines infiltrated down to the bottom of the channel and gradually piled up filling the gravel pores. He mentioned that as long as there were pore spaces in gravel deposit, fines were observed to deposit and the fines once deposited in the bed was never observed to be eroded. The experimental result of Einstein (1968) was contradictory to the field observations and the possible reason for such result as pointed by Diplas and Parker (1985) may be flow being below incipient motion, no self formation of pavement layer,

absence of pool and riffle, large size difference between gravel and silica flour and the use of recirculatory flume.

Milhouse (1973) studies the flow through Oak Creek, a typical gravel bed stream. He found a well sorted gravel (mean size 63 mm) on surface layer called pavement and poorly sorted gravel (mean size 20 mm) in subsurface layer called sub-pavement. His study reported that the pavement layer plays the most important role in limiting the availability of stream bed sediment for discharge along with flow. Milhouse (1973) observed that during low flows, the gravel bed acts as a sink and grabs fines from suspension. Whereas at high flows, the same gravel bed acts as a source and releases fines into suspension. He also observed that fine sediment tends to deposit on the top of substrate and bottom of pavement layer. He termed the interface of pavement and sub pavement a silt reservoir.

Beschta and Jackson (1979) conducted 18 experiments with 0.5 mm sand and 2 experiments with 0.2 mm sand as a filler material on 15 mm gravel bed. Experiments were conducted at different discharge, slope and Froude number. Their observations reveled Froude number as a driving hydraulic parameter (90% confidence level) affecting the intrusion process. They observed that at low Froude number (Fr<0.9), sand of 0.5 mm mostly moved within 1 cm of the gravel surface and infiltrated just 5 cm of the gravel bed. 0.5 mm sand quickly formed a seal at around 5 cm below surface and gradually moved upward filling pores. At higher Froude number (Fr>0.9) sands were accumulated into a depth range of 10 to 5 cm. They hypothesized that turbulence pulses generated at higher velocity inhibit the formation of sand seal near surface. Average bed stress, unit stream power, Reynold number didn't play significant role in intrusion process. Also the amount of fines deposited into the bed was maximum at higher sediment input rate at higher Froude number. Whereas 0.2 mm sand showed intrusion down to the bottom of gravel supporting Einstein (1968) observation. Also the amount of 0.2 mm sand accumulated in the bed was higher than that of 0.5 mm. They also studied the entrainment process and found maximum entrainment up to 1 cm depth. They finally concluded that flow condition (Froude number), sediment input rate and its particle size distribution influences the infiltration and deposition of fines into gravel bed.

Adams and Beschta (1980) selected 13 riffle areas from 5 streams of Oregon Coast Range to sample bed material up to 25 cm depth to evaluate percentage of fines present in whole sample. They observed spatial and temporal variation of fines proportion within adjacent streams,

within the stream itself and even within same riffle. Size distribution of gravel substrate and filler material, hydraulic condition of flow and the availability of fine for intrusion are main factors for spatial variation of fines. The deposition of fines in the bed of same stream was correlated with stream full discharge and sinuosity. Sinuosity is the ratio of length along the stream centre line to the length along the valley. Flow condition and the sediment transport rate variation across the single stream riffle are supposed to be responsible for in-riffle variation of fines proportion. They also observed cross sectional variation of fines in a river is more than that of longitudinal variation of fines in a river. For the temporal variation, the possible cause was attributed to the periodic flushing during high flow events. They emphasized gravel must move for flushing fines from its interstices.

Dhamotharan et al. (1980) produced a physical model of Oak Creek at St. Anthony Falls Hydraulic Laboratory using geometric scale ratio of 1:8 and Froude number similarity. The bed surface forming gravel was of median size 2.5 mm with standard deviation 2.5. The model was of recirculatory type and the flow rate was enough to move even the coarsest gravel. The study confirmed that the gravel stream phenomena can be reproduced in the laboratory. The flow was started with clear water flow. Once the system of flow reached equilibrium, fines of median size 0.12 mm was added in the flow keeping all parameters intact. A new equilibrium state was reached after adding fines. They observed that the fines predominantly accumulated at the interface of pavement and sub pavement layer. This observation was similar to that of Milhouse (1973). Accumulation of fine at that layer blocked the movement of fines down to the channel and hence bottom up filling of pores as observed by Einstein (1968). Dhamotharan et al. (1980) observed 36% reduction in bed load transport rate compared to that in clear water flow.

Filed study on Jacoby Creek was done by Lisle (1980). Cans of 17 cm diameter and 22 cm height filled with well sorted 15 mm diameter gravels were buried into the bed perpendicular to the flow direction at several locations likely to be used by salmonids for incubation. The cans were dug out, emptied and buried again in similar away after each of six flow events. In Jacoby Creek, bulk of total load transport moves as suspended load but observations in cans reveled its contribution only one fifth of total. Lisle (1980) mentioned probable reason for this as the fine particles moving as bed load has better access to pores. He observed silt and very fine sand deposited at bottom of can whereas sand and other granular materials trapped on top layers. He also reported that at higher total load transport rate, the rate of infiltration of fine in the bed

increases but the amount of infiltration reduced because of seal by grains moving as bed load. Lisle (1980) also reported more variation in infiltration across channel than along channel.

Carling (1984) conducted flume experiments with gravel of median size 15.6 mm and standard deviation 1.27 at below incipient motion condition. Three types of sands with median sizes 0.15 mm, 0.19 mm and 1.4 mm were used as filler material. He studied the effect of bottom shear stress, size distribution of filler material, Reynolds number, Froude number, water depth and mean suspended sediment concentration on the infiltration of sand. Carling (1984) concluded that infiltration of sand has nothing much to do with the gross hydraulic parameters. He justified this by sayings that mean hydraulic parameters do not provide any information about the layer adjacent to the gravel surface which actually governs the process of deposition of fines. Instead he mentioned that initial concentration of sand was a main flow parameter that well correlated the siltation rate. Some other observations were that, only the coarsest sand formed a patchy seal and siltation rate was rapid even at low concentration irrespective of hydraulic properties and sand size.

Frostick et al. (1984) conducted field study on a tributary of River Lee called Turkey Brook. They studied the spatial variation of silt infiltration and depth variation of infiltration with different size subsurface materials. The then surface material of Turkey Brook was uniform and of 27 mm median size and subsurface material was of 16 mm median size. Six matrix traps each with opening of 0.5 m and 0.33 m depth and each trap having sixteen compartments were buried into the bed. The opening of the trap was covered with surrounding materials. Ten compartments were left emptied and remaining six filled with sediment of median size 48 mm, 24 mm and 12 mm; two compartments per material. Three traps were buried across a channel bar and three across riffles. Eight compartments of each trap were emptied weekly; three compartments with different subsurface materials along with one emptied monthly and remaining were empties for every three months. Measurements of fines deposited in subsurface material filled compartments show 10 to 87% less silt compared to empty compartments for a period of three months. It was found that the cross sectional variation of fines infiltration is more dominant than that along the channel. Their observations also concluded that size distribution of subsurface material also matters a lot. More fines infiltration was observed in coarse subsurface deposit than finer subsurface deposit. They hypothesized ratio of surface to subsurface material size put impact on the amount of fines infiltration. Lower ratio allows more infiltration.

Diplas and Parker (1985) demonstrated the existence of pavement layer significantly coarse than subsurface material by conducting a clear water run on poorly sorted material. His experimental results showed that fines deposited below the surface layer didn't interact with the flow. The concentration of fines expressed in percent by weight in the pavement layer correlated well with mean flow concentration if rest all flow parameters almost remains same. There is semi logarithmic relation between percentage of fines in pavement and the mean flow concentration. Another finding of the experiment was that depth of infiltration mainly depends on relative size difference of filler material and bed material. Especially for layer close to surface, bed shield stress and ground water level also affects the process of infiltration. Diplas and Parker (1985) also observed that coarser particles of fine sediment make a seal in the gravel layer impeding further downward movement of fines. They also reported that fines in bed can be flushed to $3d_{90}$ depths if bed is mobile, if not only top layer fines can be flushed. Here d_{90} is gravel size for which 90% material is finer.

Khullar (2002) conducted several experiments on routing of suspended sediment through uniform and non uniform gravel beds. 1.8 mm and 0.96 mm sized uniform gravel and 2.1 mm sized non uniform gravels were used to form channel bed. 0.064 mm silt termed as wash load was used as filler material. He observed that when silt laden flow passed through gravel bed, the silt infiltrated into the gravel bed but couldn't reach to the bottom. He observed that proportion of silt in bed kept on increasing till the silt concentration in flow reached equilibrium. The equilibrium condition was supposed to reach when rate of entrainment of fines from bed became equal to rate of deposition. He also reported lesser silt accumulation at crest location than in trough location.

Wooster et al. (2008) conducted three flume experiments on immobile gravel bed with well sorted sand of geometric diameter 0.35mm as filler material. The sand mainly moved as bed load. Various sizes of materials were used to form surface and subsurface layer of 10 zones in single flume. Flow discharge was kept same for all runs. Experiments were designed in such a way that for each experiment, sediment feed rate increased by 10 fold and duration of feed decreased by 10 fold maintain the same cumulative feed volume. Two experiments with low feed rate produced almost similar infiltration while third one with high feed rate resulted in less sand infiltration. This indicated that a sudden release of high sediment is more beneficial than slow release from the view point of sediment infiltration in the bed.

Chapter 3

Experimental Setup and Methodology

3.1 General

The present chapter discusses in detail the experimental runs conducted for the analysis. The experiments were carried out in the Hydraulics Laboratory of the Indian Institute of Technology Roorkee, India. A series of sediment routing experiments were conducted in the laboratory to obtain data on velocity distribution, suspended load concentration, bed load transport etc. Broadly three types of experimental runs were conducted viz. clear water run, sediment laden run and the entrainment run. Those runs in which fine sediment was not mixed with water were termed as clear water runs and those carrying suspended sediment with water were termed sediment laden runs. The runs which carried clear water but with the motive to entrain the sediments deposited during sediment laden run were termed as entrainment runs. All the experimental runs were carried out under subcritical, steady and uniform flow conditions. The details of the experiments are discussed in the following sections.

3.2 Equipments

3.2.1 Flume

For the entire experiments, a recirculating tilting flume of length 13 m, width 0.40 m and depth 0.60 m was selected. Figure 3.1 shows the schematic diagram, of the flume used in the study.

The upstream of the flume has water inlet chamber and in order to reduce the high turbulence in the incoming flow, several arrangements like placing of boulders, flow straightening racks, flow suppressors etc were made. With all these arrangements the working section of the flume was about 9 m. Tailgate at the end of the flume was mechanically operated and was used to control the flow depth in the flume. Both sides of the flume were made of transparent glasses and bottom was made of fiber. On top, two adjustable rails were provided to ease the movement of trolleys carrying pointer gauge, Pitot tube and Acoustic Doppler Velocimeter (ADV). The rails were parallel to the flume bed. At the downstream end, a hopper tank was placed in such a way that the water coming out of the flume directly fall at the center of the tank. This arrangement facilitated the proper mixing of sediment and didn't allow sediment to deposit in the tank. The tank was connected to 50 hp motor through a 0.1 m diameter pipe to recirculate the water. The horizontal portion of the inlet pipe had an orifice to measure the discharge.

3.2.2 Velocity measurement

Velocity was measured with the help of Prandtl pitot tube of outside diameter 6 mm and inside diameter 3 mm and ADV. Vertical velocity distribution was measured along the centreline of the flume. For few initial runs, the velocity was measured using ADV while for rest of the runs, both pitot tube and ADV were used. Velocies measured using pitot tube were used to compute average velocity whereas ADV measurements were used for turbulent analysis only.

3.2.3 Discharge measurement

An orifice was installed in the horizontal section of return pipe to measure discharge as shown in Figure 3.1 . A 7.5 cm diameter circular orifice was installed in the pipe. The pressure head across the orifice was measured using vertical mercury manometer. Before carrying out the experiments, the orifice was calibrated and Figure 3.2 shows the calibration curve for the orifice. The calibrating equation is:

$$Q = 0.065(\Delta h)^{0.494} \tag{3.1}$$

Where Q is discharge in cumec and Δh is the difference in the manometer reading of two limbs in meter.

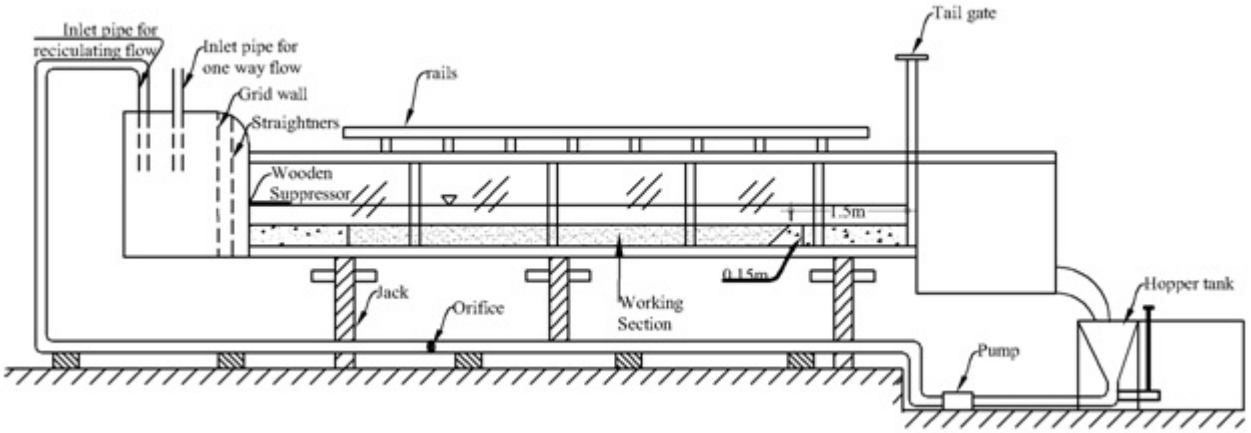

(a) Elevation

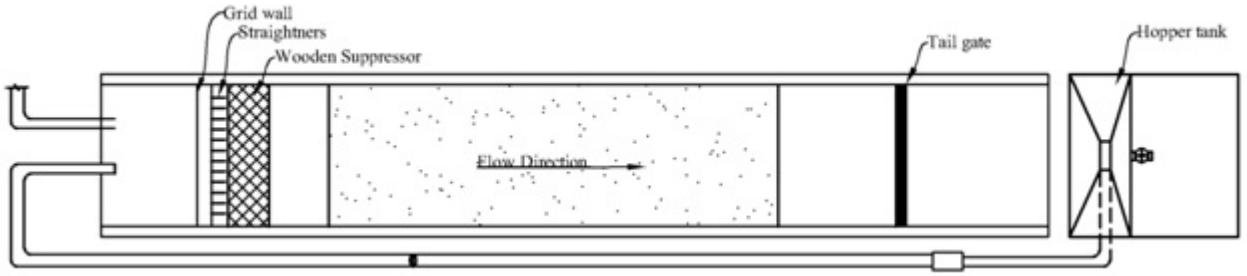

(b) Plan

Figure 3.1: General layout of flume and its component (not to scale)

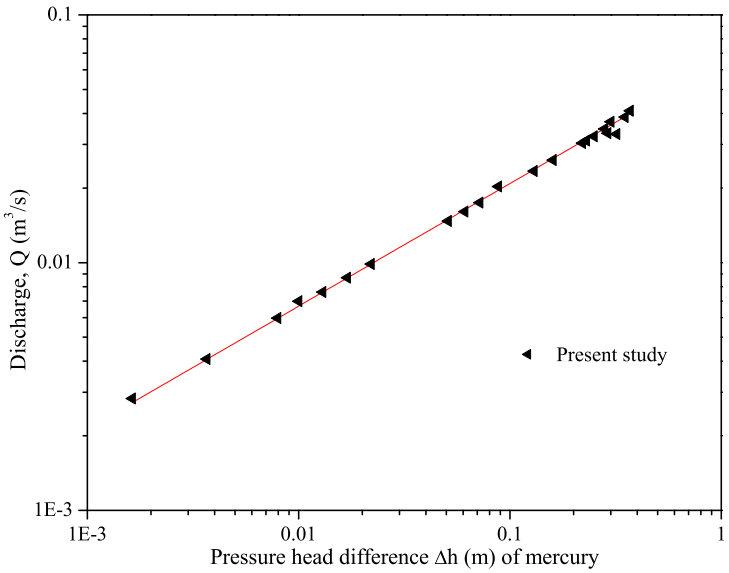

Figure 3.2: Calibration curve for orifice meter

3.2.4 Slope adjustment and measurement

The flume used for the study was of tilting type. The flume was set at a desired slope using electrically operated wheels and jacks. The slope of the flume was tested by two methods viz. two container method and dumpy level. Two empty containers connected with a flexible rubber pipe at bottom were placed at two distant locations on the flume bed. Water was filled in the upstream container and allowed to rest for a minimum of 12 hours. After 12 hours, water level in both the containers were measured. Water level difference between these containers gave the vertical drop of flume for that length. A dummy level and a staff rod were also used to measure the elevation at various sections along the flume.

3.2.5 Bed load measurement

Bed materials transported by the flow were collected at the downstream end of the flume. A nylon net (trap), with openings large enough to pass the water and fine sediment and small enough to retain bed materials was tied at the downstream end of the flume as shown in Figure 3.3 . At every half an hour interval, such traps were changed and the bed materials collected in these traps were weighed. Changing of traps used to take 10-15 seconds; hence practically there was no loss of bed material during changing of traps. After weighing, the same bed material was fed on the upstream for next half an hour to maintain the continuity of bed load.

Figure 3.3: Nylon net (trap) tied at the downstream end of flume

3.2.6 Suspended sediment feeding and measurement

Except for clear water and entrainment runs, fine sediment (silt) was fed in the flowing water. A predetermined amount of silt was carefully added in the hopper tank for a predetermined duration. The sediment was added into the hopper at such a location where the water from the flume directly strikes so that there will be proper mixing. The quantity and duration of feeding was planned in such a way that at no time concentration of fines in flow greatly exceeded the desired concentration.

Width integrating suspended sampler, manually fabricated equipment in the laboratory was installed at the downstream end of channel to collect the suspended sample. The width integrating suspended sampler used in the study is shown in Figure 3.4 . Approximately 10 liters of sample were collected at regular intervals by traversing the sampler across the full width of flow. The samples thus collected were weighed and sufficient time was allowed for sediments to settle down. The clear water was then drained out and the wet silt was dried in an oven. The average concentration of flow at the time of taking sample was then found by dividing the weight of dry silt by the given weight of water.

Similarly, a depth wise suspended sampler as shown in Figure 3.5 was used to take water samples from different depths along the centerline. Depth wise suspended sediment concentrations were taken from two locations,i.e., 2.5 m and 10 m from upstream end. Approximately 1 liter of sample was taken from each depth. Care was taken to match the velocity of sample

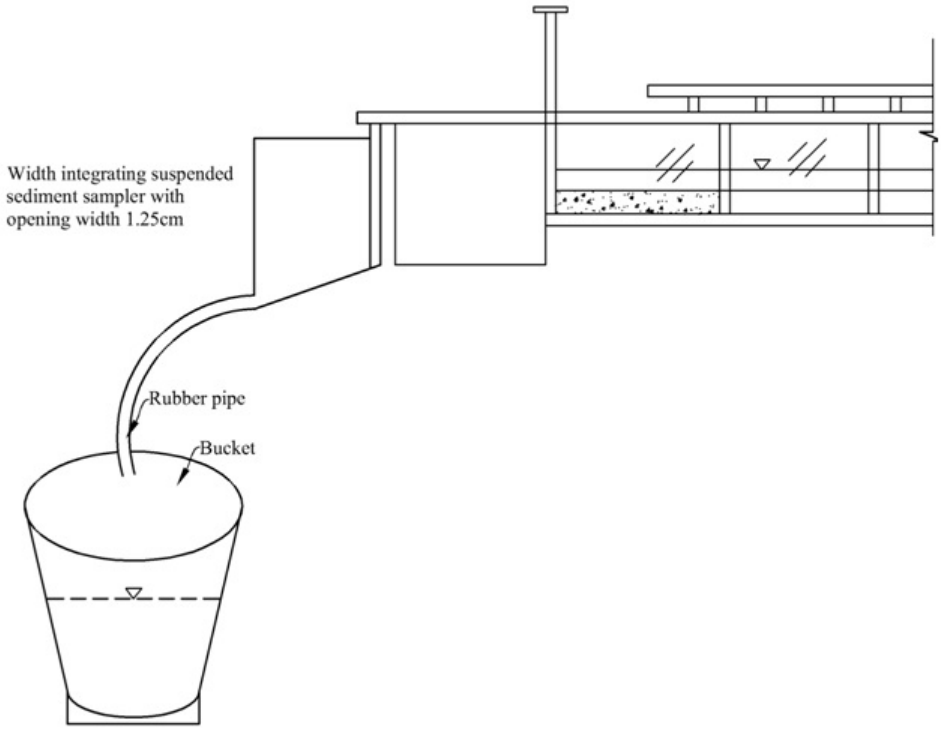

Figure 3.4: Width integrating suspended load sampler

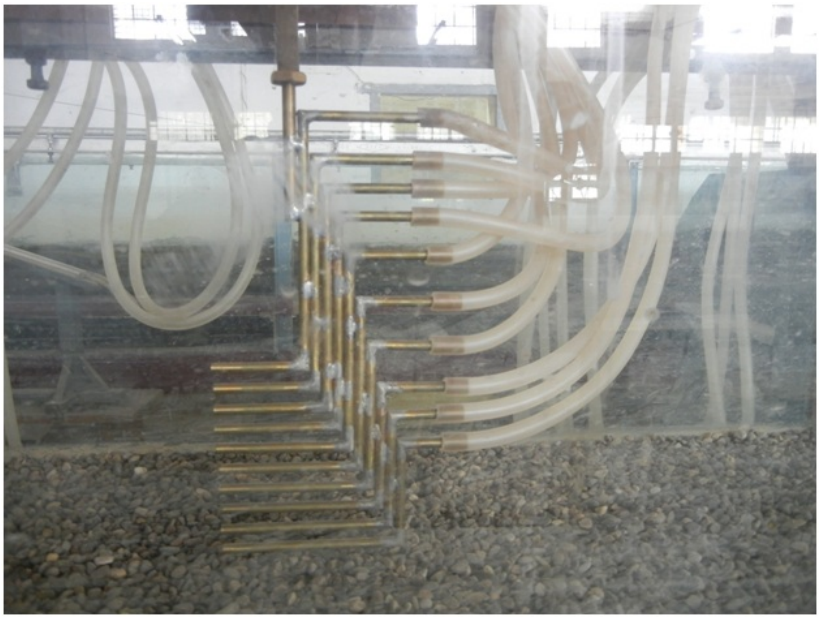

Figure 3.5: Depth wise suspended load sampler

withdrawal to the velocity of flow by adjusting the elevation of discharge end of rubber pipe connected to the tube. The samples thus collected were weighed and passed through Wattman Filter Paper No.1. The sediments trapped on the filter paper was dried in oven and the concentration was obtained as explained earlier.

3.2.7 Flow depth measurement

Flow depths during the experiments were measured using pointer gauge mounted on the trolley. Water surface profile was measured by taking the elevation of the top of flowing water. After completion of experimental runs, bed surface profiles were measured in the same manner. Both measurements were taken at every 0.5 m from the start of working section. The difference in the elevations of these two profiles gave the flow depth at each section. Since the flow was kept uniform, the flow depth at each measured sections were practically same. However an average of the flow depth at middle 3 m section was considered as the flow depth.

3.2.8 Bed sample measurements

After each sediment laden run, the bed was allowed to drain out for sufficient time. Once the bed got dried, bed samples over the entire depth were taken at three locations (3 m, 6 m and 9 m) along the flume. These samples were taken to quantify the amount of silt infiltrated through the bed. The sample encompasses the entire width of channel and of 20 cm long along the flow direction and of 2 cm thick. Two very thin but hard aluminum sheets of length 40 cm and 2 cm marked lines on it (as shown in Figure 3.6) were inserted into the bed 20 cm apart. Grab sampling was done with the help of small trowel for each 2 cm thickness of bed over the entire width. The samples thus collected were weighed and washed with clear water in a bucket. The

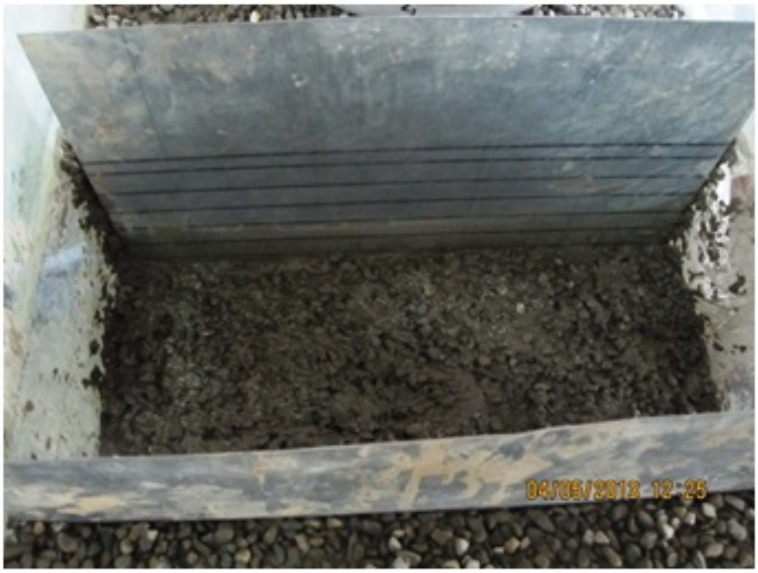

Figure 3.6: Bed material sampling in process

washed gravels were then kept back in the same sampled location and the washed water was allowed sufficient time for the settlement of silt. Clear water in the bucket was drained out and the wet silt was kept in oven for drying. The availability of silt in individual sample was obtained by dividing the weight of dry silt available in that layer with the weight of sampled material from the same layer. Figure 3.6 illustrates the sampling process of bed material.

3.3 Materials Used

3.3.1 Gravel

Material size and gradation have effect on sediment transport (Li 1987). Three uniform size gravel of median size (d_{50}) 5.2 mm, 2.7 mm and 1.9 mm were used in all the experiments. The gravel passing through 8 mm sieve and retained on 4 mm sieve had a median size of 5.2 mm and was designated as L. Gravel of median size 2.7 mm, and designated as M, was passed through 4 mm sieve and retained on 2 mm sieve. Similarly the smallest gravel, designated as S, was passed through 2 mm sieve and retained on 1 mm sieve. It had a median diameter of 1.9 mm. Gravel particles of all sizes had the specific gravity of 2.65.

3.3.2 Fine sediment

Raw material to obtain fine material of desired size was brought from the Ganga Canal at Bahadrabad in Haridwar district of India. The raw material was sun dried and sieved through 0.090 mm and 0.045 mm sieves. The material retained between these two sieves was used as fine sediment. The size of fine sediment was 0.062 mm which corresponds to the silt. Table 3.1 presents the particle size distribution characteristics of gravel and fine sediment used in the study and Figure 3.7 presents the corresponding particle size distribution curves. It is clear from Figure 3.7 that the gravel and fine sediment used in the study are of uniform size.

3.4 Experimental Procedure

The following steps illustrate in detail the experimental procedure for each experimental runs.

Table 3.1: Characteristics of materials used for present study

Sediment	d_a (mm)	d_{50} (mm)	d_{65} (mm)	σ_g	M
L	5.5	5.2	6	1.27	0.278
M	2.63	2.7	2.8	1.21	0.384
S	1.81	1.9	1.92	0.905	0.63
W	0.063	0.062	0.072	1.20	0.27

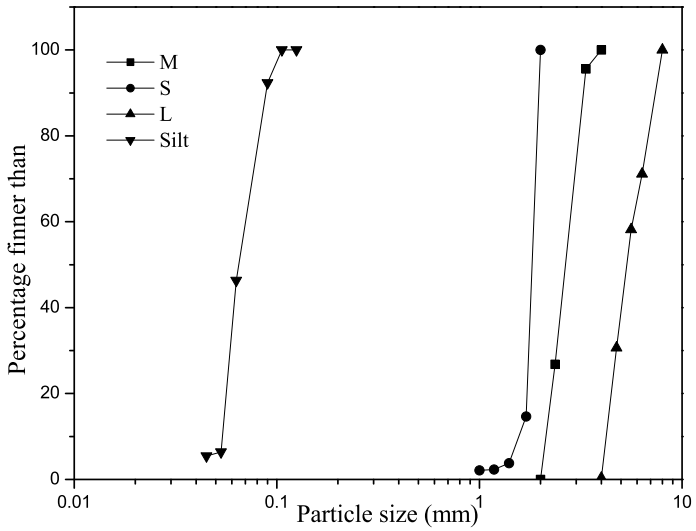

Figure 3.7: Particle size distribution of materials used in experiments

(i) Gravel to be used was neatly washed with clear water to make it fines/dust free.

(ii) Cleaned gravel was then laid on the clean bed of flume to a height of 15cm throughout the working section of the flume. The gravel bed was leveled with the wooden template and the level was checked with point gauge and dumpy level.

(iii) The re-circulatory system of the flume was brought into operation. Certain discharge was allowed to enter into the flume.

(iv) During trail runs, the discharge (Q), slope (S) and flow depth (h) were changed simultaneously to arrive at steady, uniform, and incipient flow condition at which the bed particles just start moving over the bed and these flow parameters were recorded.

(v) Now the bed was again leveled. The experimental runs for data collection was conducted with clear water corresponding to the hydraulic parameters (Q, S and h) obtained in the

trail run. This clear water run gave a set of reference data viz. discharge (Q), slope (S), flow depth (h), flow velocity (U) and bed load transport rate (q_B).

(vi) The gravel bed material moved as bed load was collected in the trap at the downstream of the flume. Right from the start of the experiment, the bed load was collected at every half an hour interval. The bed load collected was weighed and then fed at the upstream of the working section of the channel for next half an hour to maintain the bed load continuity. This process was done for the full duration of the experiment.

(vii) During each run, water surface and bed surface profiles were measured to confirm the uniformity of the flow. The velocity of the flow was also measured with Pitot tube and ADV.

(viii) The clear water run was followed by the sediment laden runs. The hydraulic parameters for these sediment laden runs were kept same as those in clear water runs. Initial sediment laden runs were conducted with low sediment concentration and the sediment concentrations were increased gradually for successive runs.

(ix) All measurements (Q, S, h, U and q_B) taken during clear water run were measured in the sediment laden runs also. In addition, silt concentration in the flowing water was also measured. Width integrating concentration and depth wise concentrations were measured as discussed in previous sections.

(x) After completion of each individual sediment laden experimental runs, the gravel was allowed to drain out the water completely. Bed samples were then taken at 3 m, 6 m and 9 m sections measured from the upstream end of flume to obtain the proportion of fines infiltrated into the gravel bed. Bed samples were taken from the whole depth.

(xi) For each gravel size the above mentioned procedures (step i to step x) were followed. For each gravel size 8 to 10 experiments with increasing concentration were conducted at particular Q, h, S. These set of experiments were considered as one series. When it was observed that sediment was no more infiltrating inside the gravel bed the series runs were stopped.

(xii) After completion of sediment laden run, next were the entrainment runs. In those runs again, clear water was passed through the one way flow system of the flume. First entrain-

ment run was at lower discharge (there might or might not be any bed load movement). In the next run discharge was bit increased; there might be some bed load movement. In this way 3-4 entrainment runs were conducted at successive increasing discharge. Discharge, velocity and bed load (if any) were measured in entrainment runs also. Again after each entrainment run, bed samples were taken as explained earlier to check the reduction in the proportion of fines that was infiltrated during sediment laden runs; also to examine the depth to which the silt can be entrained at different discharges.

As mentioned in Table 3.1 , the sediments are designated as L, M, S and W. Here L stands for the largest gravel size i.e. 5.2 mm, M stands for medium size gravel i.e. 2.7 mm, S stands for the smallest size gravel i.e. 1.9 mm and W stands for suspended sediment of size 0.062 mm. All the experimental runs are assigned run numbers. For example an experimental run has a name $2LC1$. Here 2 stands for series number, L is the type of gravel used, C is the clear water run and 1 is the run number. $2LC1$ represents a clear water experimental run of second series on bed composed of 5.2 mm gravel. Similarly, an experimental run with name $1SW4$ represents fourth sediment laden run of first series on bed composed of 1.9 mm gravel. Whereas, to denote entrainment runs, E is used. For example, 2ME2 designates the second entrainment run of second series of run on bed composed of 2.7 mm gravel.

Chapter 4

Resistance to Flow

4.1 General

Flow resistance relationships are a classical components of river hydraulic analysis, required for many hydraulic engineering studies like prediction of flow depth, flood routing etc. (Bathurst 2002). The problem of obtaining the friction factor becomes difficult if the bed is mobile, not straight, undulated etc. The friction factor or resistance to flow for the case of rigid bed straight channels is well documented (Khullar 2002). Effect of suspended sediment on flow resistance is not same in the rigid bed and mobile bed (Khullar 2010). Suspended sediment in the flow has a significant impact on the fluid and flow characteristics, and hence, has a significant influence on the resistance to flow. In the last seven decades, numerous conclusions have been arrived on the increase or decrease of the friction factor in presence of suspended sediment. The present chapter discusses the determination of friction factor in open channels carrying suspended sediment. Probable change in the Von Karman constant has been quantified and a criterion has been proposed for the determination of friction factor in presence of suspended sediment.

4.2 Karman Constant Variation with Fines Concentration

In this section, the variation of Von Karman constant with variation in sediment concentration is studied. Though log law is being applied for the full depth of flow, it is actually valid in

the region 30<y^+<0.2R_* (Nezu and Nakagawa 1993); where $y^+ = U_* y/\nu$ and $R_* = hU_*/\nu$, y is the height of the point of measurement from the bed, h is the flow depth, ν is kinematic viscosity, U_* is the shear velocity, y^+ is the dimensionless depth and R_* is the Reynolds number. It has been noticed by several researchers that Von Karman constant also gets affected due to the presence of suspended sediment in flow (eg. Guo and Julien 2001; Coleman 1986; Elata and Ippen 1961). Here an attempt has been made to study the variation of Karman constant with the concentration of suspended sediment in flow. Out of the seven series of experimental runs, the velocity distribution of the last four series (2L, 2M, 2S and 3M) are measured with pitot tube. The pitot readings have been taken from 2 mm above the bed level to the water surface. The pitot readings which lie within the depth of 30<y^+<0.2R_* are only considered in the analysis. The velocity distribution data from these series are used to analyse the variation of Karman constant with sediment concentration.

For each individual run of the above mentioned series, a plot of $log(y/k_s)$ versus velocity (U) were prepared; k_s is the equivalent roughness height. One such plot corresponding to 9^{th} run of series 2M (i.e 2MW9) is shown in Figure 4.1. The equation of the best fit line was

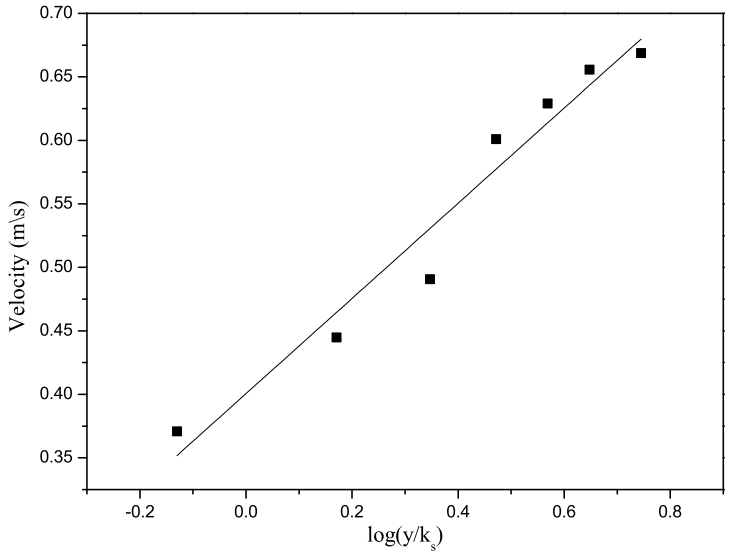

Figure 4.1: Logarithmic velocity distribution of run 2MW9

obtained; the coefficient of correlation of which was 0.975. The best fit equation thus obtained was compared with the standard log law (equation 2.1) to compute the value of Karman constant (κ). The value of the Karman constant was obtained for all runs (clear water and wash load) of the four series. A plot of (κ) and suspended load concentration (C) in respective runs are

plotted in Figure 4.2.

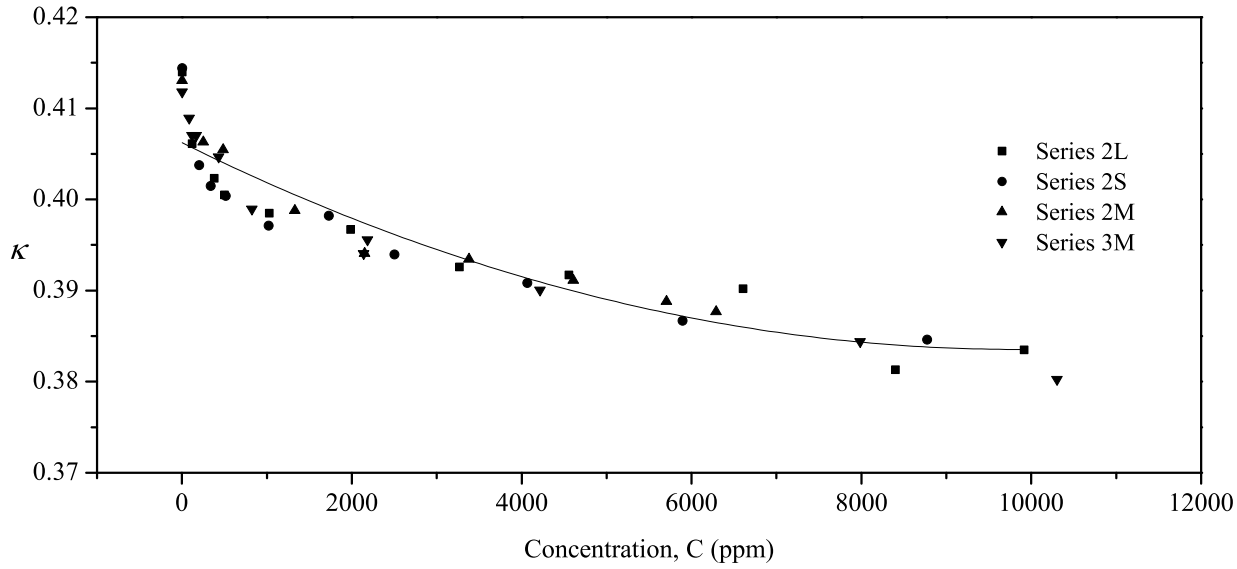

Figure 4.2: Variation of Karman Constant (κ) with sediment concentration (C)

Figure 4.2 clearly shows a decreasing trend of Karman constant with increasing concentration of fines. Towards the higher concentration, the Karman constant doesn't seem to decrease rapidly. The best fit relationship that explains the variation of Karman constant with concentration is obtained as

$$\kappa = 3 \times 10^{-10} C^2 - 5 \times 10^{-6} C + 0.407 \text{.....For} \quad C \leq 10300 ppm \tag{4.1}$$

4.3 Effect of Suspended Sediment on Resistance to Flow

It has already been mentioned in Chapter 2 that the resistance to flow due to fines concentration may increase or decrease. Resistance to flow mainly decreases due to dampening of turbulence and increases due to more energy loss in the process of suspension, increased viscous resistance and form resistance. Data of Vanoni (1946), Vanoni and Nomicos (1960), Cellino and Graf (1999), Khullar (2002) and present study which are presented in Table 4.1 have been used in the analysis of the resistance to flow. Vanoni (1946) conducted experiments on porous bed composed of 0.47 mm and 0.88 mm sand bed particles with fine particles of 0.09 mm and 0.147 mm. The concentration of his experiments varied from 445 to 1250 ppm. Vanoni and Nomicos (1960) used fine sand of size 0.1 mm and 0.16 mm as suspended material to vary

concentration between 116-3050. Cellino and Graf (1999) experiments were also on porous bed by cementing 4 mm sand on channel bed and 0.13 mm sand as suspending material. Khullar's (2002) experiments were on mobile porous bed composed of 1.8 mm and 0.96 mm uniform size gravel bed. 0.064 mm silt was used as suspended sediment. Among the data of Khullar (2002), only those data which corresponding to uniform gravels bed are selected for the analysis.

Table 4.1: Range of hydraulic parameters used for resistance analysis

Data/Series	**Q** (m^3/s)	**h (m)**	**U (m/s)**	F_r	**S x** 10^3	d_w **(mm)**	**S**	**C (ppm)**
Vanoni (1946)	0.0365-0.1490	0.07-0.17	0.61-1.11	0.57-0.93	1.25-2.5	0.091-0.148	2.65	445-1250
Vanoni and Nomicos (1960)	0.0086-0.0144	0.074-0.087	0.37-0.70	0.41-0.80	2.0-2.93	0.1-0.16	2.65	116-3050
Cellino and Graf (1999)	0.049-0.066	0.12	0.68-0.92	0.63-0.85	0.3-3	0.135	2.65	87-2375
Khullar (2002) 1UW	0.0129-0.0259	0.082-0.193	0.58-0.82	0.48-0.86	1.79-3.82	0.064	2.65	280-11369
1L and 2L	0.0214-0.0262	0.071-0.090	0.708-0.771	0.76-0.92	8.44-9.95	0.062	2.65	118-9917
1M, 2M and 3M	0.0179-0.0214	0.071-0.082	0.596-0.707	0.70-0.85	5.17-7.62	0.062	2.65	85-10302
1S and 2S	0.0170- 0.0239	0.072-0.094	0.580-0.667	0.66-0.73	4.00-6.27	0.062	2.65	251-7065

4.4 Calculation of Hydraulic Parameters

4.4.1 Friction factor

Darcy- Weisbach friction factor formula is used to compute the friction factor. Darcy- Weisbach equation relates the friction factor (f) with hydraulic radius (R), bed slope (S) and average flow velocity (U).

$$f = \frac{8gRS}{U^2} \tag{4.2}$$

Since the experiments were conducted in a narrow channel of width 0.40 m, sidewall correction has been applied using Vanoni and Brooks (1957) method which is explained below. The wall friction factor (f_w) is related to the ratio of R_e/f, where $R_e = 4UR/\nu$ and $f = 8gRS/U^2$.

$$(f_w) = \frac{1}{20(R_e/f)^{0.1} - 39} \tag{4.3}$$

To find the corrected hydraulic radius another required parameter f_b is determined from

$$(f_b) = f + \frac{2b}{h}(f - f_w) \tag{4.4}$$

The final corrected hydraulic radius can then be found using equation (4.5).

$$(R_b) = R\frac{f_b}{f} \tag{4.5}$$

4.4.2 Fall velocity

The Particle fall velocity is computed by using the method of Swamee and Ojha (1991). They proposed the equation for fall velocity of natural sediment particle as

$$\omega_* = \left[\frac{44.84{\nu_*}^{0.667}}{\left(1+4.5\beta^{0.35}\right)^{0.833}} + \frac{0.794}{[\beta^4 + 20\beta^{20} + {\nu_*}^{2.4}exp(18.6\beta^{0.4})]}\right]^{-1} \tag{4.6}$$

Where ω_* is dimensionless fall velocity of sediment. β is the shape factor of suspended sediment, the value of which is taken as 0.7 as suggested by the Swamee and ojha (1991) for round particles and ν_* is the dimensionless kinematic viscosity. The dimensionless terms are further expressed as

$$\omega_* = \frac{\omega}{\sqrt{(s-1)gd_n}} \tag{4.7}$$

$$\nu_* = \frac{\nu}{\sqrt{(s-1)g{d_n}^3}} \tag{4.8}$$

Where ω and ν are respectively fall velocity and kinematic viscosity of fluid. d_n is the particle nominal diameter. It has been found that for natural material there is a linear relation between the sieve diameter (d) and the nominal diameter (d_n) (IIHR, 1957) given as $d = 0.9d_n$. Equation (4.6) is applicable only when $\nu_* \geq 1.8 \times 10^{-4}\sqrt{\beta}$.

4.5 Validity of Arora et al. (1986) Criterion

Arora et al. (1986) observed that compared to clear water, the friction factor of sediment laden flow increases with an increase in concentration if $\frac{C\omega}{US} \geq 1200$ but decreases with an increase in concentration if $\frac{C\omega}{US} < 1200$. The validity of Arora et al. (1986) criterion for finding out the friction factor is studied by using the data of Vanoni (1946), Vanoni and Nomicos (1960), Cellino and Graf (1999), Khullar (2002) and present study. Figure 4.3 shows a relationship between nondimensional friction factor and the sediment concentration for the data under consideration along with Arora et al. (1986) criterion. In Figure 4.3 f_0 and f are the friction factors for clear water and sediment laden flow respectively. From Figure 4.3, it can be concluded that

the criteria proposed by Arora et al. (1986) doesn't seem to be valid for all these data under consideration as the friction factor for sediment laden flows are continuously decreasing with increasing concentration.

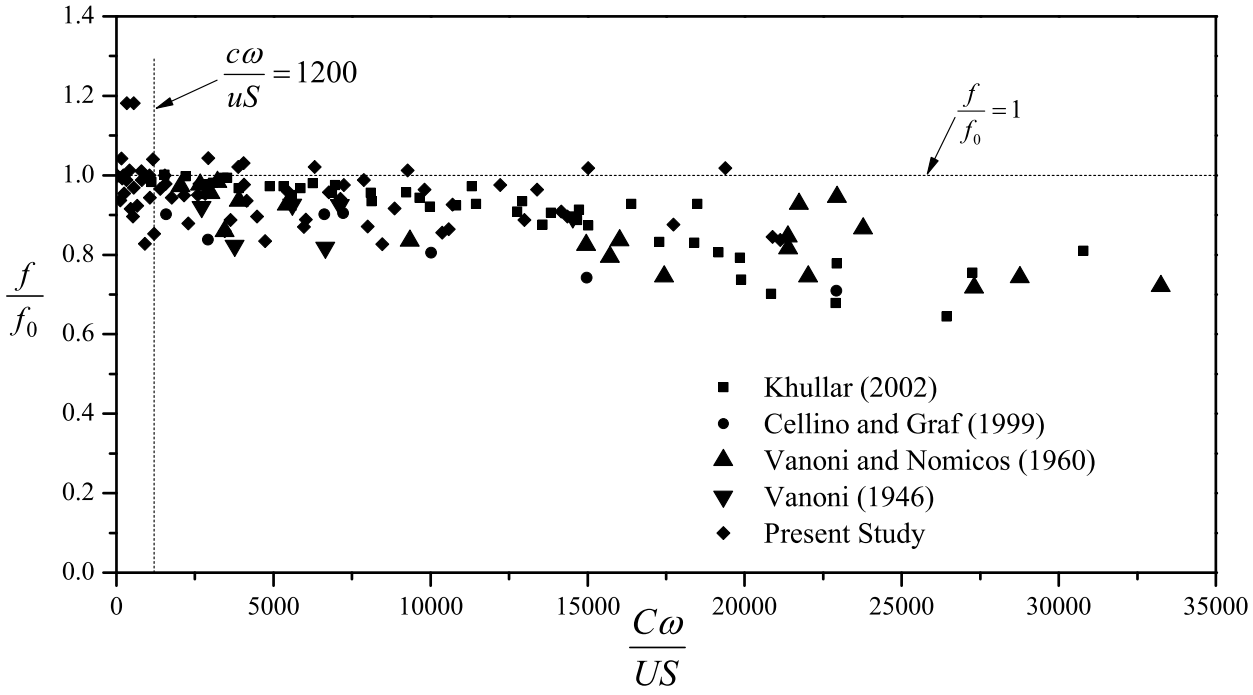

Figure 4.3: Check on Arora et al. (1986) for change in resistance to flow

4.6 Determination of Friction Factor

From section 4.5 , it can be seen that Arora et al. (1986) criterion fails to accurately predict the friction factor for the value of $\frac{c\omega}{US} > 1200$. In the present study, an attempt has been made to accurately predict the friction factor in sediment laden flows. Following Einstein and Chien (1955) and Coleman (1986), a parameter $(s-1)\frac{C\omega}{US}$ was found to be satisfactorily correlating the change in friction factor with varying sediment concentration. The proposed parameter also takes into account the change in relative density of fluid and variation in velocity. Figure 4.4 presents the variation of $\frac{f}{f_0}$ with $(s-1)\frac{C\omega}{US}$ for experimental data considered. A new relationship (equation 4.9) is proposed between $\frac{f}{f_0}$ and $(s-1)\frac{C\omega}{US}$ using data of Vanoni (1946), Vanoni and Nomicos (1960), Cellino and Graf (1999) and Khullar (2002) along with the present study data.

$$0.985 - \frac{f}{f_0} = 8 \times 10^{-6}(s-1)\frac{C\omega}{US} \tag{4.9}$$

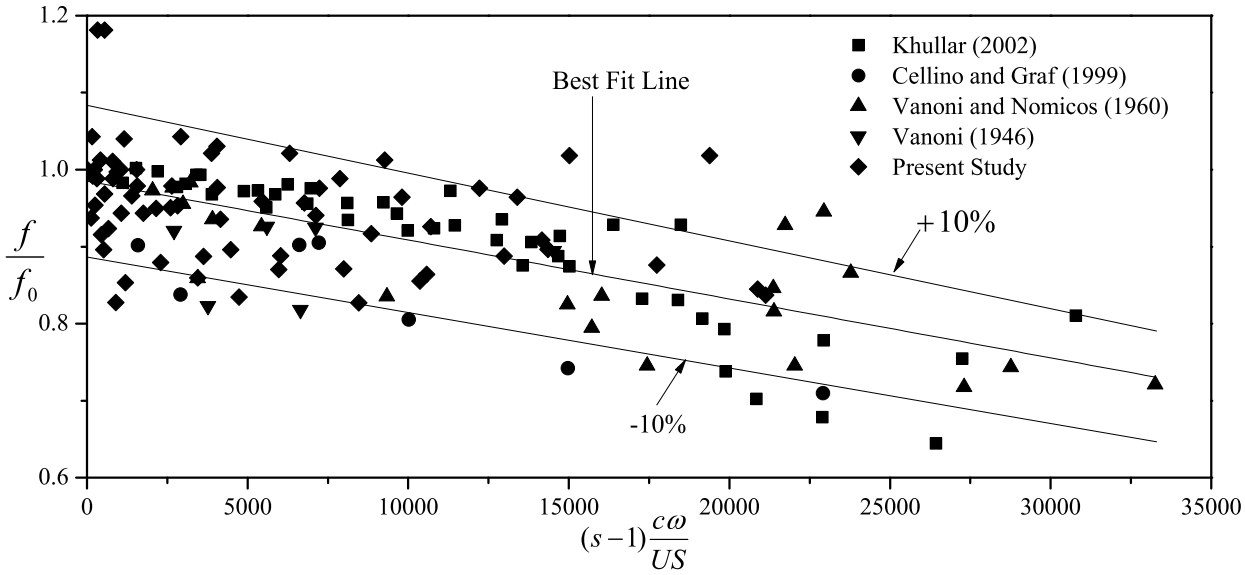

Figure 4.4: Friction factor predictor function

Figure 4.4 also shows the $\pm 10\%$ error line and it can be observed that almost 86% of data lie within the error band.

4.7 Concluding Remarks

The Von Karman constant is found to vary with the change in suspended sediment concentration in the flow. The Karman constant decreased with the increase in sediment concentration. At higher concentration, the Karman constant is observed to attain a constant value. An equation relating the Karman constant and sediment concentration is given in equation (4.1) . Arora et al. (1986) criterion for determining whether friction factor increases or decreases in presence of suspended sediment is not found good for the data obtained from the present study and the data of some others. In the present study (alluvial gravel bed), the friction factor is invariably found to decrease in the presence of suspended load provided the bed form geometry does not change significantly with change in sediment concentration. Equation (4.9) is proposed for the determination of f in an alluvial channel.

Chapter 5

Analysis of Sediment Infiltration and Entrainment

5.1 General

As mentioned in previous chapters, majority of fine sediments in the flow are the migrants of catchment area. During heavy rainfall in catchment area, flow joining the river carries huge amount of fine sediments. In case of a gravelly bed rivers, a part of the fine sediments infiltrates into the pores of the gravel bed and remaining gets washed away depending upon the flow characteristics and sediment concentration. Infiltration of fine particles in the pores of gravel bed mainly depends on the ratio of sizes of gravels of the bed and fine sediments in the flow. Besides, flow characteristics also plays a vital role in the infiltration process. The process of infiltration and deposition of fines continues till the equilibrium condition is reached i.e. the rate of deposition becomes equal to the rate of entrainment. On the contrary, when the hungry water passes through the gravel bed having fine sediment in its pores, the flow picks up the fine sediments from bed and carries them away. The Process of deposition in and removal of fine sediments from the coarse bed of channel have been modeled mathematically. The results from the mathematical model are verified by using the experimental data collected in the present study. Hence, this chapter analyses the process of infiltration/ deposition and entrainment of fine sediments in the gravelly bed rivers from the experimental runs along with the modeling of the deposition of the fine sediment has also been attempted.

5.2 Fine Sediment Deposition and Entrainment Process

When fine sediment laden water passes through the gravel bed, it deposits part of the sediment in the pores of bed. The particles first infiltrate down to a certain depth, gets deposited into the pores and gradually piles up to the surface to the bed. The depth of infiltration mainly depends upon the size ratio of gravel and fine sediment. Until and unless the water is not hungry it keeps on depositing fines. The amount of fines infiltration and deposition mainly depends on sediment concentration in the flow, sediment characteristics and the flow characteristics. If clear water or sediment laden water with very little sediment concentration flows through gravelly bed channels and in case where the hydraulic conditions permit, the flow takes with it the fine sediments attached to the gravels on the bed. The hydraulic condition of the flow in which flowing water can extract the sediments from the bed is called hungry water. Hungry water when passes through gravel bed, entrains the fine sediment deposited in the pores. Depth of entrainment mainly depends on the flow characteristics and gravel size distribution of the bed. The following sections discusses in detail the process of sediment deposition and entrainment observed from the experimental runs carried out in the present study. The analysis involves the visual observations, measurements of depth of infiltration along the channel, vertical distribution of sediment in the gravel bed.

5.3 Visual Observations

Visual observation are made to get an understanding of the sediment infiltration process during sediment laden runs. The sides of the channel was made of transparent glasses. This facilitated the observation of the particle movement initiation as well as fines infiltration and entrainment. The bed surface obtained after different equilibrium runs were photographed. Also the accumulation of fines in the gravel bed were photographed from sides of channel. It has been observed by Diplas and Parker (1992) that the fine sediments initially infiltrates freely to a certain depth where the deposited fines bridge the gap among the bed particles and restricts the later incoming fine particles to infiltrate further below. The deposition then gradually piles up. This phenomenon of deposition was not observed in all the runs with larger size of gravel forming the channel bed. However, in the series of runs with smallest gravel size (1.9 mm), the phenomenon was observed.

5.4 Sediment Deposition on Gravel Bed

As mentioned earlier, the fine sediment deposition on gravel bed mainly depends on the size ratio of sediment and gravel and the flow characteristics. To understand the deposition phenomenon in detail, experiments were carried out with three gravel sizes (5.2 mm, 2.7 mm and 1.9 mm). In all the experiments, the sediment size was 0.062 mm. The experimental observations for each gravel size is discussed in the following Sections.

5.4.1 Bed composed of 5.2 mm gravel

At the beginning of experimental runs with 5.2 mm gravel, the bed of the channel wa level. In none of the experiments (clear water, sediment laden and entrainment runs) with bed composed of 5.2mm gravels, the bed features changed. It remained in level and practically unchanged. Though there were bed load movements, it was uniform throughout the flume length and hence no bed forms were observed. Figure 5.1 the bed surface after completion of 11^{th} sediment laden run of series 2L.

Figure 5.1: Bed surface at the start and at the end 11^{th} run of series 2L

In all the runs conducted with this gravel size, the thickness of gravel bed was 15cm and the fine sediment infiltrated down to the bottom of the bed. Since channel bed was impervious, there was no scope of fine sediment going further down. Fines then started depositing in the

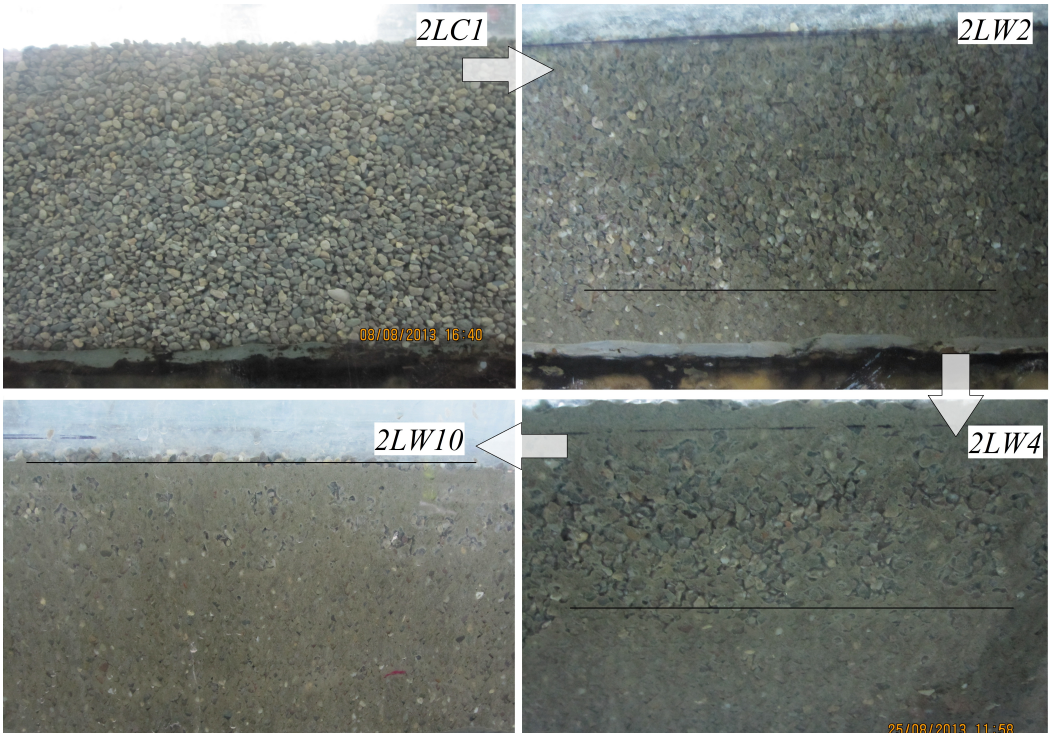

Figure 5.2: Gradual piling of sediment in the series 2L

pores. Once the pores at bottom level got completely filled with sediment, it moved upward. With increasing concentration of fine sediment in the flow in successive runs, the deposition of fines in pores gradually piled up filling the pore spaces completely. It was observed that fine sediment deposited per unit depth was more at the bottom of the bed and decreased as one moves up. However, this difference is marginal. Figure 5.2 shows the gradual piling of fine sediment in the successive sediment laden runs of series 2L.

After the completion of sediment laden run, entrainment runs were carried out. The entrainment runs were conducted by increasing clear water discharge in successive runs. The first run was at very low discharge in which there was hardly any bed material movement. In that run, it was observed that the clear water just washed the top surface of gravel. The flow was not able to extract the fines deposited in the gravel interstices. At successive higher discharges, the flow extracted the fines from deeper and deeper bed. With increasing discharge, the bed load transport also increased. It was observed with all entrainment runs that flows are only able to extract the deposited fines from top few centimeters under normal hydraulic condition. Sediments that have gone deeper are almost impossible to get extracted. Figure 5.3 shows the gradual entrainment of fine sediment due to the successive entrainment runs of series 2L.

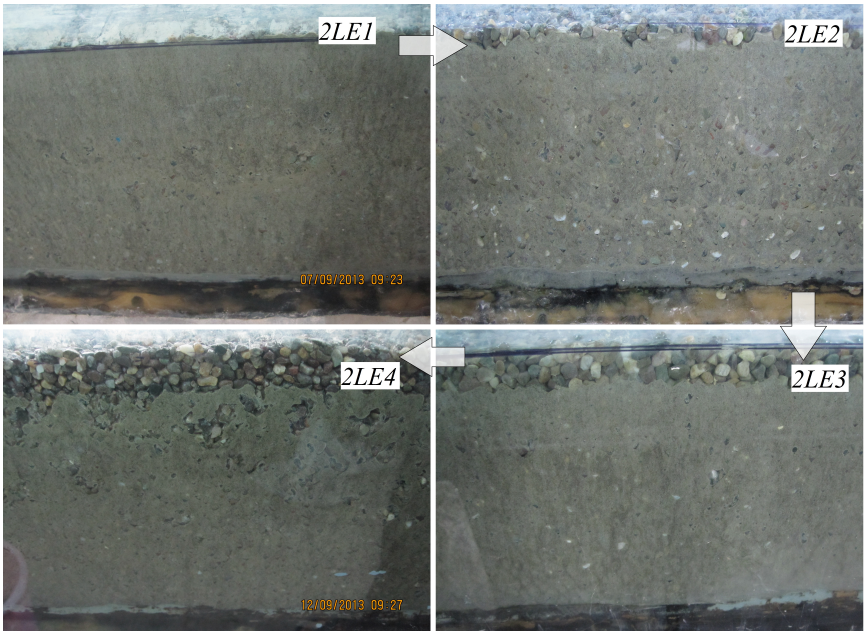

Figure 5.3: Gradual entrainment of sediment in the series 2L

5.4.2 Bed composed of 2.7 mm gravel

Similar to experimental runs with 5.2 mm gravel, the bed surface before and after the runs remained practically leveled and unchanged. The deposition and entrainment of fine sediment within and from the pores of the channel bed composed of 2.7 mm gravel were same as that in the case of bed composed of 5.2 mm. During the sediment laden runs, the fine sediments infiltrated down to the bottom of the gravel bed. The deposition gradually started in the bottom up direction. It was observed that fine sediment deposited per unit depth was more at the bottom of the bed and decreased as one moves up. However, this difference is marginal. Starting from top left corner (clock wise direction), Figure 5.4 shows the gradual piling of fine sediment in the successive sediment laden runs of series 2M. One series of run with 2.7 mm gravel was conducted with 20 cm bed thickness to check whether fines can infiltrate 20 cm depth or not. It was found that fines infiltrated the entire depth of 20 cm.

Once the pores of the bed composed of 2.7 mm gravels were completely filled with suspended sediment, clear water was allowed to pass through it to study the entrainment process. Each successive entrainment runs was with an increasing clear water discharge. It was observed that the depth of entrainment by the flowing water gradually increased with the increasing discharge. Figure 5.5 (clockwise) shows the gradual entrainment of sediments from the gravel pores deposited during the sediment laden runs of series 2M.

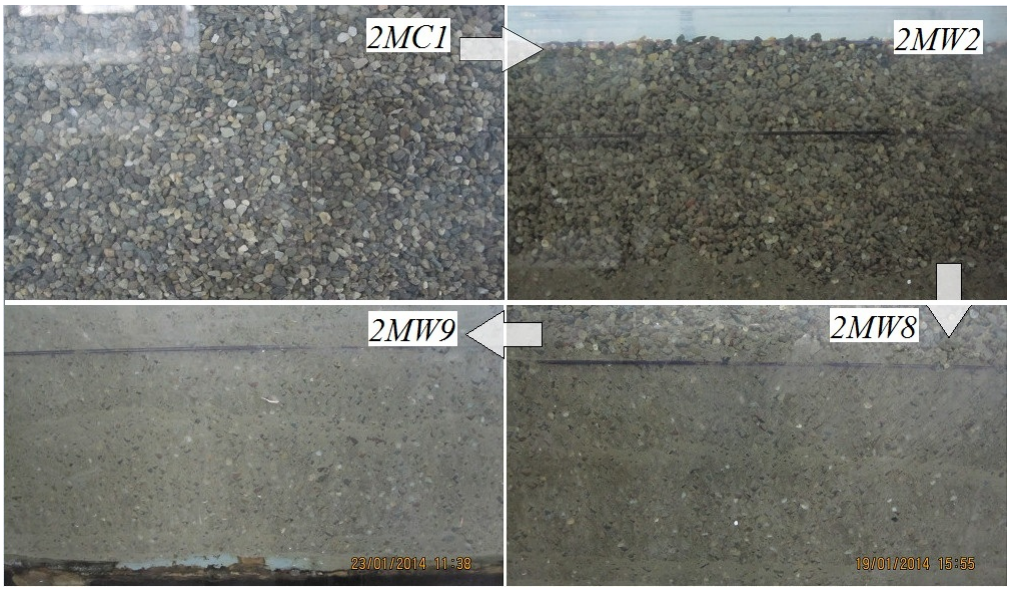

Figure 5.4: Gradual piling of sediment in the series 2M

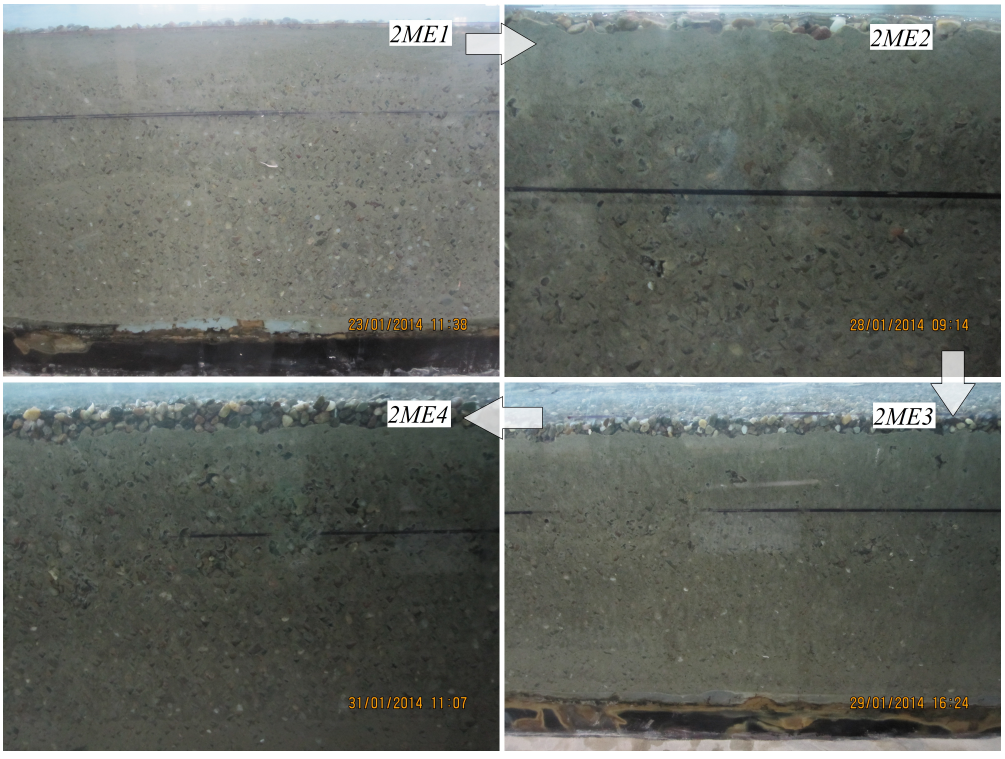

Figure 5.5: Gradual entrainment of sediment in the series 2M

5.4.3 Bed composed of 1.9 mm gravel

The sediment deposition in the bed composed of 1.9 mm gravel was different from that observed in 5.2 mm and 2.7 mm gravel beds. The fine sediments were unable to infiltrate down to the bottom of the channel and instead trapped in the midway of the gravel depth. Diplas and Parker (1992) mode of infiltration and deposition of fines seemed to be followed in this gravel bed. Though some traces of fines infiltration into gravel bed was observed down to 10 cm but the majority of sediments were trapped in the top 6 cm thickness of bed. According to Diplas and Parker (1992) it is hypothesized that, in first phase fine sediment infiltrates into the gravel bed without any obstruction and this phase continues till second phase starts in which deposited fines bridge the gap among bed particles thus creating a seal that restricts deeper infiltration of fines. Figure 5.6 shows the gradual infiltration of fine sediments into the bed.

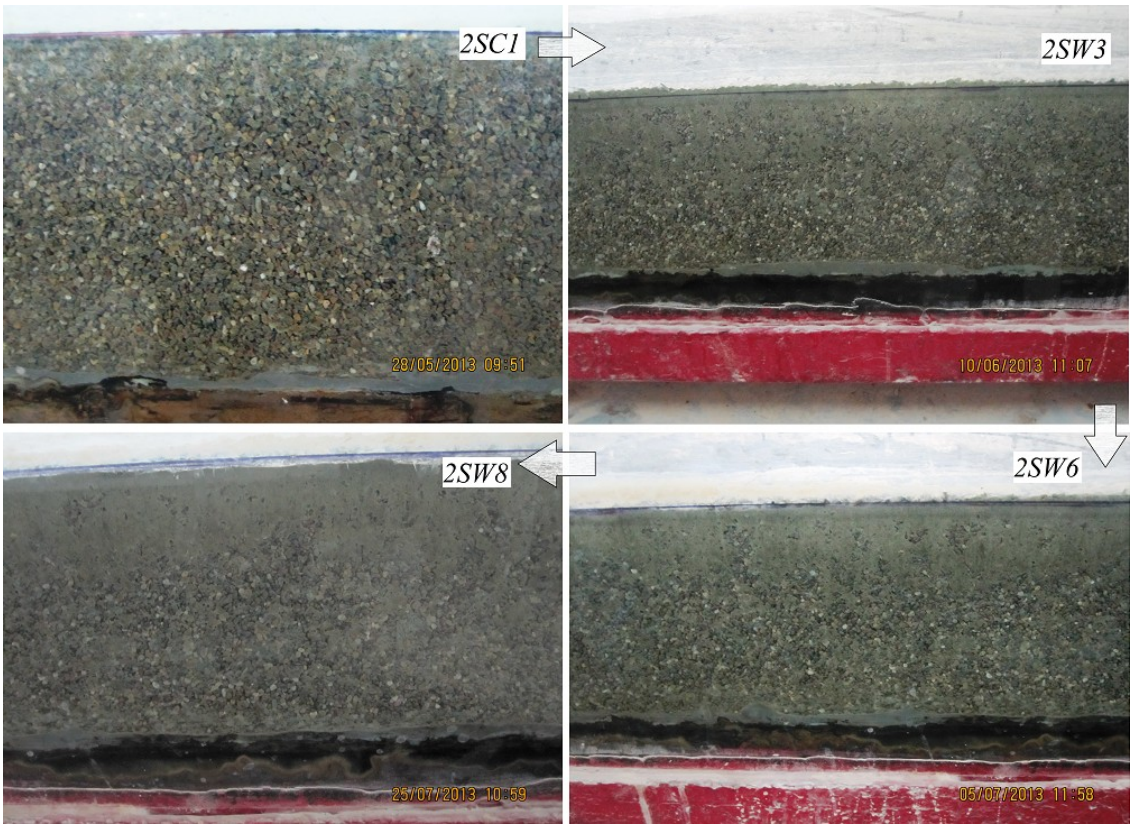

Figure 5.6: Gradual piling of sediment in the series 2S

However in this case also, it was observed that fine sediment entrainment process was similar to that observed with 5.2 mm and 2.7 mm gravel beds. With an increasing clear water discharge, the depth of entrainment increased.

5.5 Analysis of Deposited Fine Sediment in Gravel Bed

As explained in Chapter 3, bed material samples were taken from three locations along the flume to study the amount of fine sediments infiltration at various depths of each three locations. The data collected regarding the proportion of fine sediments present at various sections of channel bed were analysed to evaluate its longitudinal and vertical variation in gravel bed, average proportion of fine sediments in bed layer (AVE) and standard Deviation (STDEV) of proportions of fine sediment in various layers. The above mentioned parameters were computed next for the respective samples separately and these are reported in Appendix B. The average of the samples at representative locations is adopted as the parameter value for the deposition of fine sediments in the bed layer. The detailed analysis is discussed in the following sections.

5.5.1 Longitudinal variation of deposited fines into the bed

After each run, the bed samples were taken from entire depth of bed material making slices of 20 cm x 40 cm x 2 cm from three locations along the flume. The percentages of fine sediment found in each layer of a single section were added up. Figure 5.7 shows run wise longitudinal variation of proportion of fine sediment present in the bed layer for sediment laden runs of series 2M. Figure 5.7 shows the decreasing trend of infiltrated fine sediment in bed along the flow direction. This type of infiltration pattern was observed in all sediment laden experimental runs of all series. Longitudinal variation of fines in bed tells that flow started depositing the fine sediment from the start of porous bed. As the flow moved downstream, it kept on losing its fine sediment content and as a result when it reached at the end of porous bed it had relatively low fine sediment content and hence the deposition in the bed was lesser than the upstream. Though there was gradual decrease in fines availability in bed along the flow direction, the variation was not very significant because the length of porous bed was not long.

5.5.2 Vertical variation of proportion of fines at single location

As mentioned in previous sections, bed samples were taken from entire depth at each of the three sections. Figures 5.8 to 5.10 shows the variation of fine sediment proportion at a various depths of particular location with increasing concentration for series 1L, 1M and 2S respectively. It

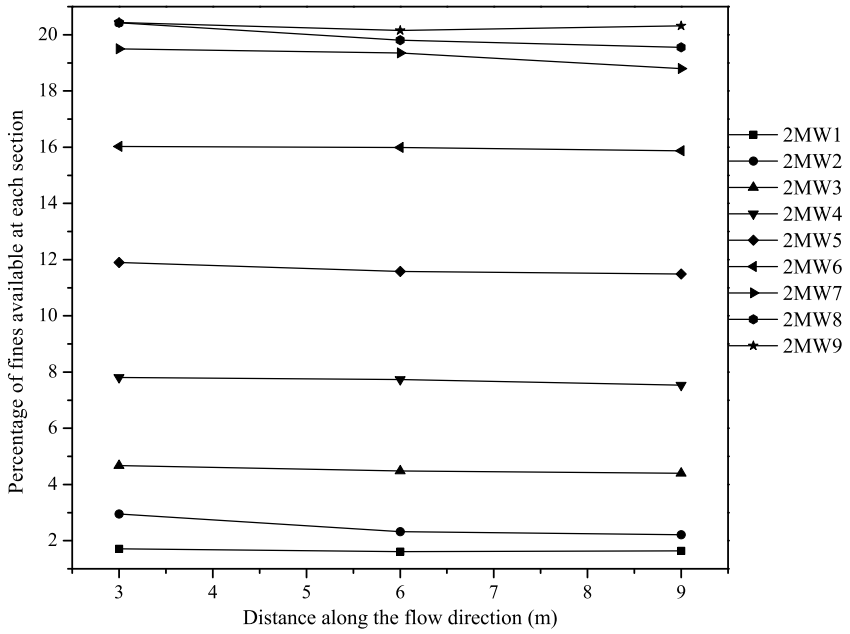

Figure 5.7: Spatial variation of fines infiltrated during sediment laden runs of series 2M

shows that in case of runs of series 1L (5.2 mm gravel) and 1M (2.7 mm gravel), fine sediment accumulation started from bottom of the bed. It also shows that maximum amount of sediment accumulated at the bottom. However, in case of 1S (1.9 mm gravel), the observation was little different as seen in Figure 5.10 . Figure 5.10 shows that no fines infiltrated down to the bottom of the gravel bed. Maximum amount of fines deposited on the top layer of the bed. The possible reason for this difference in the case of 5.2 mm, 2.7 mm and 1.9 mm gravels can be attributed to the difference between size ratios of gravel and fine sediments.

5.5.3 Average

Proportions of fine sediment found in various layers at a single section were arithmetically averaged. A plot of average value of fines infiltrated at various sections (at 3m and 9m sections) along the flow direction with equilibrium concentration is shown in Figure 5.11. This figure and other such figures clearly illustrate that the average value increases with the increasing concentration in flow. This observation is supported by findings of Einstein and Chien (1955), Diplas (1994), Khullar (2002) and Samaiya (2009). Data in Appendix B is evident that maximum average value was 23.53% among all the runs of all series. It is to be noted that this maximum average value didn't exceed the theoretical limit of 27.43% obtained from equation (5.8) .

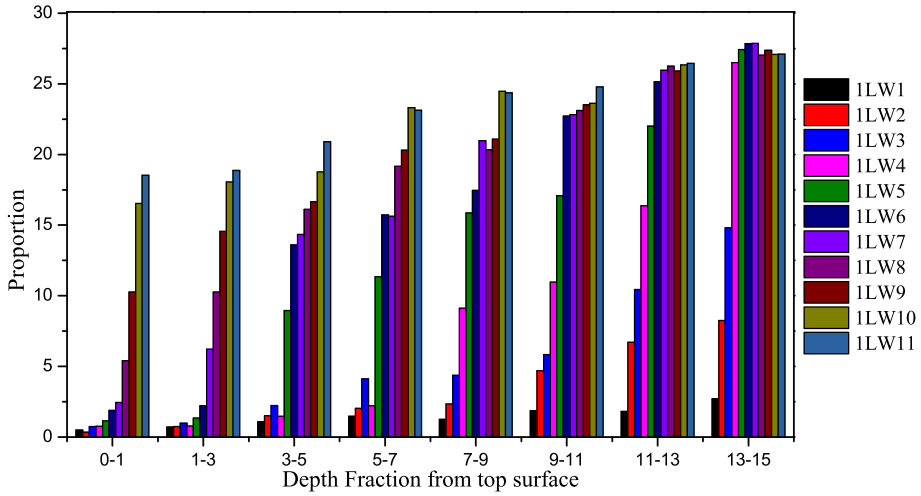

(a) 3m section

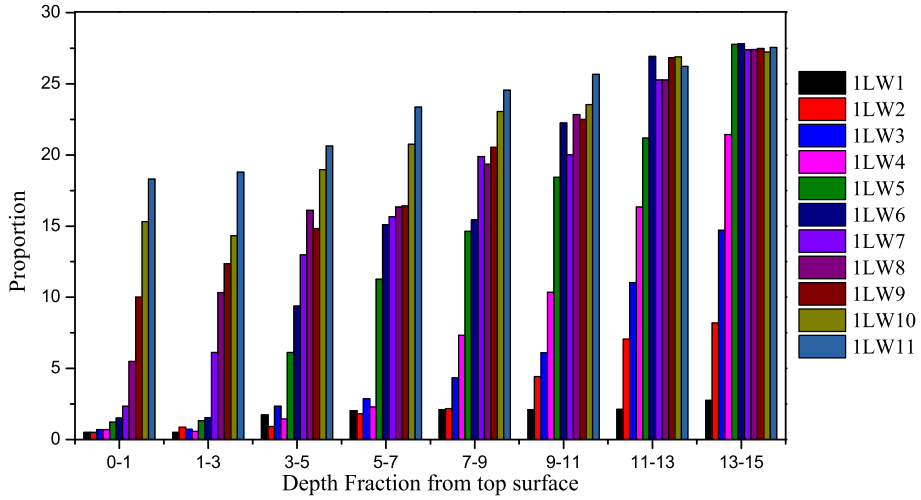

(b) 6m section

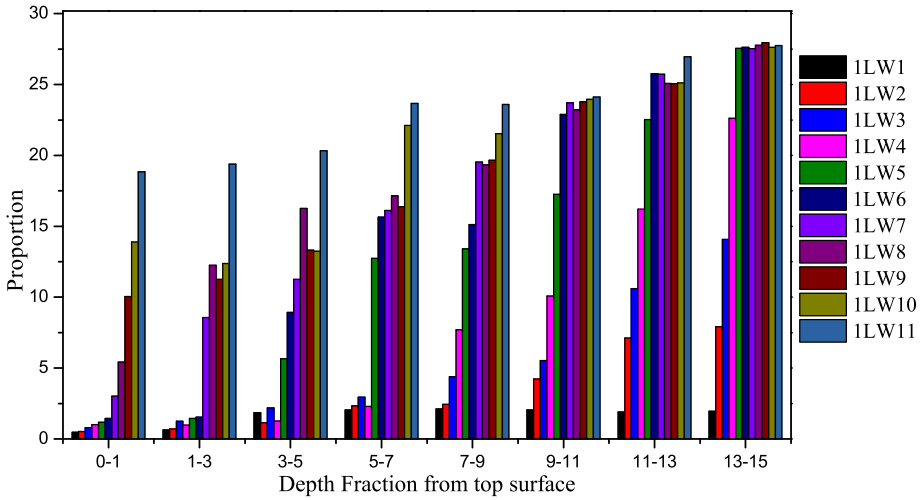

(c) 9m section

Figure 5.8: Deposition of silt in various layers of gravel of series runs 1L

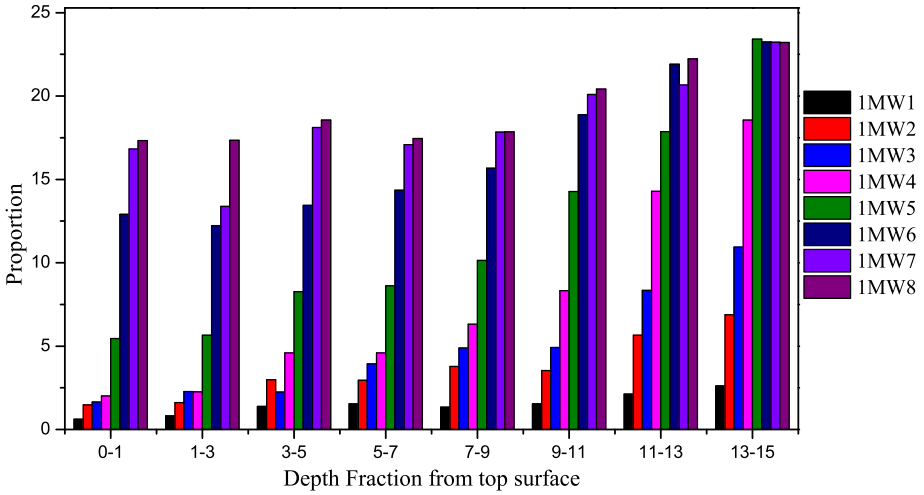

(a) 3m section

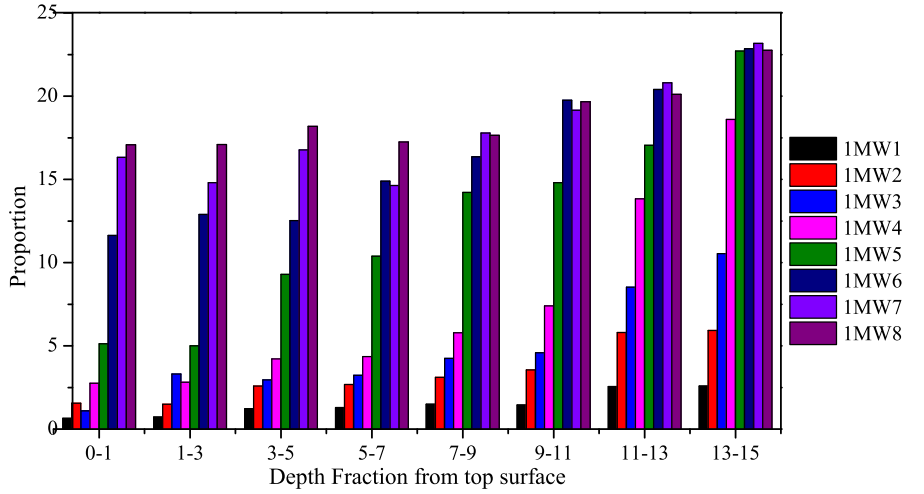

(b) 6m section

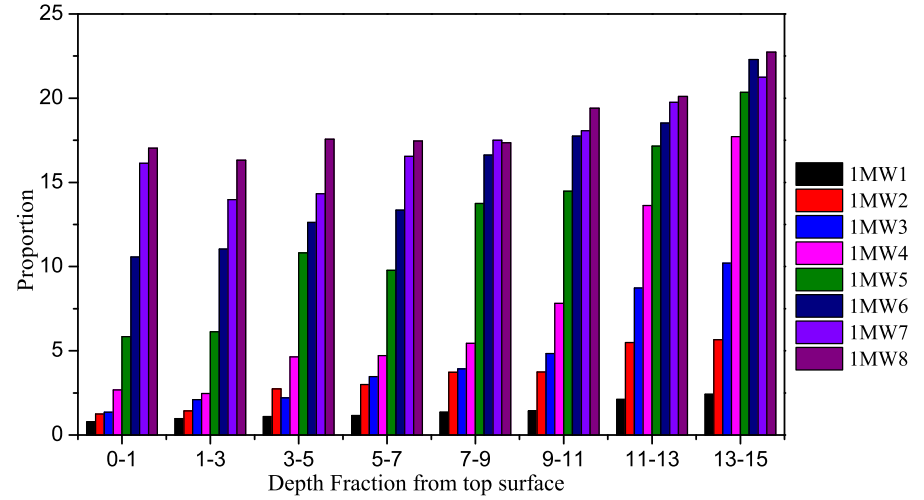

(c) 9m section

Figure 5.9: Deposition of silt in various layers of gravel of series runs 1M

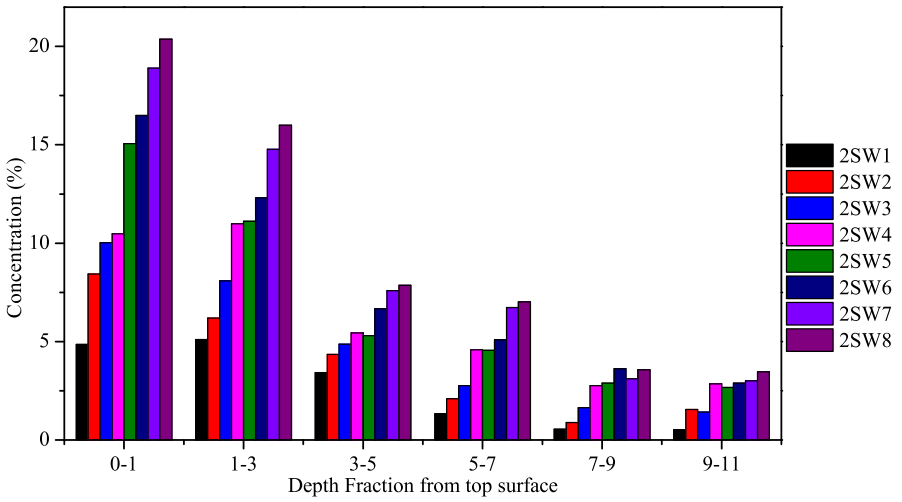

(a) 3m section

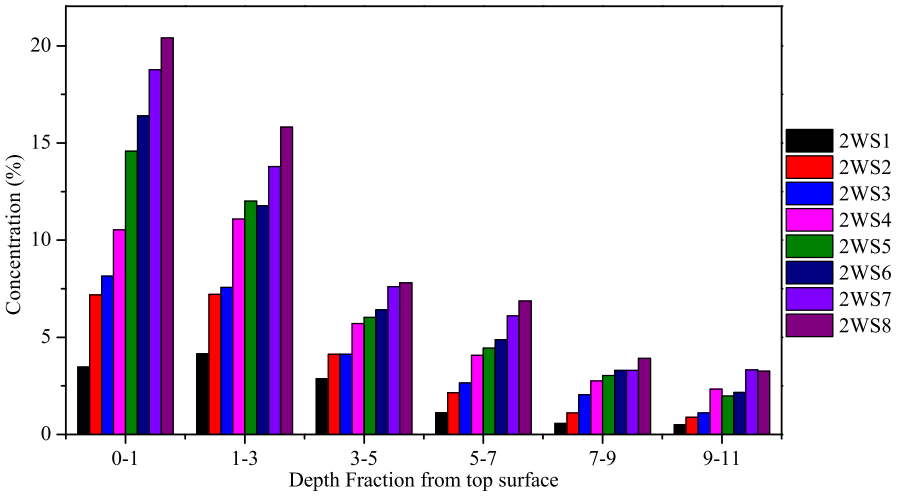

(b) 6m section

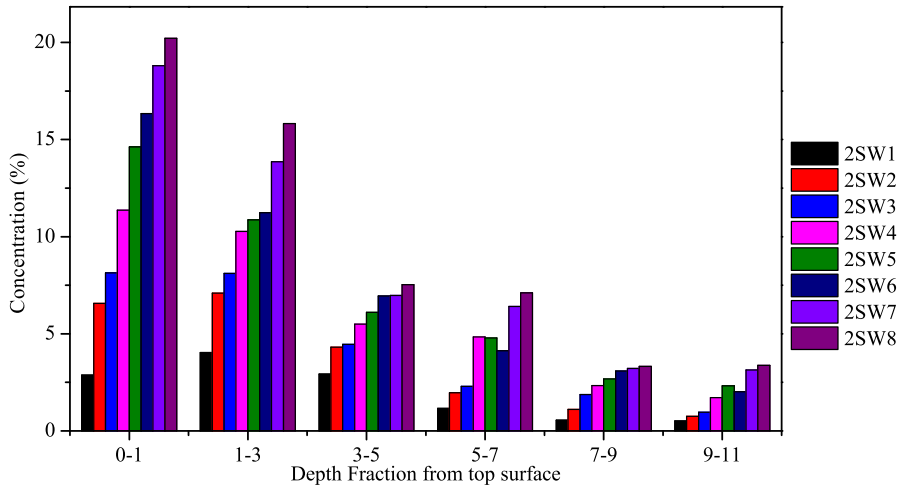

(c) 9m section

Figure 5.10: Deposition of silt in various layers of gravel of series runs 2S

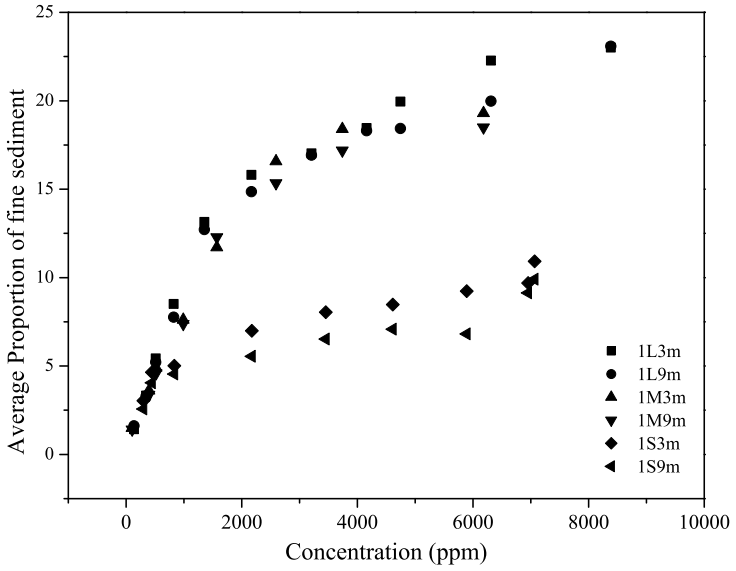

Figure 5.11: Proportion of fines at 3 m and 9 m sections of bed

5.5.4 Standard deviation

Standard deviation is a measure of deviation of average value of individual run compared to the series average. Standard deviations of proportion of fine sediment in different layers were computed for each run using the following formula.

$$STDEV = \sqrt{\sum_{i=1}^{N} \frac{(x_i - AVE)^2}{N-1}} \tag{5.1}$$

Where x_i is the proportion of fine sediment in individual run $(i^{th}run)$, AVE is the average value of proportion of sediment at a section for single series and N is the total number of samples.

Figure 5.12 shows the variation of standard deviation of proportion of fine sediment in the bed layer (along the flow direction) with the increasing sediment concentration in successive runs. Quantitatively, the total amount of fines deposited on the upstream location was more than that deposited on the downstream locations. That is after every individual run or at the end of the series, the total amount of silt deposited in the bed layer gradually decreased towards downstream end of flume. This phenomenon was quite clear but their deviation from the average value was not following any specific trend as evident from the Figure 5.12 . But towards the saturation (bed getting completely filled with silt), the standard deviation dramatically fell indicating that there were not much variation in the fines proportion in different layers.

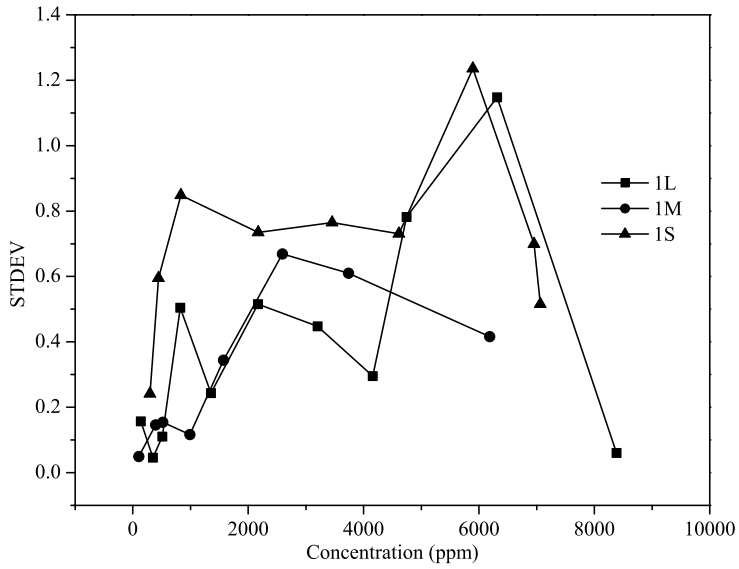

Figure 5.12: STDEV of fines proportion in bed layer with concentration of wash load in the flow

5.6 Modeling of Fines Deposition in Channel Bed Pores

During heavy rainfall, a river flow carries huge amount of suspended sediment. Some of them infiltrate the coarse bed and get deposited into the pore spaces. During subsequent low flow period with relatively clear water, the fines deposited during high flow get entrained. These fine sediments are actually foreign migrants and hence are not found in bed material sample after the recession of flood.

The depth of infiltration of the fines into the gravel bed depends on the size ratio of gravel to fines. More the size ratio, deeper will be the infiltration. This has been observed in the experiments conducted in this study. If the sediment concentration in the flow is high enough, fines keep on infiltrating until the pore spaces get completely filled with fines. In order to compute the porosity of the bed layer, it is assumed that fine sediments get deposited only on the top layer of bed, herein called as active bed layer. It has also been assumed that there are no aggradation of fine sediment on the bed surface.

5.6.1 Active bed layer

Continuous exchange of bed particles and suspended particles was evident from the visual observation of the experiments. The exchange is only limited to certain thickness of bed layer.

This fractional thickness of the whole gravel depth which actively participates in sediment deposition and entrainment process is called active bed layer. Kumar (1988), Rahuel et al. (1989) related the active bed layer thickness with flow depth whereas Borah et al. (1982), Parker (1990) and Correia (1992) related with gravel size.

Kumar (1988) active bed layer function is given by

$$\Delta z = 0.3h \tag{5.2}$$

Where Δz is the thickness of active bed layer and h is the flow depth. Niekerk et al. (1992) related active bed layer to sediment size and shear stress as;

$$\Delta z = 2d_{50}\frac{\tau_0}{\tau_{0c}} \tag{5.3}$$

Where d_{50} is the particle median size (particle size for which 50% sediment is finer), τ_0 is total stress and τ_{0c} is the critical shear stress. A new approach has been developed by Khullar (2002) in order to include both (flow depth and sediment size) effect on the demarcation of active bed layer thickness and is given as;

$$\Delta z = 0.3h\left(1 - \frac{\tau_{0c}}{\tau_0}\right) + 2d_{50} \tag{5.4}$$

In the above equation, when $\frac{\tau_{0c}}{\tau_0} \simeq 1$, Δz becomes a function of particle size only i.e. the case of flat bed where average and critical shear stresses are nearly same but when $\frac{\tau_{0c}}{\tau_0} \ll 1$, the active bed layer thickness becomes function of flow depth and shear stress also. This situation resembles the dune bed.

5.6.2 Theoretical limit of fine sediment proportion in coarse bed pores

When flow carrying suspended sediment pass through the coarse bed (here gravel bed), a part of suspended sediment may infiltrate and deposit into the pores of gravel bed. But the process, depth and quantity of infiltration depends on flow, fluid, bed material characteristics and sediment concentration. The proportion of sediment in the pores increases with an increase in concentration of suspended sediment. In order to obtain the maximum quantity of sediment a coarse bed can accommodate, the knowledge of porosities of original bed and the suspended sediment are required. Let P_G be the porosity of gravel bed and P_S be the porosity of suspended sediment. Let V be the bulk volume (solid volume +void volume) and V_{SG} be the volume of

the solid gravels only. Porosity is defined as the ratio of volume of voids to the total volume. Hence

$$p_G = \frac{V - V_{SG}}{V} = 1 - \frac{V_{SG}}{V}$$

$$V_{SG} = V(1 - P_G) \tag{5.5}$$

Where volume of void is $V.P_G$. That is maximum volume of suspended sediment that can be accommodated in gravel bed of porosity P_G is $V.P_G$. Let the volume of solids of suspended sediment be V_{SS}.

$$V_{SS} = V.P_G - P_S.V.P_G = V.P_G(1 - P_S) \tag{5.6}$$

Where $P_S.V.P_G$ is the volume of voids inside the total volume of suspended sediment. Equation (5.6) is the theoretical limit of maxim solids of suspended sediment that can be accommodated in the gravel pores. Let the combined volume of solids only be V_{SC}.

$$V_{SC} = V_{SG} + V_{SS}$$

$$V_{SC} = V(1 - P_G) + V.P_G(1 - P_S) \tag{5.7}$$

Maximum possible proportion (P_{max}) by weight of suspended sediment in the composite bed is given by

$$P_{max} = \frac{\gamma_s V_{SS}}{\gamma_s V_{SC}}$$

$$P_{max} = \frac{V.P_G(1 - P_S)}{V(1 - P_G) + V.P_G(1 - P_S)}$$

$$P_{max} = \frac{P_G(1 - P_S)}{(1 - P_G) + P_G(1 - P_S)} \tag{5.8}$$

For the case of materials used in present study, the porosity of the flume bed made of 5.2 mm gravel was 0.31 and the porosity of the suspended sediment was 0.331. Substituting these values in equation (5.8) , the maximum proportion of fine sediment that can deposit in the pore of gravel bed is 27.43% of the volume of composite bed. For alluvial channels, the limiting condition of suspended sediment transport may be said to have been reached when the pores get completely saturated with fine sediments. In the following sections, a numerical model is developed for obtaining the porosity of gravel bed when sediment laden flow takes place. MacCormack (1969) based explicit finite difference scheme is used to solve the governing equations numerically.

5.6.3 Governing equations

The flow in an alluvial river can be well defined by the sediment continuity equation, flow continuity equation and flow dynamics/ momentum equation.

a) Sediment continuity equation

The following assumptions are made for drawing the sediment continuity equation.

- The voids in initial bed of the channel is free from sediments. The first clear water run through the bed sweeps away the fines particle if any existing in the pores and increases the bed porosity.
- Only the active bed layer participates in the process of sediment infiltration, deposition and entrainment.
- Bed material transport has no effect on the process of infiltration.
- Prior to attaining the limiting condition (bed being fully saturated with fines), it can attain equilibrium condition at different concentrations of fine sediment.
- Equilibrium condition is said to have attained when the rate of deposition becomes equal to the rate of entrainment.
- Once limiting concentration is achieved, the aggradations may take place if flow keeps carrying fines at higher concentrations.
- The bed acts like a sink for fine sediment.

Let's consider a control volume bounded by section $1-1$ and $2-2$ in a river reach as shown in Figure 5.13 . The length of the control volume is Δx. Let Q_S be the suspended sediment volume per unit time entering the control volume through section $1-1$. Then the volume per unit time of suspended sediment coming out of section $2-2$ is $Q_S + \frac{\partial Q_S}{\partial x}\Delta x$. Q_S is the function of both distance (x) and time (t) . For small duration of time (Δt),

Mass of sediment entering the control volume = $\rho_s \times Q_S \times \Delta t$

Mass of sediment leaving the control volume during the same time = $\rho_s\left(Q_S + \frac{\partial Q_S}{\partial x}\Delta x\right)\Delta t$

$$\text{Change in mass within control volume} = -\rho_s \frac{\partial Q_S}{\partial x}\Delta x \Delta t \tag{5.9}$$

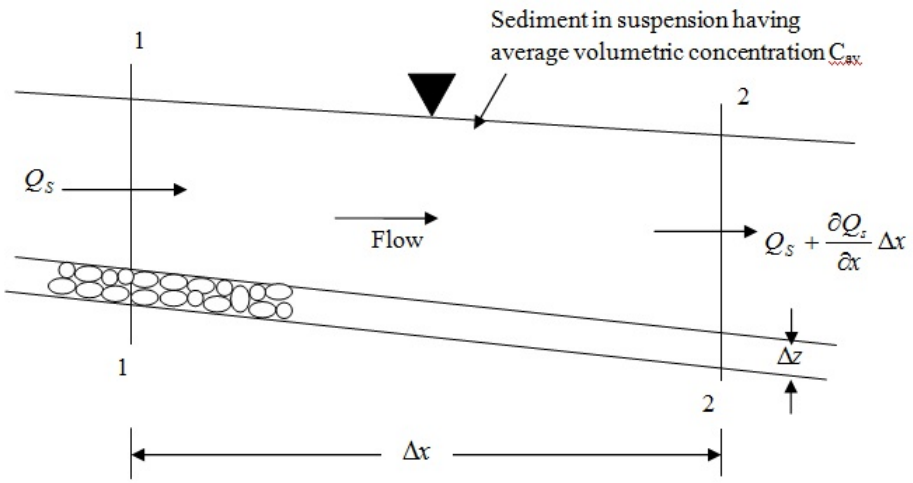

Figure 5.13: Control volume used for derivation of sediment continuity equation

This change in storage is reflected in the bed and the flow by decreasing the bed porosity and decreasing the average sediment concentration in flow. Let's assume that fines deposition occurs uniformly over the whole area of active bed layer. Initial mass of sediment (solids only) in the active bed layer of thickness Δz and initial porosity P_{G1} is given by

$$\rho_s(\Delta z b \Delta x - \Delta z b \Delta x P_{G1}) = \rho_s \Delta z b \Delta x (1 - P_{G1}) \tag{5.10}$$

After the infiltration and deposition, porosity of bed changes (decreases). Let the new porosity be P_{G2} and hence new mass of sediment (solids only) in the thickness Δz is

$$\rho_s \Delta z b \Delta x (1 - P_{G2}) \tag{5.11}$$

Then change in mass before and after infiltration is

$$-\rho_s \Delta z b \Delta x \Delta P_G \tag{5.12}$$

Where $-\Delta P_G = P_{G2} - P_{G1}$ is the change in porosity. The negative sign is due to the decrease in porosity after time Δt . With time as the infiltration continues, the porosity also changes, hence let $\Delta P_G = \frac{\partial P_G}{\partial t}\Delta t$. Equation (5.12) becomes

$$-\rho_s \Delta z b \Delta x \frac{\partial P_G}{\partial t}\Delta t \tag{5.13}$$

Let the cross sectional area of control volume is A and average concentration of suspended sediment is C_{AV}. As the flow releases sediment, the average concentration also changes with time. The change can be expressed as

$$\rho_s \frac{\partial A.C_{AV}}{\partial t}\Delta x \Delta t \tag{5.14}$$

Total change in the mass of sediment stored in control volume is

$$\rho_s \Delta x \Delta t \left(-\Delta z b \frac{\partial P_G}{\partial t} + \frac{\partial A.C_{AV}}{\partial t} \right) \tag{5.15}$$

Equating equations (5.9) and (5.15) . C_{AV}can be substituted by Q_S/Q

$$\rho_s \Delta x \Delta t \left(-\Delta z b \frac{\partial P_G}{\partial t} + \frac{1}{U} \frac{\partial Q_S}{\partial t} \right)$$

$$\frac{\partial P_G}{\partial t} + \frac{1}{-U \Delta z b} \frac{\partial Q_S}{\partial t} + \frac{1}{-\Delta z b} \frac{\partial Q_S}{\partial x} = 0$$

$$\frac{\partial P_G}{\partial t} + a_1 \frac{\partial Q_S}{\partial t} + a_2 \frac{\partial Q_S}{\partial x} = 0 \tag{5.16}$$

Where $a_1 = \frac{1}{-U \Delta z b}$ and $a_2 = \frac{1}{-\Delta z b}$. Equation (5.16) is the sediment continuity equation for transport of suspended sediment through coarse bed alluvial rivers.

b) Flow continuity equation

The flow continuity equation is given as

$$\frac{\partial h}{\partial t} + U \frac{\partial h}{\partial x} + h \frac{\partial U}{\partial x} = 0 \tag{5.17}$$

c) Flow momentum equation

The flow momentum equation is given as

$$\frac{\partial q}{\partial t} + U \frac{\partial q}{\partial x} + gh \frac{\partial h}{\partial x} + gh \frac{\partial z}{\partial x} + ghS_f = 0 \tag{5.18}$$

Where q is discharge per unit width of channel and S_f is the friction slope. Equations (5.16) to (5.18) are used to study the transport of suspended sediment under various conditions. Since the experiments were conducted under steady and uniform flow condition, the same conditions are assumed while solving the above set of equations. Since flow considered here is steady and uniform, the flow parameters used in equations (5.17) and (5.18) are easily known. Equations (5.16) to (5.18) forms a set of non linear hyperbolic equation. The only difficulty in above set of equations is the solution of equation (5.16) , the analytical solution of which is not possible. Therefore, a numerical solution of equation (5.16) is proposed. The aim of this mathematical modeling is to study the deposition of fines in the pores and hence resulting porosity is considered to be the unknown variable in equation (5.16). The values of Q_S present in equation (5.16) should be obtained from any appropriate suspended sediment transport law (eg. Khullar 2002). Similarly friction slope can be obtained from any resistance equation.

5.6.4 Numerical scheme

Finite difference numerical scheme of MacCormack (1969) based on two levels of predictor and corrector steps is utilized for the solution of equation (5.16). It is an explicit scheme and simple to use. MacCormack (1969) scheme is second order accurate in space and time. MacCormack (1969) scheme have also been used by Bhallamudi and Chaudhry (1991, 1992), Mohapatra and Bhallamudi (1994) among many others. Forward finite difference is used for approximating the spatial partial differential term during predictor step and backward finite difference during corrector step or vice versa. The variables estimated during the predicted step are used in corrector step. The approximation of the derivatives of function are done with reference to the numerical grid as shown in Figure 5.14 .

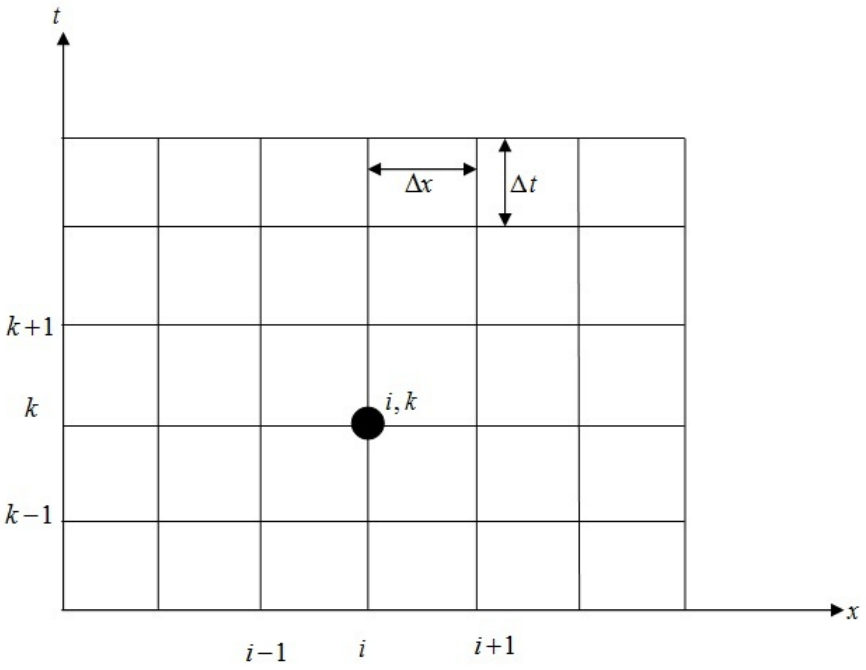

Figure 5.14: Finite Difference grid

a) Predictor step

Using forward difference scheme to equation (5.16) , the predicted values of p and Q_S at next time step are attained as

$$\frac{1}{\Delta t}\left({P_{Gi}}^* - {P_{Gi}}^K\right) + \frac{a_1}{\Delta t}\left({Q_{Si}}^* - {Q_{Si}}^K\right) + \frac{a_2}{\Delta x}\left({Q_{Si+1}}^* - {Q_{Si}}^K\right)$$

$${P_{Gi}}^* = {P_{Gi}}^K + a_1\left({Q_{Si}}^K - {Q_{Si}}^*\right) - a_2\frac{\Delta t}{\Delta x}\left({Q_{Si+1}}^K - {Q_{Si}}^*\right) \tag{5.19}$$

In equation (5.19) , terms with $*$ denote predicted values. ${P_{Gi}}^*$ and ${Q_{S_i}}^*$ are two unknown predictors in equation (5.19) . Both are dependent on each other; hence its direct solution is not possible. It is solved iteratively. As a first approximation, consider ${Q_{S_i}}^* - {Q_{S_i}}^K$ and compute ${P_{Gi}}^*$. Using this value of ${P_{Gi}}^*$, the percentage of fine material in active bed layer is computed as follows. The change in porosity of active bed layer is

$$\Delta P_G = P_{G1} - {P_{Gi}}^* \tag{5.20}$$

Where P_{G1} is initial porosity of bed. The weight of fines, W_f , in the bed for the change in porosity by ΔP_G is given by

$$W_f = \Delta P_G \Delta z b \Delta x \gamma_s \tag{5.21}$$

The percentage weight of fines in the active bed layer is given by

$$W_f(\%) = \frac{W_f}{W_f + W_0} \tag{5.22}$$

Where W_0 is the initial dry weight of active bed layer. ${Q_{S_i}}^k$ is computed next by using suspended load transport law eg. Khullar (2002). The above iteration is stopped when the difference between computed and utilized value of ${Q_{S_i}}^*$ in equation (5.19) is not significant.

b) Corrector step

The corrected values of variables P_G and Q_S at next time are obtained during this step by following the backward difference scheme and by using the values obtained during predictor step.

$$\frac{1}{\Delta t}({P_{Gi}}^{**} - {P_{Gi}}^*) + \frac{a_1}{\Delta t}({Q_{S_i}}^{**} - {Q_{S_i}}^*) + \frac{a_2}{\Delta x}({Q_{S_i}}^* - {Q_{S_{i-1}}}^*)$$

$${P_{Gi}}^{**} = {P_{Gi}}^* + a_1({Q_{S_i}}^* - {Q_{S_i}}^{**}) - a_2\frac{\Delta t}{\Delta x}({Q_{S_i}}^* - {Q_{S_{i-1}}}^*) \tag{5.23}$$

Variables with $**$ stand for the corrected values at the end of time Δt. In equation (5.23) also, there exists two unknown variables ${P_{Gi}}^{**}$ and ${Q_{S_i}}^{**}$. They are again mutually dependent and hence need to be solved iteratively. The iterative procedure explained above is followed here also.

c) Final values

$${P_{Gi}}^{K+1} = \frac{1}{2}\left({P_{Gi}}^K + {P_{Gi}}^{**}\right) \tag{5.24}$$

$$Q_{Si}{}^{K+1} = \frac{1}{2}\left(Q_{Si}{}^{K} + Q_{Si}{}^{**}\right) \tag{5.25}$$

Following the above procedure, the values of unknown at next time level $k + 1$ can be found at all interior nodes of the grid. But the same values at boundaries are determined by using boundary conditions. Flow properties h and U are known at end nodes as well because the flow is steady and uniform i.e. initial and boundary conditions are known.

5.6.5 Stability of numerical scheme

The MacCormack (1969) scheme must satisfy the Courant - Freidrichs - Lewy (CFL) condition at every grid for its stability. Since the water wave travels at much higher velocity than bed transitions, the condition for stability is given by:

$$C_n = \left(\frac{q}{h} + \sqrt{gh}\right)\frac{\Delta t}{\Delta x} \leq 1 \tag{5.26}$$

Where C_n is the Courant number.

5.6.6 Model application

The model described above is for simulating the process of deposition of fine sediment within the pores of gravel bed. Data collected during the present study are used for the verification of the proposed model output. As motioned earlier that model is used to compute the change in porosity, a flow chart showing the steps of calculation is shown in Figure 5.15 . In order to determine the change in porosity, the required initial and boundary conditions are:

a) Initial Condition

Initial porosity of bed i.e. $P_G(i, 1) = 0.383$ and initial sediment inflow $Q_S(i, 1) = 0.00$ where $i = 1, N$. The last node is $N + 1$.

b) Boundary Condition

The boundary condition is required at the upstream end for model application. The condition was $Q_{S_0}{}^{k+1} = Q_{S_N}{}^{k} + \Delta Q_S$. Here ΔQ_S was the rate of increase of incoming sediment load at upstream node. Since the condition was not so straightforward, it was translated

into a convenient equation so that porosity (P_G) at node 1 can be easily found out. A fictitious node upstream of node 1 was considered and discharge at that node was supposed to be ${Q_{S_0}}^{k+1} = {Q_{S_N}}^{k} + \Delta Q_S$. Using sediment continuity equation and applying the backward difference on spatial term, the following equation was obtained for P_G at node 1.

$$ {p_{G1}}^{k+1} = {p_{G1}}^{k} + a_2 \frac{\Delta t}{\Delta x}\left[\left({Q_{S_N}}^{k} + \Delta Q_S\right) - {Q_{S1}}^{k}\right] \tag{5.27} $$

A computer program was written in FORTRAN 95 to implement the steps in flow chart. Data of runs at different equilibrium conditions were used to test the model. The spatial variation was kept 1 m. The computational time step was selected according to the Courant condition for stability by adopting $C_n = 0.73$. So Δt varies for each individual run.

5.6.7 Comparison of computed and observed equilibrium porosity

The computed values obtained from the model discussed above and the observed values obtained by using the measured percent of suspended material within the active bed layer of the channel at the end of corresponding runs are plotted in Figure 5.16. The figure shows that model though predicts a bit higher value but still it very well simulates the final equilibrium porosity with all computed values falling within ±10% of observed porosity.

5.6.8 Computation of porosity during sediment laden flow

Measurement of porosity (by measuring sediment proportion in bed) during the run was not possible. Hence the comparison was only possible with the value at the end of equilibrium run. Variation of porosity (computed only) with time at a particular section of a particular run is shown in Figure 5.17. It shows that the porosity at a particular section gradually decreased with the time. The figure shows the variation in porosity at two locations. The porosity at all locations are not much varying because they were not much distance apart. Still there exists slight variation with porosity at upstream section being lower than it's downstream. This indicates that slightly higher amount of fine sediment infiltrated at the upstream section. However as the flow progresses towards equilibrium condition, the porosity at both locations become same.

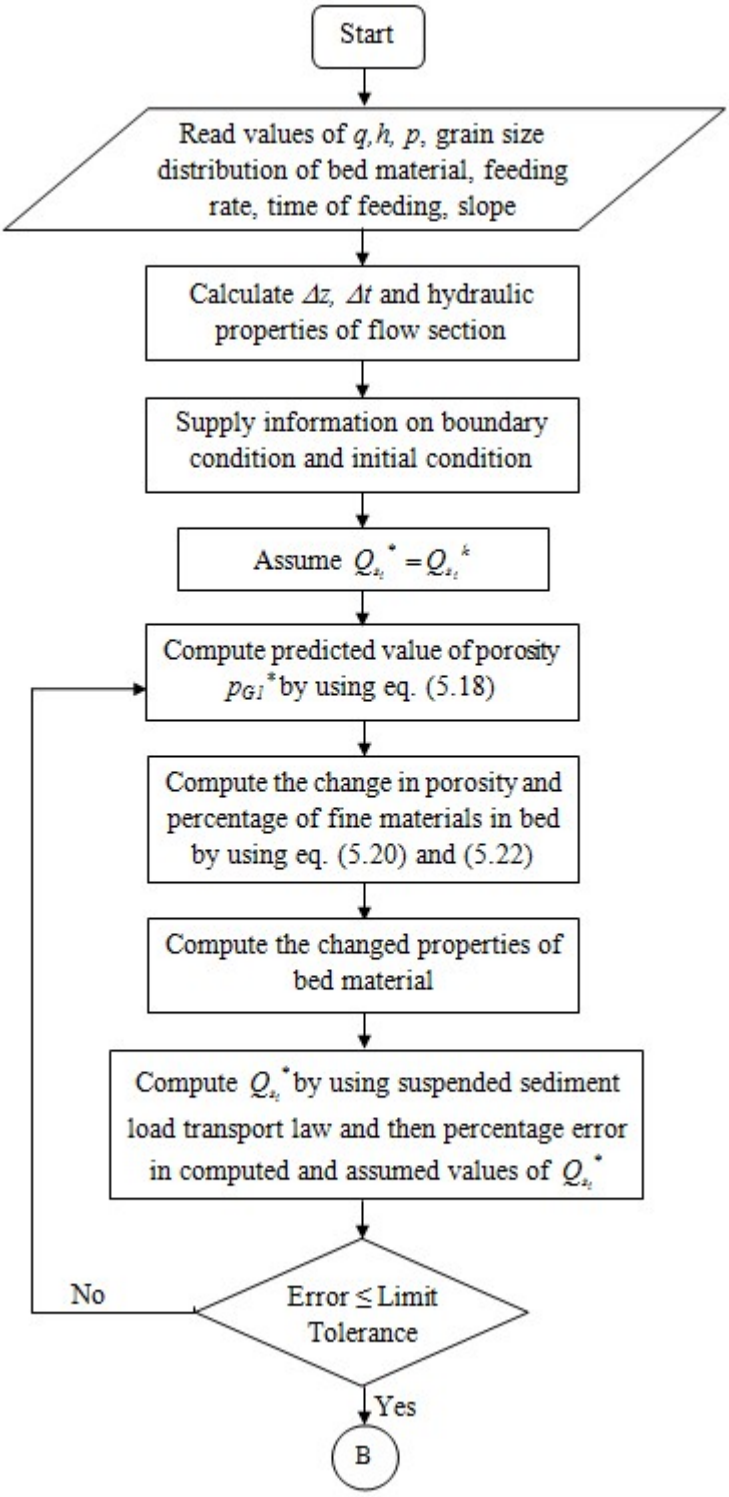
Start
Read values of q, h, p, grain size distribution of bed material, feeding rate, time of feeding, slope
Calculate Δz, Δt and hydraulic properties of flow section
Supply information on boundary condition and initial condition
Assume $Q_{s_i}^{*} = Q_{s_i}^{k}$
Compute predicted value of porosity p_{G1}^{*} by using eq. (5.18)
Compute the change in porosity and percentage of fine materials in bed by using eq. (5.20) and (5.22)
Compute the changed properties of bed material
Compute $Q_{s_i}^{*}$ by using suspended sediment load transport law and then percentage error in computed and assumed values of $Q_{s_i}^{*}$
Error ≤ Limit Tolerance
No
Yes
B

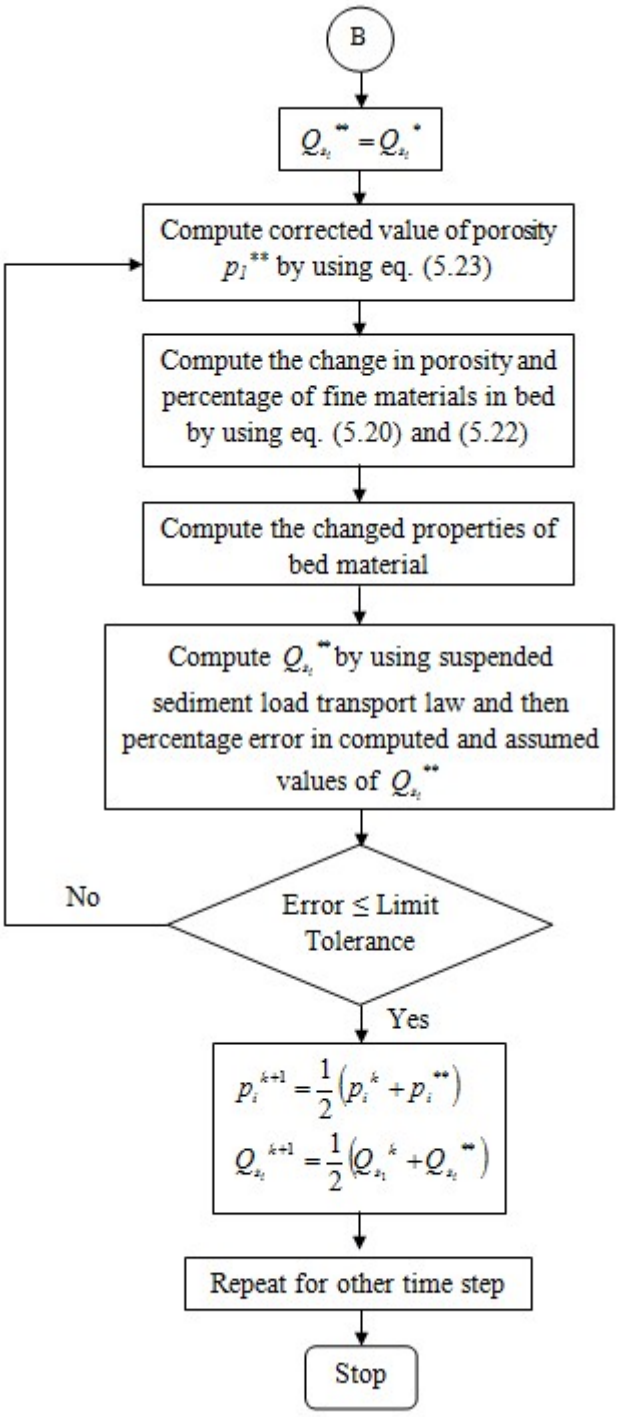

Figure 5.15: Flow chart showing the steps involved in the application of mathematical model

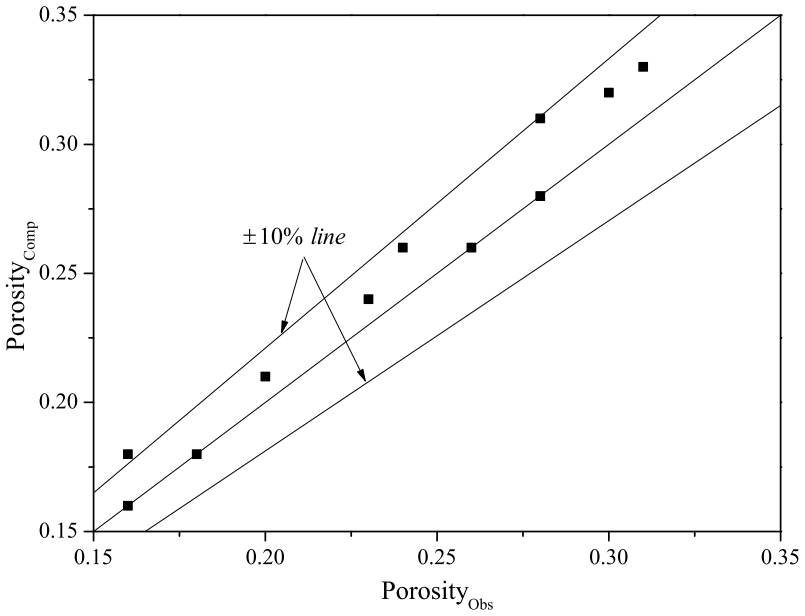

Figure 5.16: Comparison of observed and computed porosities of runs of series 1L

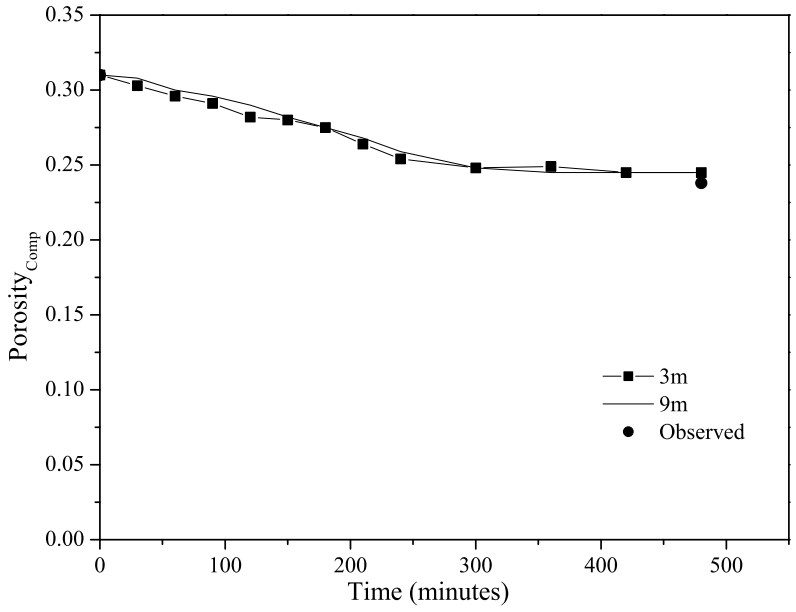

Figure 5.17: Variation of porosity with time at section 3m and 9m of run 1LW1

5.7 Concluding Remarks

This chapter presented the detailed description of visual interpretation of the process of sediment infiltration and deposition and modeling of the fines infiltration. It has been concluded from the observations that sediment infiltration continues till equilibrium condition is reached. The moment when the pores are completely filled, is called the limit deposition condition. Visual observation reported that for larger size ratio of gravel to suspended sediment, the depth of infiltration is more. Relatively more sediment infiltration was observed at the upstream section than downstream at the end of various equilibrium runs. But as the successive flow proceeds towards limiting condition, the amount of fines at all section along bed becomes more or less same.

Mathematical model developed for estimating the porosity proved to be successful. The calculated porosity resembled well with that of observed. Sediment continuity, flow continuity and flow momentum equations were used for the modeling. The differential equation of sediment continuity was solved by two step predictor and corrector based on numerical scheme of MacCormack (1969). Model predicted that as the sediment concentration in flow increases, the porosity decreases. Porosity of the upstream section decreases rapidly than lower sections.

Chapter 6

Bed Load Transport

6.1 General

In nature, bed and bank of a channel are composed of cohesionless or cohesive or composite materials such as gravel, sand, silt, clay or mixture of these. Knowledge of transport of cohesionless and cohesive material or its mixture is very essential (Kothyari and Jain 2010; Kothyari et al. 2014). The present chapter discusses the transport of bed load on gravel bed rivers and the applicability of few of the existing methods of bed load estimation when the flow contains the suspended sediment. Experiments were conducted to measure the bed load at different sediment concentration. A modified equation is also proposed to estimate the bed load.

6.2 Bed Load Transport at Various Sediment Concentration

In all the experiments performed in the present study, bed load transport was observed. With increasing concentration of fines in flow, the bed load transport was observed to increase. Figure 6.1 shows the variation of bed load with suspended sediment concentration for all the clearwater and sediment laden runs. Figure 6.1 shows an increasing trend of bed load transport rate with sediment concentration. However, the increment is not uniform. The probable cause of increase in bed load transport rate with sediment concentration can be attributed to the decrease in the resistance to flow. As discussed in Chapter 4, the Von Karman constant was observed to decrease with increasing concentration. In Figure 6.1 the concentration value of clear water

flow is considered as 1 ppm to facilitate the plotting on log scale.

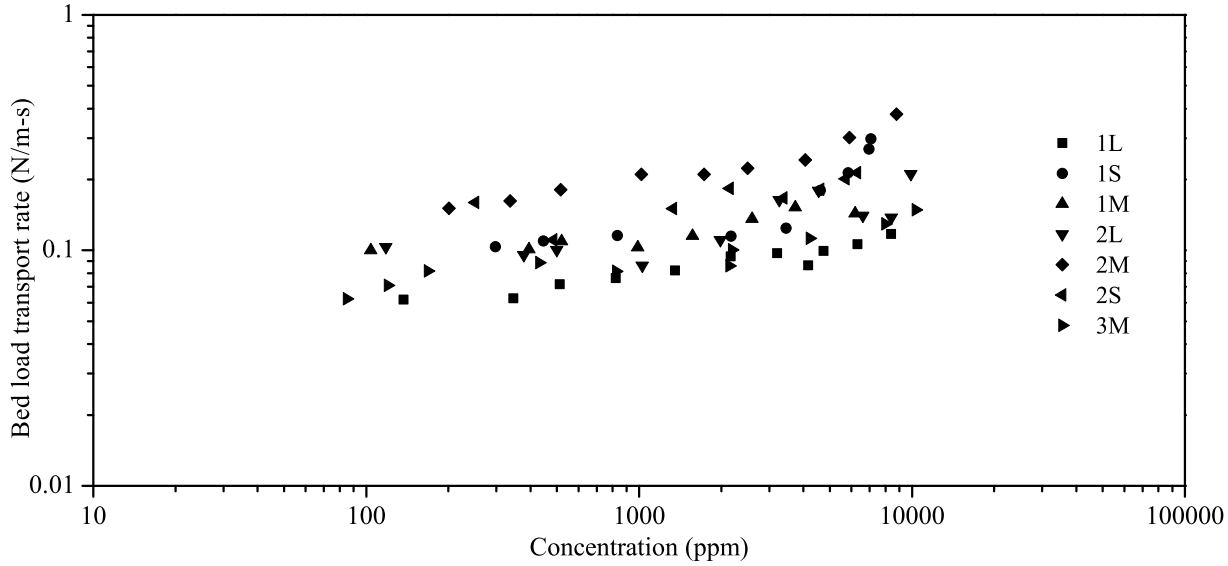

Figure 6.1: Variation of bed load transport rate with suspended load concentration

6.3 Composition of Active Bed Layer

In the bed load transport process, only the upper layer of the bed takes part. Theoretically the top layer which actively takes part in the movement is called active bed layer. As already discussed in Chapter 5, different proportions of fine sediments were present in the pores of the gravel bed under different equilibrium concentrations of suspended load in transport of the flow. The characteristics of the active bed layer after transport of suspended load through it were thus different from its original characteristics. Thus the values of the parameter like (d_a, d_{50}, d_{65}, M) for the active bed layer were different from those for the original bed. These parameters were computed from the experimental data for the active bed layer.

It is also important to mention here that the fine sediment used in the present investigation was very fine compared to the original size of bed material. Also as discussed in Chapter 5, the fine sediment is observed to settle within the pores of the gravel bed. Therefore, the presence of fines in the pores of the gravel bed does not significantly change the exposure of the coarse particles of the parent bed material. Nevertheless, the fine sediments retained in the pores of the bed are sheltered by the coarse bed materials. Hence for all practical and computational purpose, it would not be wrong to consider mixed sediment parameter same as that of parent

bed material. The same conclusion has been reached by Khullar (2002) and Samaiya (2009) after analyzing their bed load transport data. Hence in this study the sediment parameters of the active bed layer are considered same as that of parent bed material.

6.4 Check on Some of the Existing Methods of Bed Load Transport

Numerous bed load transport estimation methods are available in literature. These methods are based on either theoretical approach, empirical approach, or dimensional approach. However, the major constraint in applying these formulations is that most of them are formulated considering relatively clear water. Existing bed load transport formulae may overestimate the transport rate in mountain rivers by two order of magnitude or more (Bathurst 2007). There are very few studies which have taken into account the effect of suspended sediment on the bed load transport (eg. Simons et al. 1963; Colby 1964 etc). Among these few also, only couple of methods considers very fine non cohesive (in the range of silt size) sediment as suspended sediment. Here an attempt has been made to check the obtained bed load data with few of the existing formulae.

As reported by Samaiya (2009), Misri et al. (1984) and Samaga et al. (1986) have tested the Einstein and Chien (1955) and Hayashi et al. (1980) methods. He also reported that Patel and Ranga Raju (1996) checked the applicability of equations proposed by Egiazaroff (1965), Ashida and Michue (1971), Hayashi et al. (1980), Nakagawa and Tsujimoto (1980), Wiberg and Smith (1987) and Bridge and Bennet (1992) and observed that these methods were not accurate. The results of those tests were not satisfactory and hence they proposed their own formulation. Khullar (2002) checked his data against Patel and Ranga Raju (1996), Karim (1998) and Wu et al. (2000). He found that Patel and Ranga Raju (1996) method of estimation of bed load transport rate of uniform and non uniform sediment was found to be satisfactory for his data.

In the present investigation, the equation proposed by Meyer- Peter and Müller (1948), Misri et al. (1984) and Patel and Ranga Raju (1996)were tested for their applicability in predicting bed load transport when the flow contains suspended sediment.

6.4.1 Meyer-Peter and Müller (1948) equation

Meyer-peter and Müller (1948) equation is among one of the most widely used empirical bed load transport equation. Meyer-Peter and Müller (1948) realized that a part of total stress is used in overcoming the resistance due to bed undulation and the remaining is used for bed particle movement hence they divided the total slope (S) into two parts.

$$S = S_b + S_g \tag{6.1}$$

Where, S_b is slope required for overcoming form resistance due to bed undulation and S_g is slope required to overcome grain resistance. The value of S_g was estimated using Manning-Strickler equation, i.e.

$$U = \frac{1}{n_g} R^{2/3} {S_g}^{1/2} \tag{6.2}$$

$$U = \frac{1}{n} R^{2/3} S^{1/2} \tag{6.3}$$

$$n_g = \frac{{d_{90}}^{1/6}}{26.0} \tag{6.4}$$

where d_{90} (in meter) is particle size such that 90% of particles are finer than this size. From equations (6.2) and (6.3)

$$\frac{S_g}{S} = \left(\frac{n_g}{n}\right)^2 \tag{6.5}$$

In the similar way if hydraulic radius (R) is divided into R_b (hydraulic radius required to overcome form resistance due to bed undulation) and R_g (hydraulic radius to overcome grain resistance) then

$$\left(\frac{n_g}{n}\right)^{3/2} = \frac{R_g}{R} \tag{6.6}$$

Substituting S_g in place of S in their 1934 equation and making some manipulations for best fit, Meyer-Peter and Müller (1948) arrived at a non-dimensional equation as

$$\left(\frac{n_g}{n}\right)^{3/2} \frac{\gamma_f R S}{(\gamma_s - \gamma_f) d_a} = 0.047 + 0.25 \left(\frac{\gamma_f}{g}\right)^{1/3} \left(\frac{q_B}{\gamma_s}\right)^{2/3} \frac{1}{(\gamma_s - \gamma_f)^{1/3} d_a} \tag{6.7}$$

where, γ_s and γ_f are respectively sediment and fluid specific weights and q_B is bed load transport rate. Whole of the equation (6.7) can be written as

$${\tau_*}' = 0.047 + 0.25\phi^{2/3} \tag{6.8}$$

where

$$\phi = \frac{q_B}{\gamma_s} \sqrt{\frac{\rho_f}{\rho_s - \rho_f \left(\frac{1}{g {d_a}^3}\right)}} \tag{6.9}$$

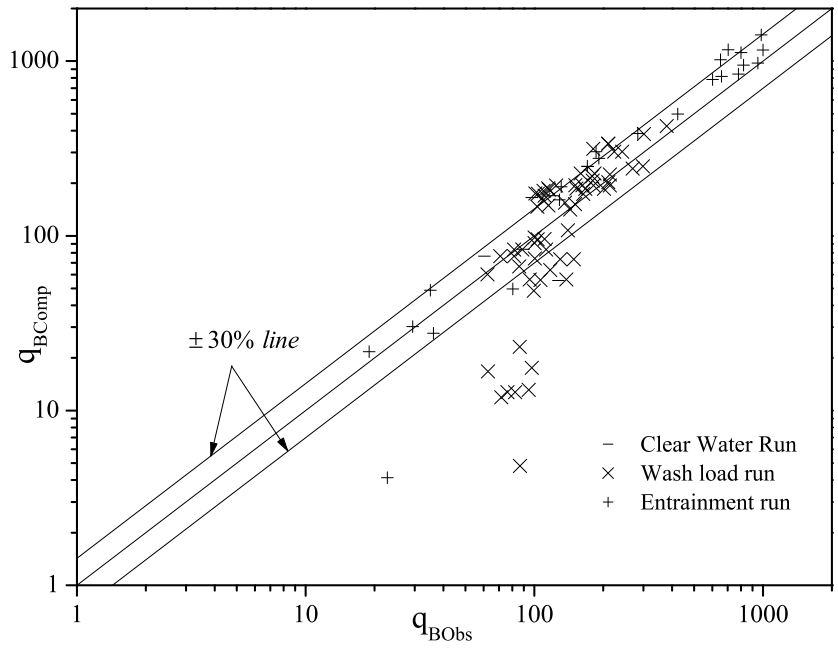

Figure 6.2: Comparison of observed versus computed bed load transport considering original U (Meyer-Peter and Müller 1948)

and

$$\tau_*{}' = \frac{\gamma_f R_g S}{(\gamma_s - \gamma_f) d_a} \tag{6.10}$$

Equation (6.8) can also be reduced to

$$\phi = 8\left(\tau_*{}' - 0.047\right)^{3/2} \tag{6.11}$$

Equation (6.11) suggests that bed load movement starts only when normalized shear stress exceeds 0.047. Hence $(\tau_*{}' - 0.047)$ is considered as the effective shear stress. $\tau_*{}'$ and ϕ are respectively dimensionless shear stress and dimensionless bed load transport.

A comparative plot of observed and computed bed load transport using Meyer- Peter and Müller (1948) formulation is shown in Figure 6.2 . It can be seen from Figure 6.2 that Meyer-Peter and Müller (1948) equation overestimates the bed load for majority of the data. In addition, about 40% of the data lies beyond the ±30% error lines. Figure 6.2 shows that little more number of transport data is on higher side of the line of agreement. About 40% of data still lies beyond the error band of ±30%. Meyer-Peter and Müller (1948) method was unable to compute the bed load transport for some of the experimental runs because of the binding criterion of effective shear stress. Such data were unable to be plotted and hence ignored. The incapability of calculating bed load transport by this method for few experimental runs were due to the

assumption that bed particles only moves when the effective shear stress becomes greater than 0.047. Hence the Meyer-Peter and Müller (1948) formulation seems to be unsatisfactory.

6.4.2 Misri et al. (1984) equation

Misri et al. (1984) and Samaga (1986) argued the rational of considering a constant value (0.047) for critical shear stress by Meyer-Peter and Müller (1948) by saying that this constant value is valid only for large particles and proposed that bed materials even move at value of $\tau_*' \leq 0.047$. They mentioned that smaller particles may move at much lower values of dimensionless critical stress. Based on the analysis of large volume of experimental data they arrived with a set of expressions to find the ϕ value in Meyer-Peter and Müller (1948) equation.

$$\phi = 4.67 \times 10^{-7}\left(\tau_*'\right)^{8} \text{.....For} \quad \tau_*' \leq 0.065 \tag{6.12}$$

$$\phi = \frac{8.5{\tau_*'}^{1.8}}{\left[1 + 5.95 \times 10^{-6}\left(\tau_*'\right)^{-4.7}\right]^{1.43}} \text{.....For} \quad \tau_*' \geq 0.065 \tag{6.13}$$

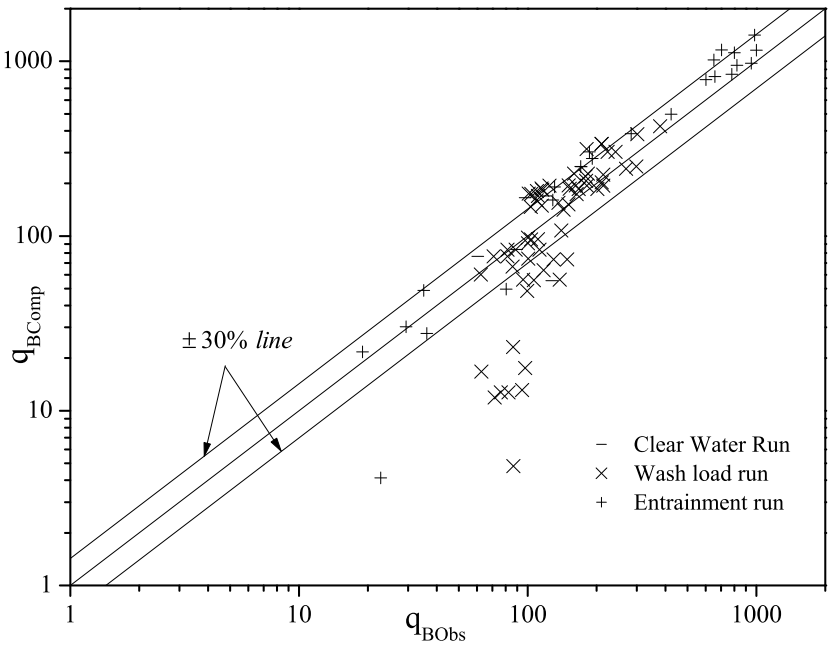

Figure 6.3: Comparison of observed versus computed bed load transport considering original U (Misri et al. 1984)

Figure 6.3 shows the comparison of experimentally observed and computed bed load transport by Misri et al. (1984). It can be observed from the figure that majority of the data lie

between the ±30% error bands. Still it can be seen that about 30% of data lie out of the ±30% range. Almost 93% of the data lie below the line of agreement indicating that Misri et al. (1984) method under predicts the bed load transport rate for the given gravel and flow condition.

6.4.3 Patel and Ranga Raju (1996) equation

Patel and Ranga Raju (1996) proposed a semi graphical approach to estimate the bed load transport. They proposed a fractionwise bed load transport computation for bed composed of non uniform materials. They used exposure cum hiding coefficient ξ to incorporate the effect of coarser particles on the smaller ones. They also mentioned that if the bed particles are uniform, the same formulation can be implemented by considering ξ as unity. Since in the present study, the bed material is uniform in nature, ζ in Patel and Ranga Raju (1996) equation is considered as unity.

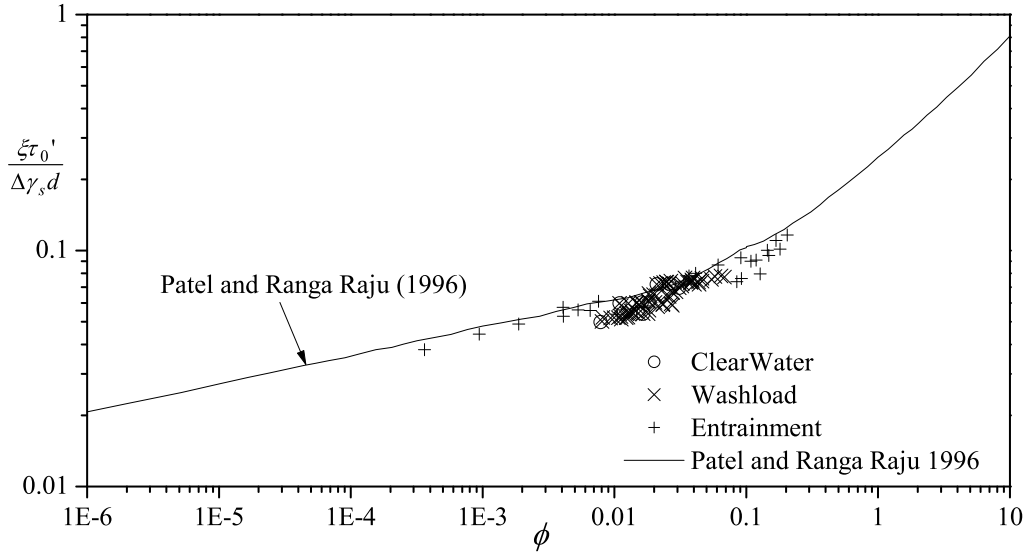

Figure 6.4: Check on Patel and Ranga Raju (1996) bed load transport law for uniform sediment

A plot of ϕ versus $\xi\frac{\tau_0{}'}{\Delta\gamma_s d}$ where $\xi = 1$ is prepared and shown in Figure 6.4 . A line representing the relationship proposed by Patel and Ranga Raju (1996) is also shown in Figure 6.4 . It can be concluded from the Figure 6.4 that the method of Patel and Ranga Raju (1996) over predicts the bed load transport rate for the case of flow carrying suspended sediment.

Figure 6.5 is a comparative plot of observed and computed bed load transport. It can be observed from the figure that majority of the data lies above the line of agreement. Most of the

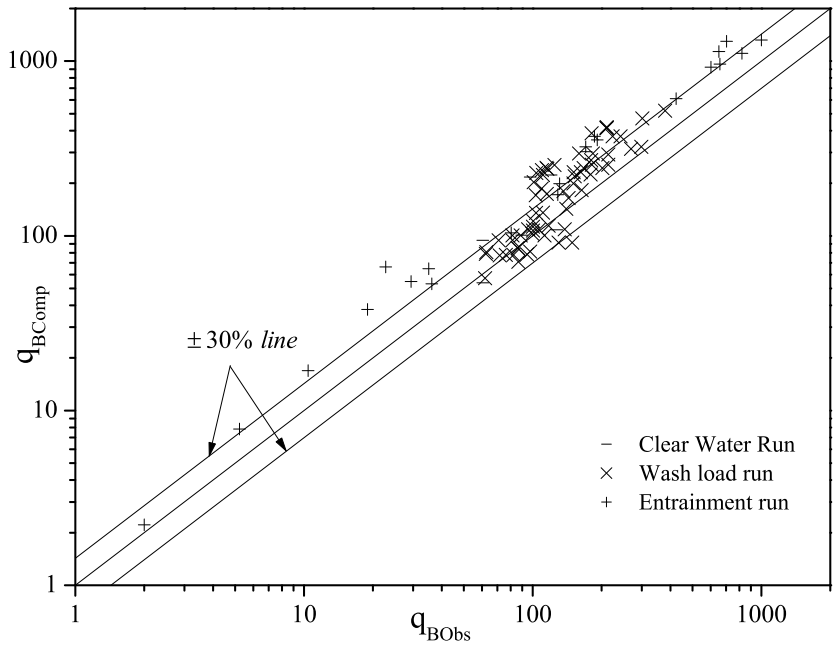

Figure 6.5: Comparison of observed versus computed bed load transport considering original U (Patel and Ranga Raju 1996)

data even lies beyond the error band of +30%. It indicates that Patel and Ranga Raju (1996) over predicts the bed load transport rate. This conclusion is in agreement with the conclusion obtained from Figure 6.4 . It can be further noted that almost 40% of data is still lying beyond the error band of ±30%.

Though the result from Misri et al. (1984) came closer to that of observed value of bed load transport, the overall result of all the methods deemed to be unsatisfactory. Hence there is a need to find the better equation that fits the present study data.

6.5 Proposed Approach for Bed Load Computation

Check on some of the existing methods of bed load transport revealed that none of them performed satisfactorily. Even with an error band of ±30%, majority of the data fell out of the error band. Hence a modified approach has been proposed here to estimate the bed load transport rate of uniform sediment in the flow carrying suspended sediment.

It has been assumed that the possible deviation in the observed and calculated value of bed load transport might be due to the non consideration of effect of suspended sediment on bed load

transport. It is to be mentioned that silt used as suspending material was very fine compared to the channel bed materials. The silts infiltrated into the gravel bed and completely filled the pores but couldn't completely flush the gravel top layer as the top layer was mobile. Hence it is assumed that the exposure of the gravel top layer was not affected by the presence of fines in the pores to the extent where size of gravel need to be modified. The size of the gravel, therefore is retained same as that of parent bed material in the modified approach proposed herein. Since the geometric properties of the gravel is considered same, the only option to include the effect of suspended sediment on bed load transport is to consider the possible change in the hydraulics of the flow due to the fine sediment in suspension.

In Chapter 4, while analyzing the variation of friction factor, it was concluded that compared to that of clear water flow, the friction factor of sediment laden flow decreases with an increase in sediment concentration in the flow. The change in flow characteristics due to change in friction factor has been discussed and the same has been incorporated in the proposed approach to estimate bed load transport rate. The friction factor for clear water flow (f_0) can be written as

$$f_0 = \frac{8g{h_0}^3 S}{q^2} \tag{6.14}$$

Where h_0 is the clear water flow depth, and hydraulic radius is considered to be equal to the flow depth. q is the discharge per unit width of channel. From Chapter 4, the friction factor (f) for a flow carrying suspended sediment can be computed using the following equation.

$$\frac{f}{f_0} = 0.985 - 8 \times 10^{-6}(s-1)\frac{C\omega}{US} \tag{6.15}$$

The value of friction factor due to clear water (f_0) can be obtained from equation (6.14) and for any known concentration of suspended sediment; the value of friction factor (f) can be obtained from equation (6.15) . Knowing the value of (f) , the modified flow depth h_{mod} can be computed for the same value of q as

$$h_{mod} = \left(\frac{fq^2}{8gS}\right)^{1/3} \tag{6.16}$$

The modified flow velocity U_{mod} due to presence of suspended sediment can thus be obtained as

$$U_{mod} = \frac{q}{h_{mod}} \tag{6.17}$$

Substituting the modified values of h_{mod} and U_{mod} at appropriate places in the Meyer-Peter and Müller (1948), Misri et al. (1984) and Patel and Ranga Raju (1996) equations, the bed load is

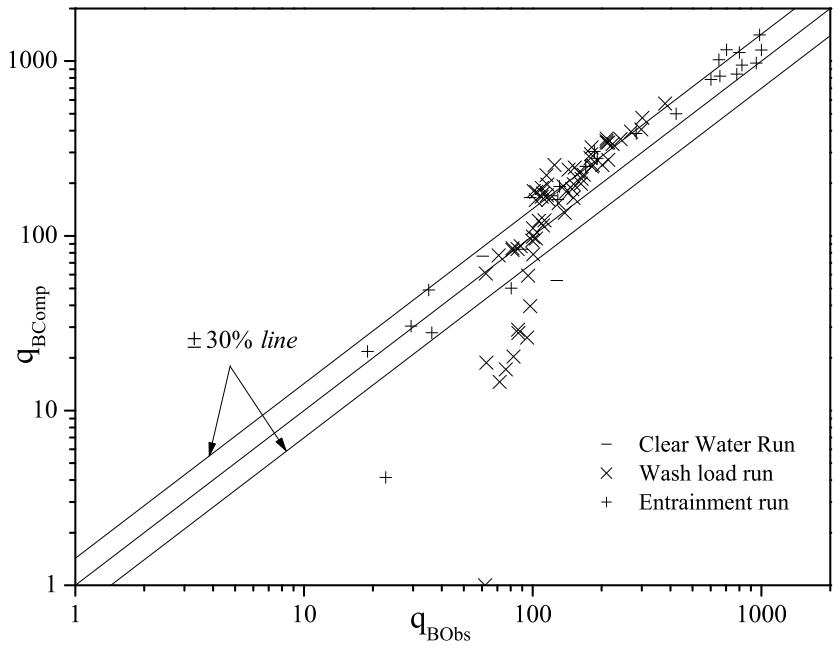

Figure 6.6: Comparison of observed versus computed bed load transport considering modified U (Meyer-Peter and Müller 1948)

computed. Figures 6.6 to 6.8 present the comparison of model computed and experimentally observed bed load for Meyer-Peter and Müller (1948), Misri et al. (1984) and Patel and Ranga Raju (1996) respectively.

A comparison of Figures 6.6 and 6.2 indicate that due to the modification of flow characteristics, Meyer-Peter and Müller (1948) bed load transport equation tries to over predict the bed load as compared to that without modification of flow characteristics. After modification, the flow velocity was observed to increase. Increase in velocity increased the bed load transport rate. However even with modified approach, about 40% of data lie beyond ±30% error band. The change in velocity occurred due to the varying concentration of suspended sediment in flow. Since during the clear water run and entrainment run, the fines concentration in the flow was nil or very low, there was almost no change in the velocity of those runs as computed by proposed approach. The bed load transport calculated for these run remained same as that in the earlier computations.

A comparison of Figures 6.7 and 6.3 shows that the modification of flow characteristics due to the proposed new approach has significantly improved the prediction of bed load by Misri et al. (1984) method. The majority of data follows the line of agreement indicating that the bed load transport rate predicted by the Misri et al. (1984) method is almost same

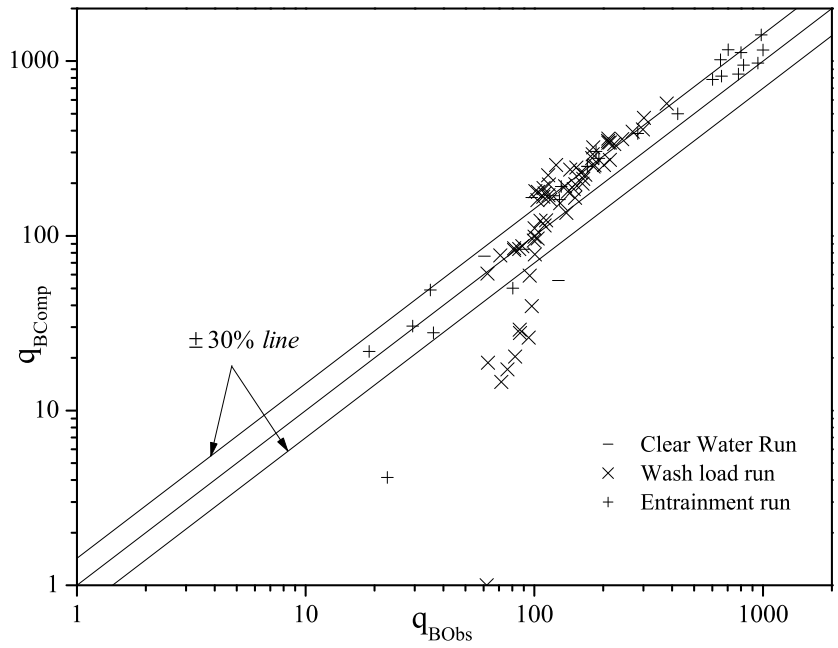

Figure 6.7: Comparison of observed versus computed bed load transport considering modified U (Misri et al. 1984)

as that observed experimentally. Considering the original velocity of flow (ignoring the effect of suspended sediment), about 30% of data were falling out of the range of ±30% error band, whereas considering the modified velocity (considering the effect of suspended sediment) the data lying out of the same error band has reduced to just 10%. There have been no changes in the predictions of bed load transport for clear water and entrainment runs.

A comparison of Figures 6.8 and 6.5 indicate that due to the modification of flow characteristics, Patel and Ranga Raju (1996) bed load transport equation tries to over predict the bed load as compared to that without modification of flow characteristics. It can be observed from the Figure 6.8 that majority of the data lies above the line of agreement. Around 50% of data have fallen out of the error band of ±30%. Here also the computed rates for clear water and entrainment runs remained unaffected.

The results obtained by the method of Meyer-Peter and Müller (1948) and the Patel and Ranga Raju (1996) even after adopting the modified approach are not satisfactory; whereas the same obtained by the method of Misri et al. (1948) deemed to be quite satisfactory. Hence it is proposed to estimate the bed load transport of the flow carrying suspended sediment considering the change in the friction factor due to presence of suspended sediment. The procedure to estimate the transport rate has been explained below.

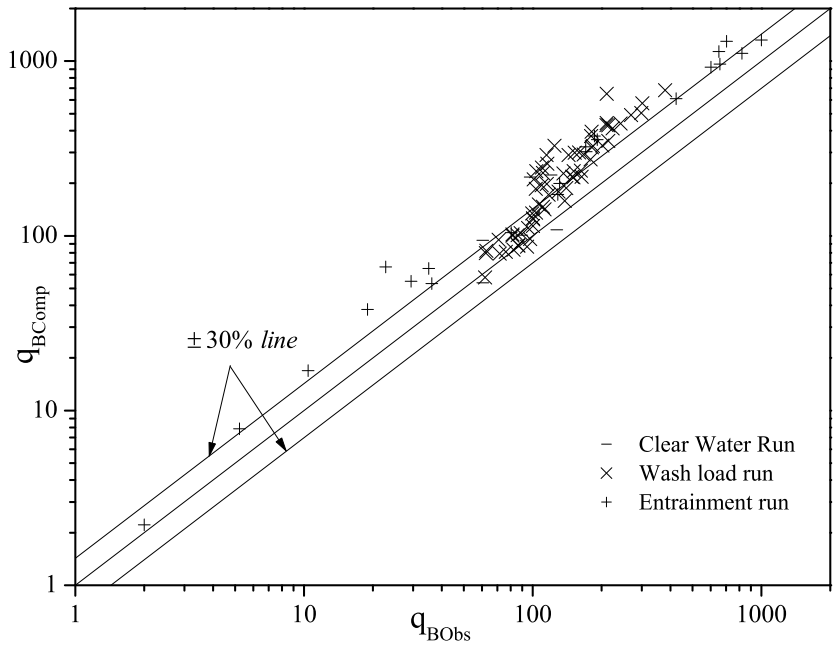

Figure 6.8: Comparison of observed versus computed bed load transport considering modified U (Patel and Rang Raju 1996)

6.6 Procedure for Computation of Bed Load Transport Rate

The following procedure explains the step by step procedure for computing bed load transport in the flows carrying suspended sediment.

- Compute the friction factor (f_0) due to clear water run using the equation (6.14) .
- Compute the friction factor due to sediment laden run (f) using equation (6.15) for individual concentrations.
- Compute the value of modified flow depth h_{mod} using equation (6.16) .
- Compute the modified flow velocity U_{mod} using equation (6.17) .
- Compute $n_g = \frac{{d_{90}}^{1/6}}{26.0}$, $R_g = (\frac{u_{comp} n_g}{\sqrt{S}})^{1.5}$ and then ${\tau_*}'$ from equation(6.10) .
- Compute ϕ using equation (6.12) or (6.13) .
- Compute q_B using equation (6.9) .

6.7 Concluding Remarks

Analysis of all the experimental data revealed that the bed load transport is a function of suspended sediment concentration as well. It has been observed that the bed load transport rate increases with an increase in suspended sediment concentration. Many methods of bed load transport estimation have been tested my several previous researchers and found to have produced unsatisfactory result. Among the methods tested in this study, methods proposed by Misri et al. (1984) found to be satisfactory. In order to arrive at a better estimation, a new approach has been proposed. The proposed new approach is based on the effect of suspended sediment on the friction applied to the channel bed. The effect on this friction factor is then used to estimate the modified value of flow parameter. The same models when tested in combination the proposed criterion, Misri et al. (1984) method produced a satisfactory result.

Chapter 7

Turbulence Analysis

7.1 General

A clear understanding of particle movement near the bed is essential to make accurate predictions of sediment transport. Apart from other parameters, turbulence characteristics also influence the complex process of entrainment, suspension, transportation and deposition of sediment (Balachandar and Reddy 2013). Turbulence is also an another affecting factor for scouring around riverine structure (Goel 2008). The present chapter presents the turbulence characteristics of the flow carrying the suspended sediment over mobile gravel bed. The turbulence characteristics across and along the flume were analyzed with the help of time averaged three dimensional velocity components, turbulent stresses, turbulence intensity component and quadrant analysis. The required data for the analysis is obtained with the help of Acoustic Doppler Velocimeter (ADV). The ADV data are recorded for all the experimental runs carried out in this study.

7.2 Data Collection and Filtering

A four receiver Nortek's Vectrino Plus ADV working at an acoustic frequency of 10 MHz and sampling frequency of 100 Hz was used to measure the real time three dimensional velocity of flow at any particular point. Figure 7.1 shows a typical ADV measurement during an experimental run.

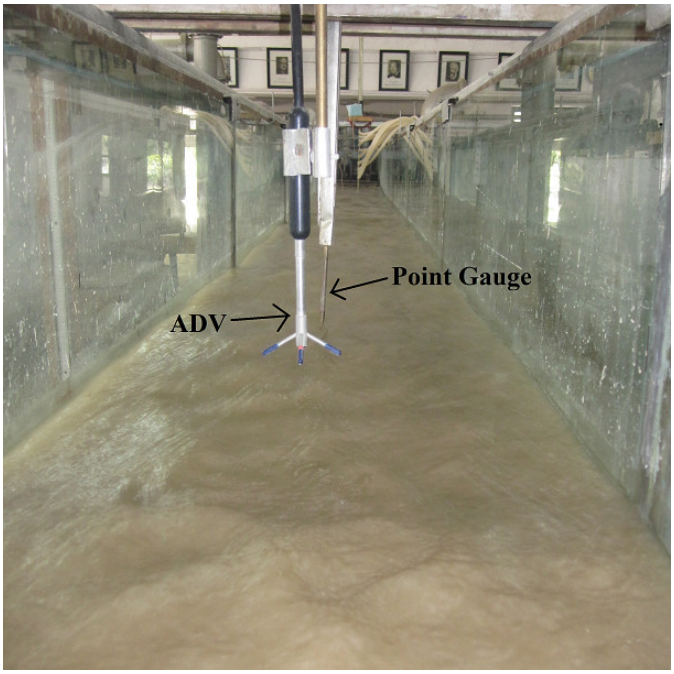

Figure 7.1: ADV ready to measure the velocity data

The ADV measures the velocity within a cylindrical sampling volume of 6 mm diameter and 4 mm height. The closest point where measurement can be made was 2 mm above the channel bed. For few centimeters from the bed, the measurements were made at 2mm interval, while the interval was kept 3 mm or 4 mm at higher region. The minimum duration of measurement of velocity was 2 minutes. However, at each point close to the bed, the duration of measurement ranged between 3 minutes to 5 minutes. Owing to the constraint of instrument, the velocity measurements of top 5 cm of flow was not made. Velocities were measured vertically along the centreline of the flume. Positive x- axis was along the flow direction, positive y- axis was across the right of flow and positive z- axis was vertically upward. The centre point of start of working section was considered as (0, 0, 0). Throughout this study, since, measurements were made only along the centre line of flow (in $x - z$ plane), thr point location system was followed as (x, 0, z). For the purpose of data processing using software, the coordinates of the points were mentioned in the form $(x_m, 0, z_{mm})$. For example if coordinate of a point is written as (5.5, 0, 10); it means the point of velocity measurement was 5.5 m downstream of the working section, at the centreline and 10 mm above the channel bed. A snap shot of the process of data collection is shown in Figure 7.2 .

The data collected from the ADV had the file extension ".adv" Using the Vectrino Plus software, the ".adv" files were converted to ".vno" files that were readable by the WinADV

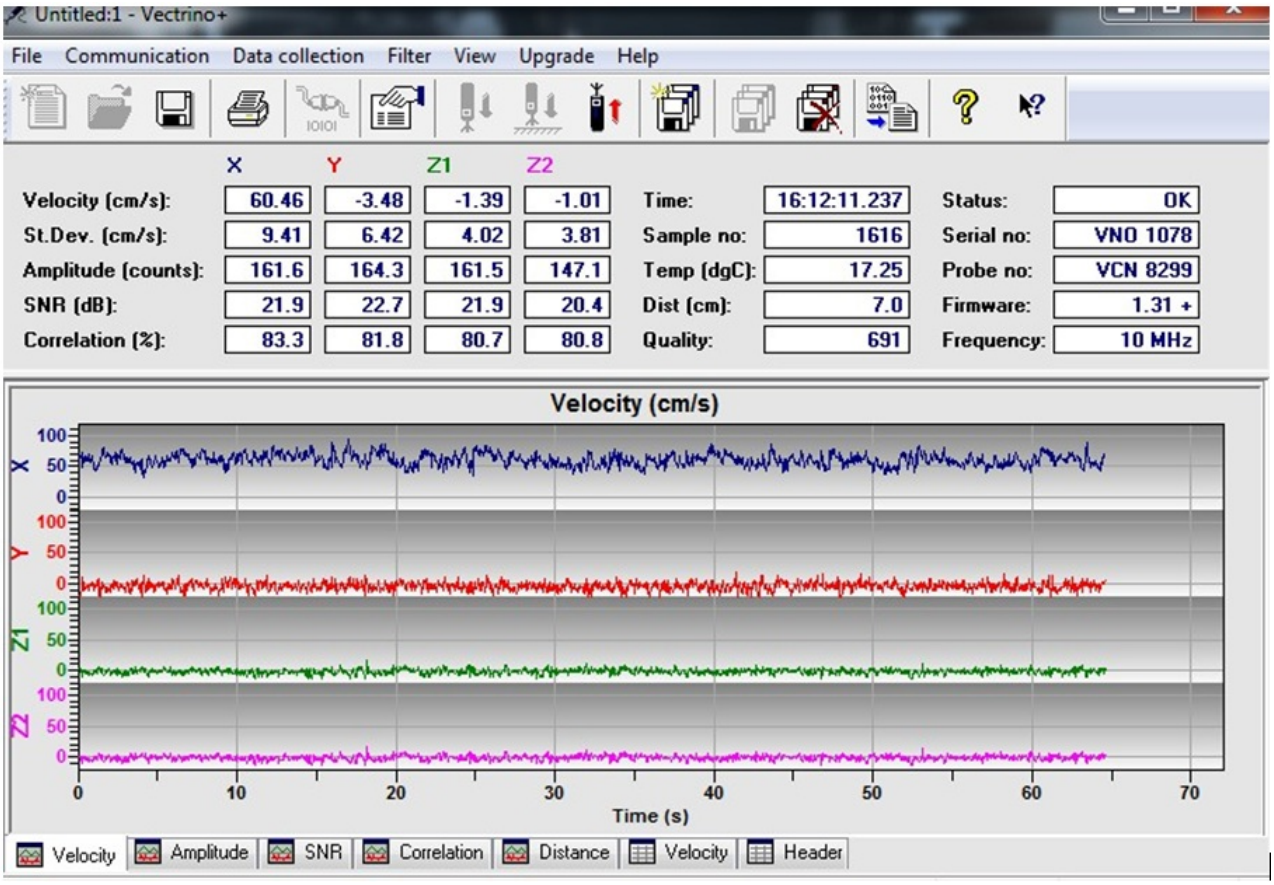

Figure 7.2: Interface of Vectrino+ software collecting the three dimensional velocity

software. WinADV has the capacity of processing multiple files at a time. A screen shot of data conversion and data processing have been shown in Figure 7.3 and 7.4 respectively.

Data processing by WinADV is actually a data filtering mechanism. Those data which satisfied the filtering criteria were only retained and processed by the software. The filtering criteria were;

- Signal - to - noise ratio (SNR) minimum 15
- Correlation between transmitted and received pulses minimum 70%
- Acceleration threshold equal to one
- Despiking by Phase- Space threshold method
- The bad samples were removed rather than interpolating them

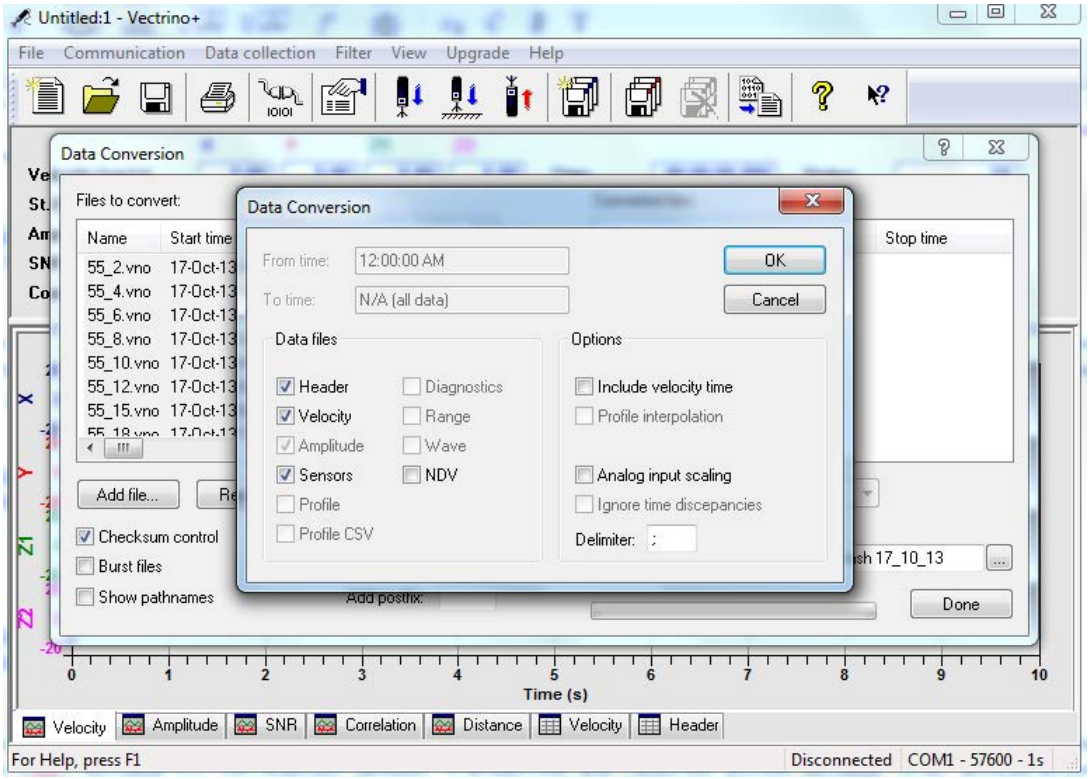

Figure 7.3: Data conversion interface of Vectrino+

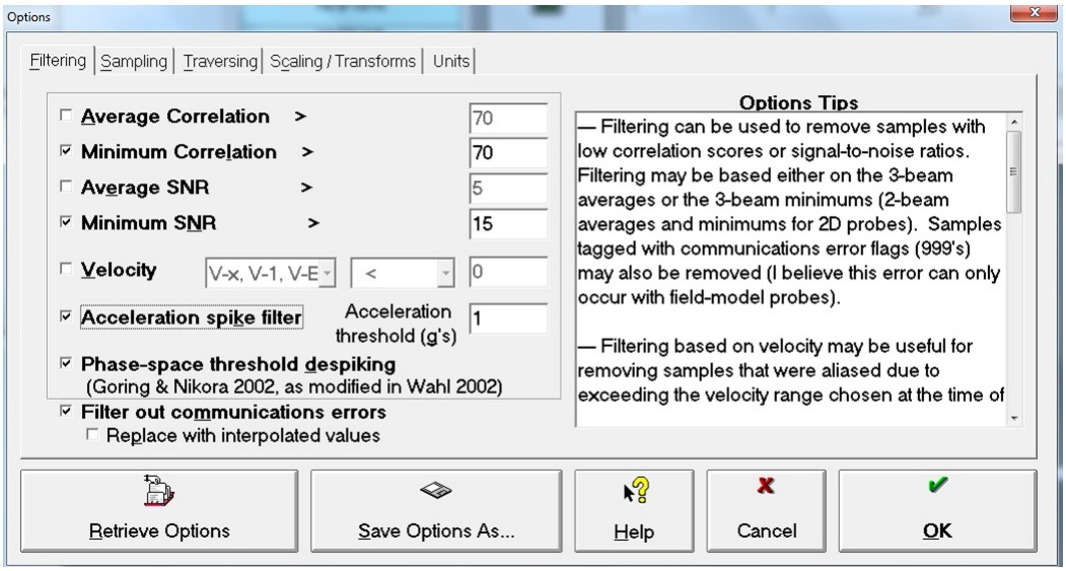

Figure 7.4: WinADV interface showing filtering criteria

7.3 Vertical Distribution of Time Averaged Velocity

The vertical distribution of dimensionless time averaged velocity in all the three directions are shown in Figure 7.5 . The velocity components $\overline{u}, \overline{v}, \overline{w}$ were normalized by dividing them with the shear velocity U_* and the height of each point of measurement z was normalized by dividing them with flow depth h.

$$u^+ = \frac{\overline{u}}{U_*} \qquad v^+ = \frac{\overline{v}}{U_*} \qquad w^+ = \frac{\overline{w}}{U_*} \qquad z^+ = \frac{\overline{z}}{h} \tag{7.1}$$

1S series includes nine sediment laden runs, one clear water run and four entrainment runs. Figure 7.5 shows the vertical distribution of non dimensional velocities in all the three directions of all the runs of series 1S. Non dimensional stream wise velocity distribution clearly shows the increasing trend of velocity towards the flow surface. The non dimensional velocity distribution in y and z directions varied between $\pm 1.0 cm/sec$; which can be considered close to zero, indicating the unidirectional flow. The distribution of flow velocity across the flow and in vertical direction was observed to be same for all the runs of all the series. Since the velocity measurement were not carried out at the top 5 cm of the flow depth due to the limitation of ADV, the velocity dip phenomena (the reduction in velocity) near the flow surface is not recorded.

In series 2L, velocities were measured at seven different locations along the flow direction. The velocity in y and z directions were observed to be close to zero. Non dimensional stream wise velocity distribution at 5.5 m and 6.75 m sections of the runs of series 2L are shown in Figure 7.6 .

The velocity profiles drawn from the data were quite similar to the standard open channel velocity distribution profile. Close observation of the plots showed that there was not much variation in the velocity profile taken at various longitudinal locations. This indicated a steady and uniform flow in the study reach of the flume. Plots that show the velocity distribution at particular location with increasing concentration (successive runs) showed that as the concentration of silt increased, average flow velocity has also marginally increased. In Chapter 4, it has been mentioned that flow velocity increased due to decreased friction factor in the presence of increasing concentration. This has been supported by Figures 7.5 and 7.6 .

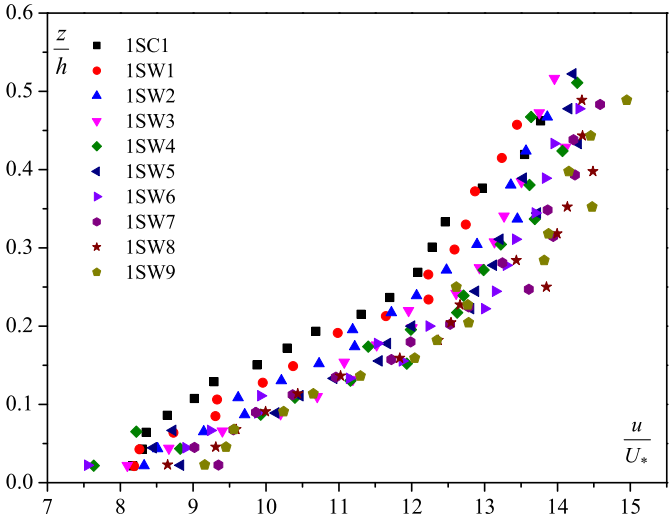

(a) Streamwise velocity distribution (u)

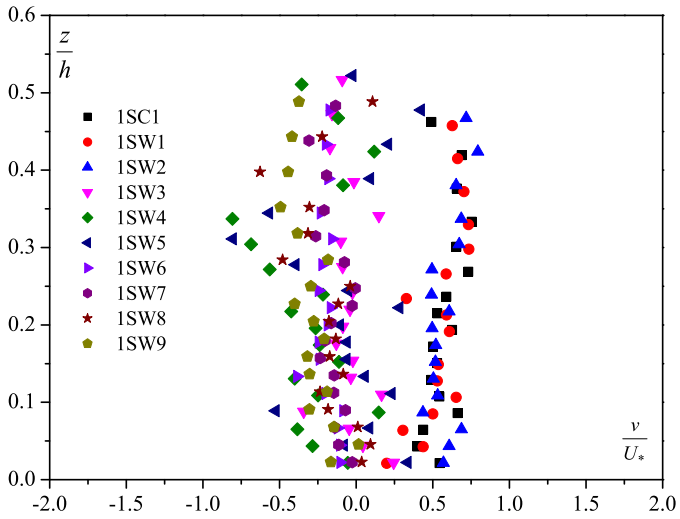

(b) Across the flow velocity distribution (v)

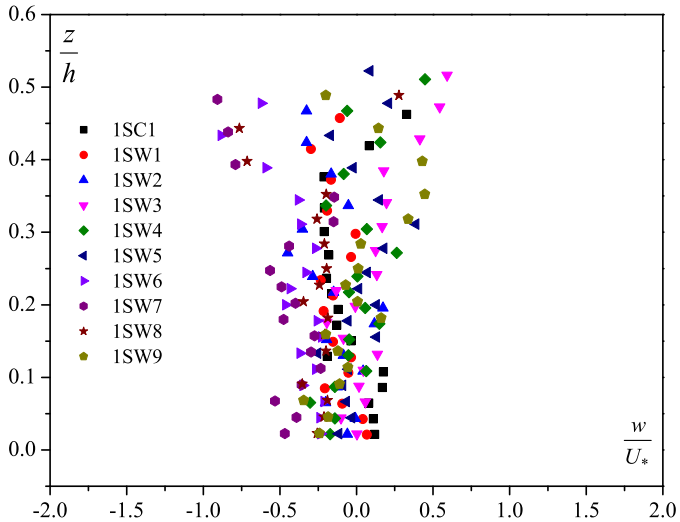

(c) Vertical velocity distribution (w)

Figure 7.5: Normalised profiles of mean velocities at 5.5 m section for series 1S

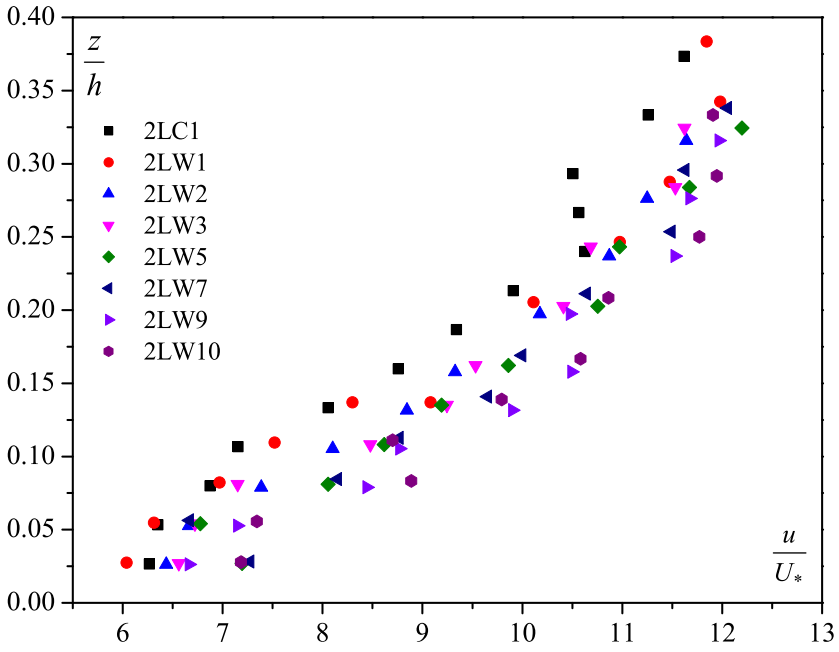

(a) Streamwise velocity distribution (u) at 5.5 m section

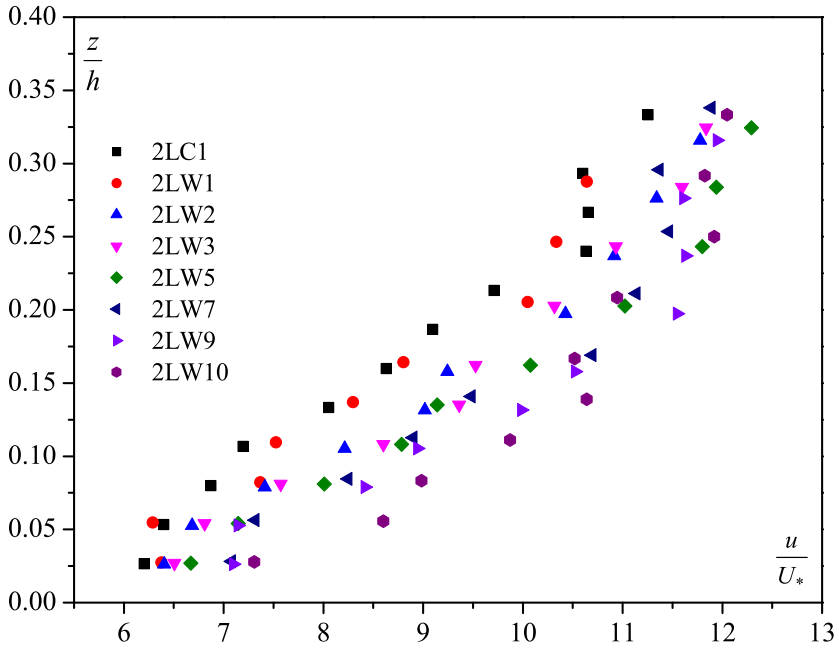

(b) Streamwise velocity distribution (u) at 6.75 m section

Figure 7.6: Normalised profiles of mean streamwise velocities for series 2L

7.4 Vertical Distribution of Turbulence Intensities

Profiles of the non dimensional turbulence intensities and non dimensional turbulent kinetic energy of the experiments of series 1S and 2L have been shown and discussed here. Turbulence intensities have been normalized by dividing with shear velocity. Figures 7.7 and 7.8 present the streamwise and vertical non dimensional turbulence intensities at section 5.5 m from the start of the working section for series 1S and 2L respectively. From Figures 7.7 and 7.8, it can be clearly seen that both the streamwise and vertical non dimensional turbulence intensities increase to a certain height from the bed followed by a decrease beyond this height. A close observation of these Figures reveal that turbulence intensities increases within the wall region $z/h \leq 0.2$ and decreases afterward.

Carollo et al. (2005) mentioned that elements roughness available on bed has direct impact on the turbulence intensities. They also mentioned that turbulence intensity increases to a certain peak value. The rough elements available on the bed penetrate the flow and hence forcefully decompose the large scale vortices into small vortices. Based on this hypothesis Nezu and Nakagawa (1993) also observed an increase in non dimensional turbulence intensity to a certain height above bed.

Two series of runs discussed in this section have different size of bed materials viz. 1.9 mm gravel in 1S and 5.2 mm gravel in 2L series. The present study was on fully rough bed. The maximum value of non dimensional streamwise turbulence intensity $({TI_u}^+)$ for series 1S and 2L were found to be 2.38 and 2.31 respectively. It can be seen that peak turbulence intensity decreases with an increase in bed roughness. Nezu and Nakagawa (1993) have reported the maximum value of ${TI_u}^+$ for smooth and fully rough bed as 2.8 and 2.0 respectively. Ramesh (2012), obtained a peak value of 2.30 and 2.02 for transitionally rough bed with bed roughness of 0.3 mm and 0.84 mm respectively. It has been reported by several researchers that turbulence intensity, turbulence kinetic energy and in particular peak turbulence intensity decreases with increasing relative roughness value.

The ratio of transverse turbulence intensity and streamwise turbulence intensity (TI_v/TI_u) were found to be 0.63 with standard deviation 0.062 for series 1S and 0.68 with standard deviation 0.07 for series 2L ; whereas 0.71 and 0.75 were reported by Nezu and Nakagawa (1993) and Song and Chiew (2001) respectively. Similarly values reported for the ratio of vertical

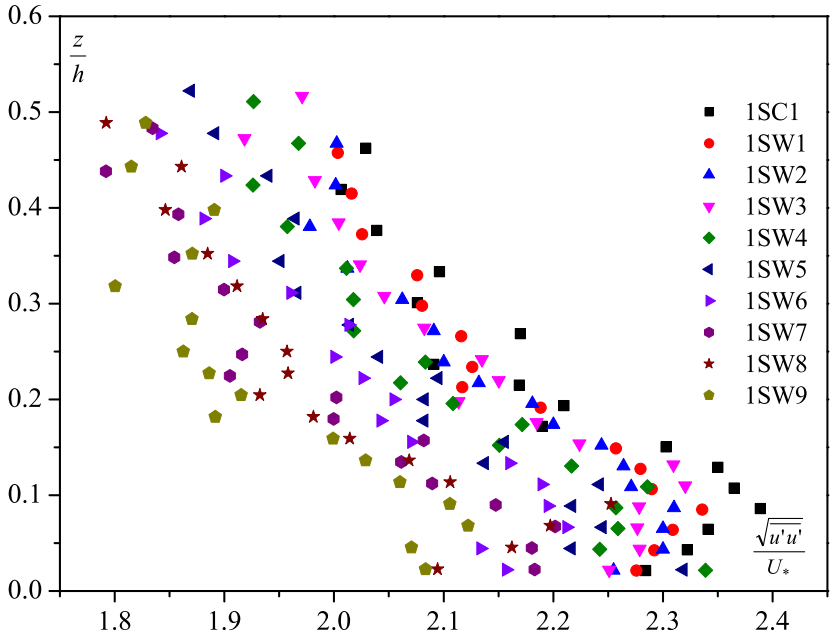

(a) Non dimensional streamwise turbulence intensity ($TI_u{}^+$)

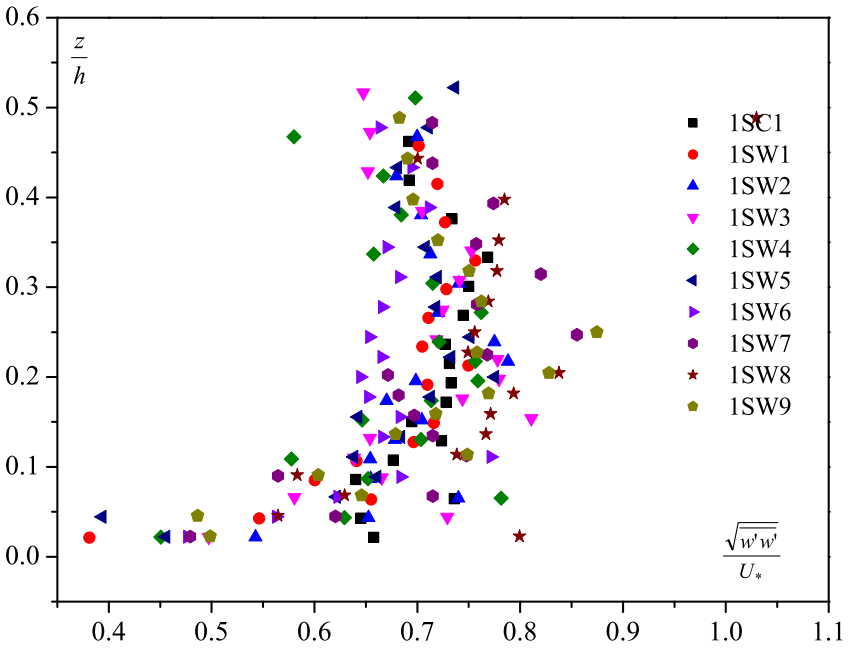

(b) Non dimensional vertical turbulence intensity ($TI_v{}^+$)

Figure 7.7: Non dimensional turbulence intensity profiles at section 5.5m for series 1S

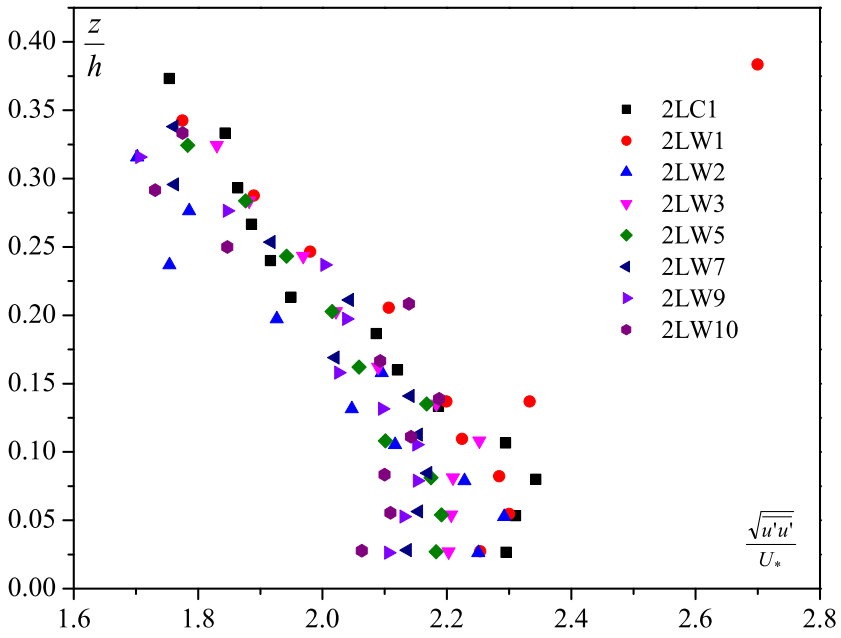

(a) Streamwise turbulence intensity distribution (TI_u)

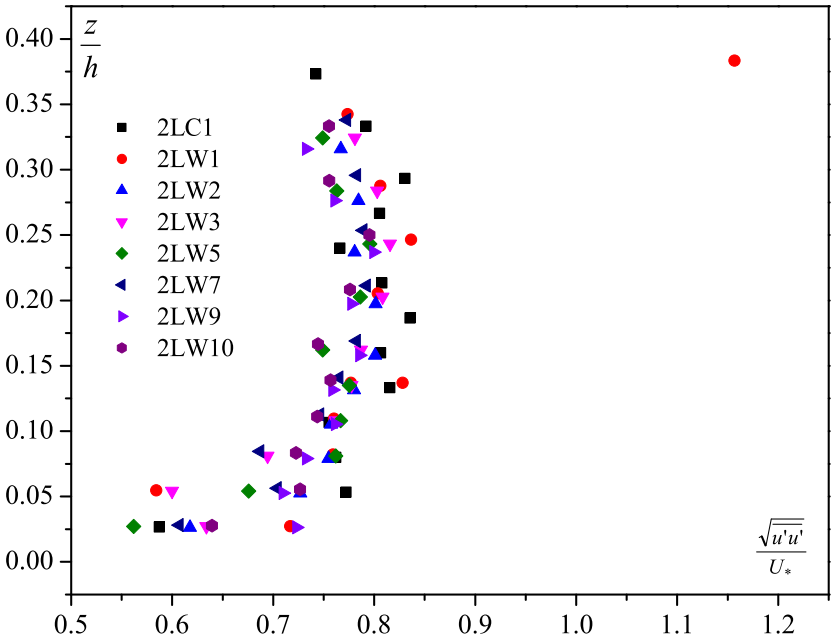

(b) Vertical turbulence intensity distribution (TI_v)

Figure 7.8: Non dimensional turbulence intensity profiles at section 5.5m for series 2L

turbulence intensity and streamwise turbulence intensity (TI_w/TI_u) by Nezu and Nakagawa (1993) and Song and Chiew (2001) were 0.55 and 0.5 respectively. For the present study the value of TI_w/TI_u (plot of TI_w not shown here) is 0.35 with standard deviation 0.06 for series 1S and 0.37 with standard deviation 0.05 for series 2L.

The turbulent kinetic energy (TKE) of all the runs have been obtained using equation (2.20) . The normalized TKE (divided by square of shear velocity) is plotted against normalized flow depth (z/h) as shown in Figure 7.9 . The plot of TKE seems to be in synchronization with that of turbulence intensity.

7.5 Vertical Distribution of Reynold Shear Stress

For two dimensional uniform flow in open channels, the total shear stress is the sum of viscous shear stress and Reynold Shear Stress (RSS) expressed as;

$$\tau_R = \mu \frac{d\bar{u}}{dz} - \rho\overline{u'w'} \tag{7.2}$$

Where τ_R is the total shear stress, μ is dynamic viscosity, $\frac{d\bar{u}}{dz}$ is vertical velocity gradient, ρ is the fluid density and $\overline{u'w'}$ is time averaged cross correlation coefficient between streamwise (u) and vertical (w) velocity components. For the same experimental runs 1S and 2L as discussed earlier, Reynold shear stress distribution have been discussed in this section. Figure 7.10 shows the normalized Reynold shear stress variation with the normalized flow depth for the runs of series 1S and 2L.

In both the figures, it can be noticed that RSS attains a certain maximum value and then decreases towards bed. Similar results have been reported by Grass (1971), Nikora and Goring (2000) and Antonia and Krogstad (2001) for rough bed channels. Nikora and Goring (2000) attributed the probable reason for this observation to the existence of roughness sub layer where additional mechanism for momentum extraction emerges. It has been recommended by Nezu and Nakagawa (1993) that for all analysis purpose, it is better to use the shear velocity (if needed) extracted from the plot of Reynold shear stress distribution i.e. evaluating equation 7.10 at $z = 0$. For example for run numbers 1SC1 and 1SW8 of series 1S, computed shear velocities were 0.049 m/s and 0.048 m/s respectively and their graphical shear velocities were 0.041 m/s and 0.043 m/s respectively. Results seem to be close. Similarly for run numbers

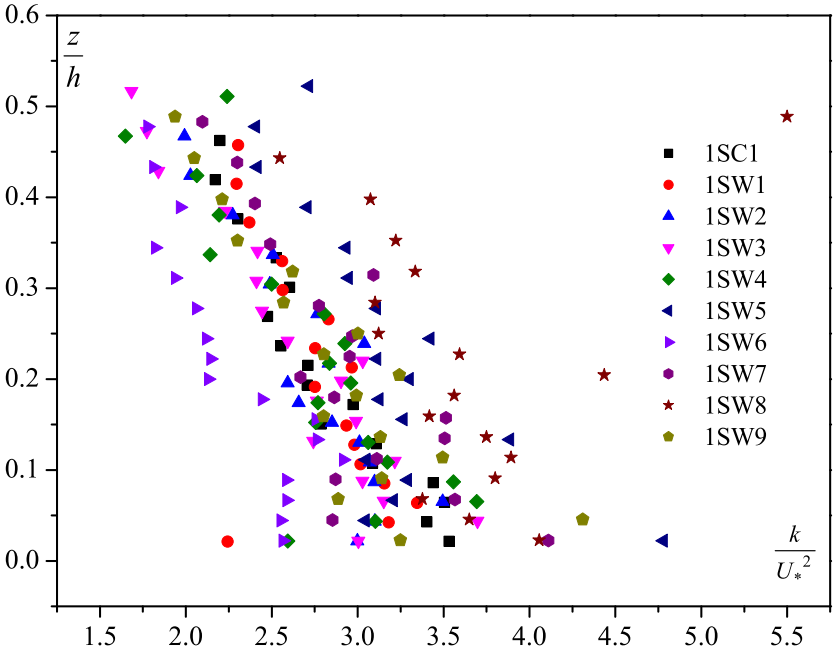

(a) TKE variation for series 1S

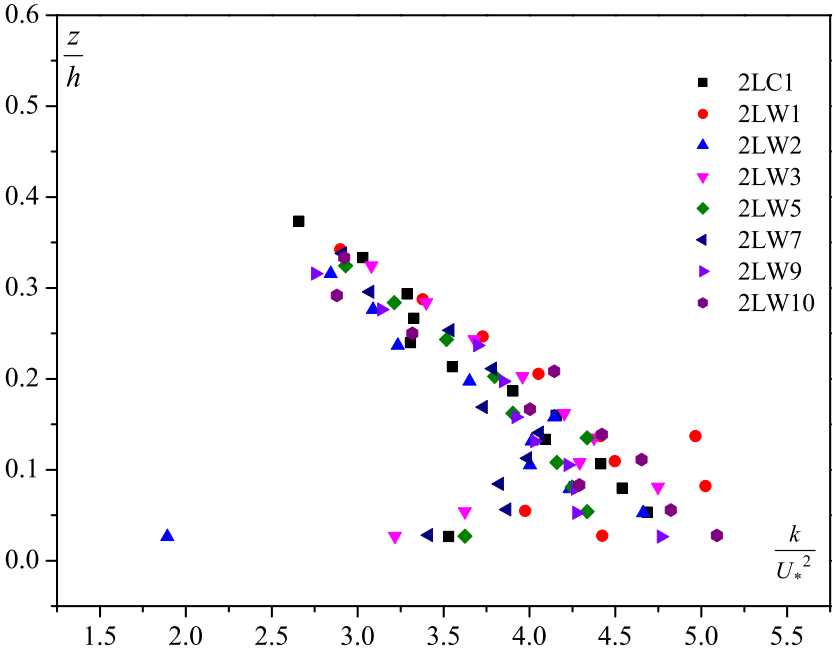

(b) TKE variation for series 2L

Figure 7.9: Non dimensional turbulent kinetic energy variation with depth

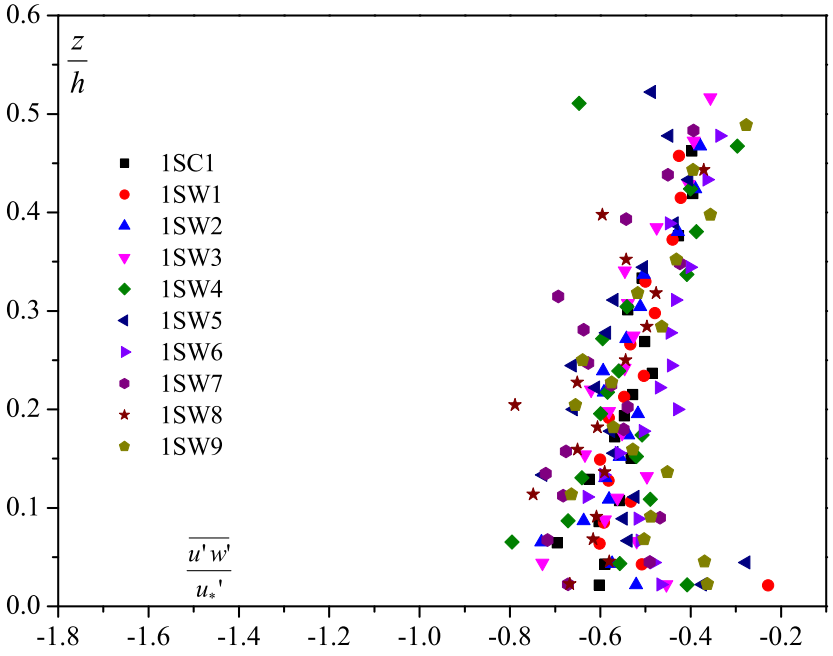

(a) RSS variation for series 1S

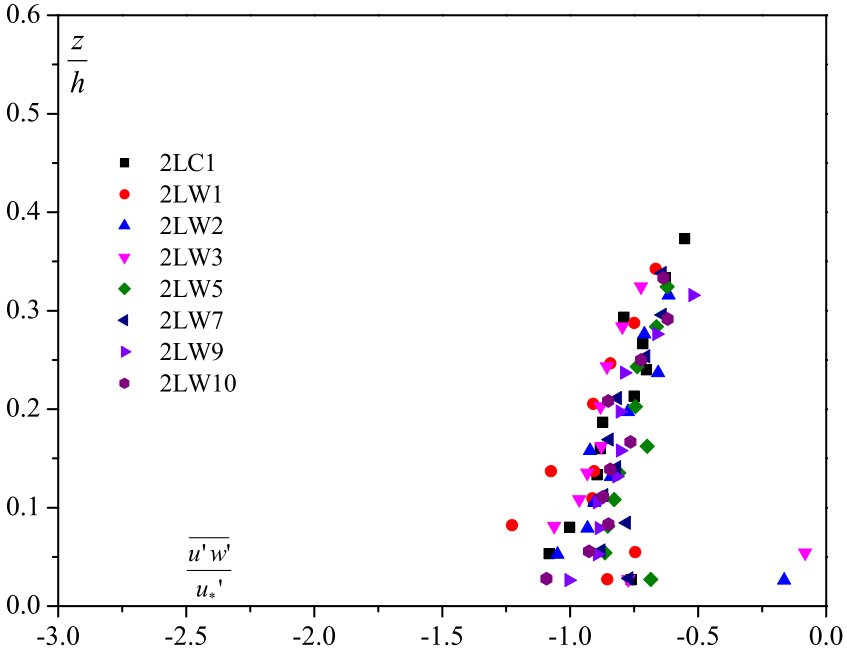

(b) RSS variation for series 2L

Figure 7.10: Non dimensional streamwise Reynold shear stress distribution

2LW1 and 2LW7 of series 2L, the computed shear velocities were 0.072 m/s and 0.071 m/s respectively and there graphical shear velocities were 0.0713 m/s and 0.0717 m/s respectively. These results were almost matching.

7.6 Quadrant Analysis

The quadrant technique elaborated in section 2.4.4 is used to investigate the shear stress production by coherent structures. For quadrant analysis, the instantaneous velocities u and w obtained by the ADV were decomposed into mean velocity and fluctuations using Explore V software. A code developed in FORTRAN 95 was used to obtain outward interaction, ejection, inward interaction and sweep out of all the data. For a particular value of z/h , the probability of occurrence $(S_{i,H})$ for each event at each depth was obtained using the above mentioned code. This analysis was done for all the experiment of each series. The analysis was done taking the hole size (H) zero. Here the quadrant analysis of all the runs of series 1S and 2L are presented and discussed.

Figure 7.11 show the contribution of bursting events for the experimental runs of series 1S and 2L. It can be observed from the figures that the fractional value of Q_2 event (ejection) increases with increasing distance from water surface. On an average, it reaches highest value in the region near to that corresponds to the near wall region. Towards bed the ejection again decreases gradually.

The decrease in Q_2 is compensated by the increase in Q_4 contribution. Increase in Q_4 contribution towards bed indicates high speed in-rushes. The contribution of Q_1 and Q_3 are more near the water surface. The sign of the probability of occurrence $(S_{i,H})$ changes at a point where the sweep overtakes the ejection. The ratio of sweep contribution to ejection contribution for series of 1S and 2L are presented in Figure 7.12 .

A ratio of around 0.8 is observed at the middle part of the flow in both series. Similar pattern of observations have been reported by Balachandar and Bhuiyan (2007) after performing tests over smooth and rough bed and Ramesh (2012) over transitionally rough bed. Both the researchers have obtained the above said ratio of 0.7. Balachandar and Bhuiyan (2007) reported that there was no difference in the Q_1, Q_3 and Q_4 contributions between smooth and rough wall flow and difference was noticed only in Q_2 profile.

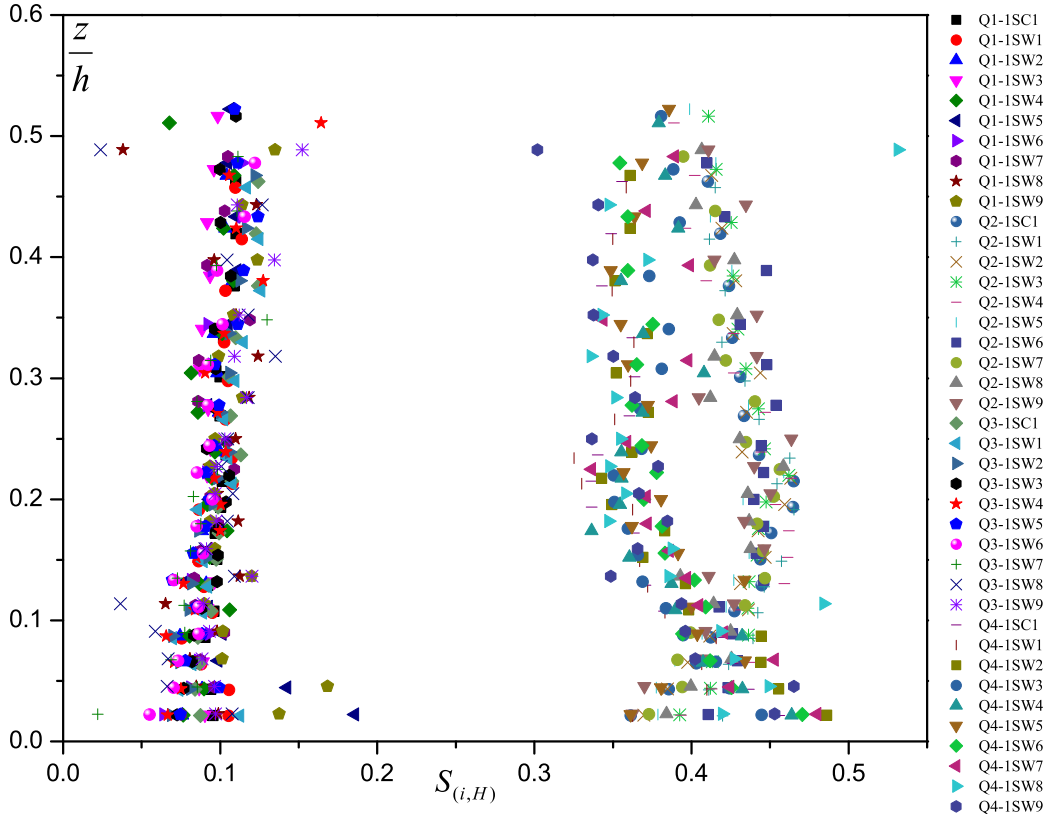

(a) Bursting events for series 1S

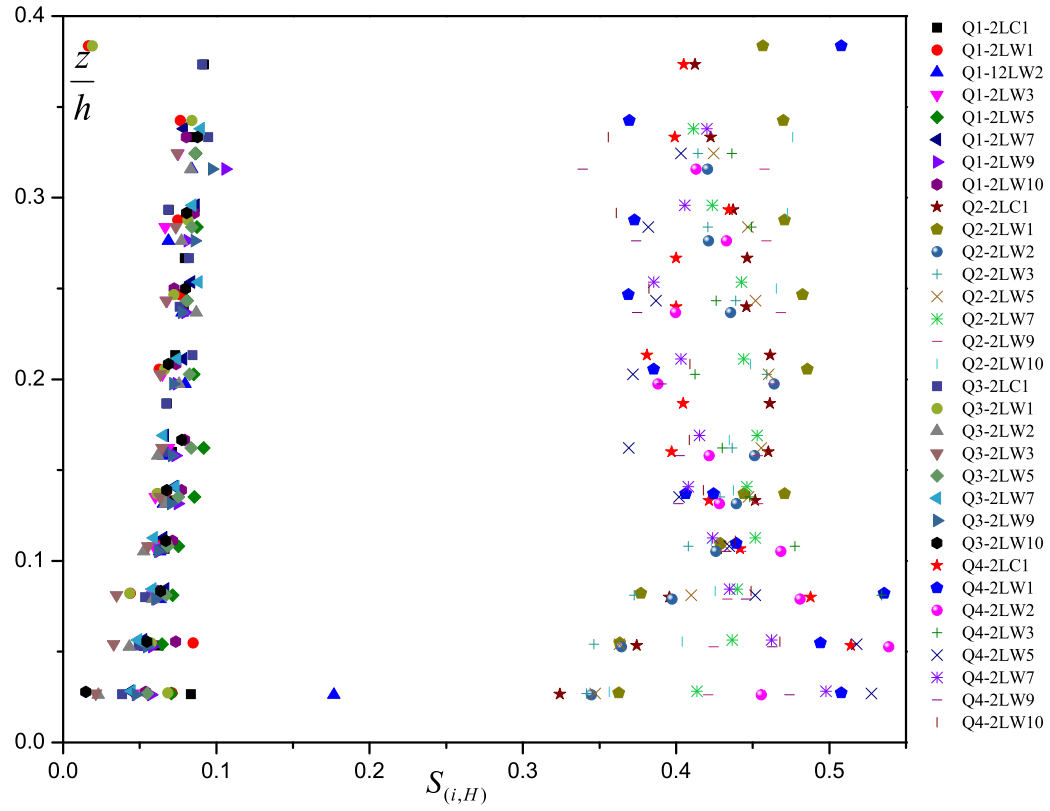

(b) Bursting events for series 2L

Figure 7.11: Distributions of four different bursting events

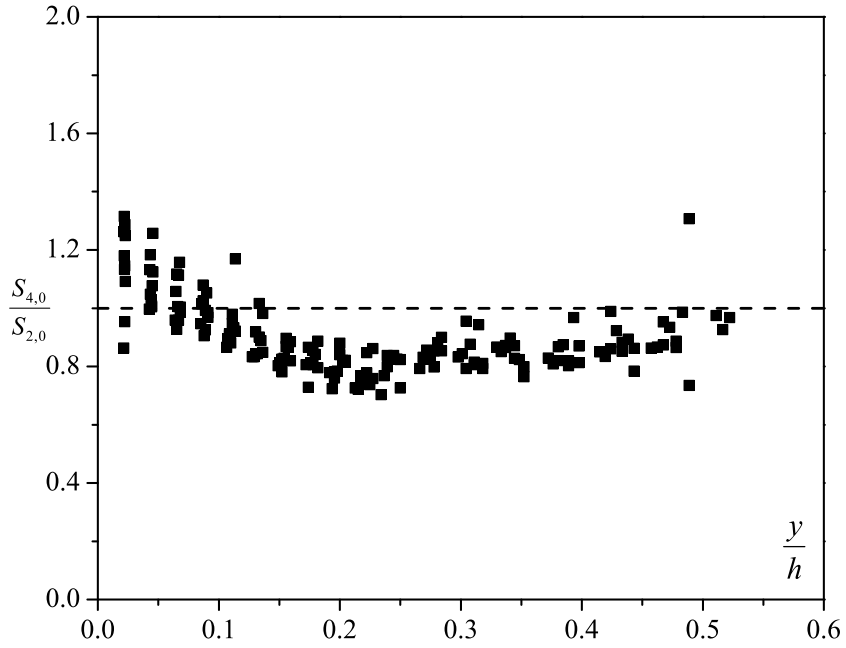

(a) Sweep to ejection ratio for series 1S

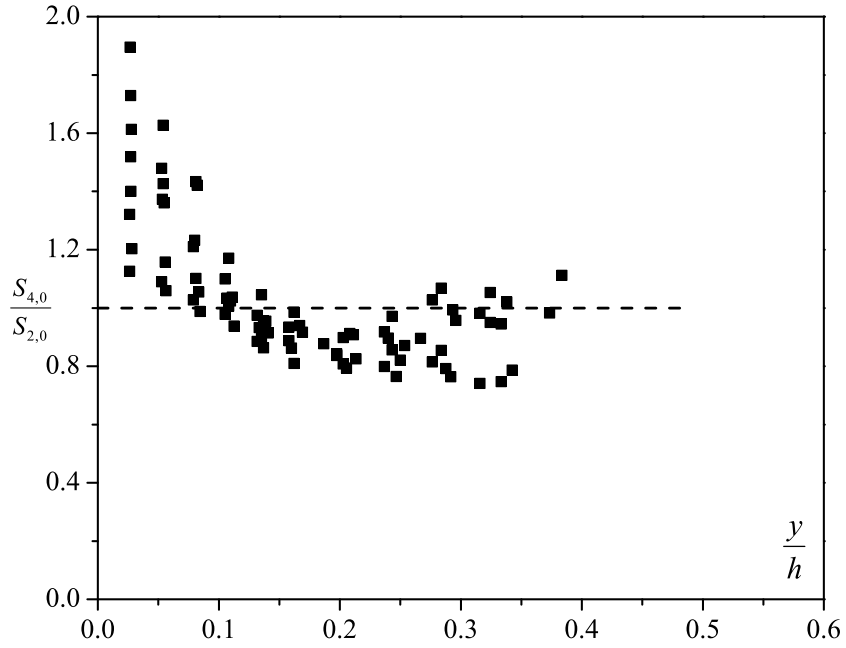

(b) Sweep to ejection ratio for series 2L

Figure 7.12: Vertical distributions of the ratio of contributions by sweep to ejection

7.7 Concluding Remarks

One of the main objectives of the study was to experimentally investigate the turbulence characteristics of open channel flow carrying suspended sediment over mobile bed. The same has been done in this chapter with the help of data collected using ADV. Two different series (1S and 2L) each consisting of several experimental runs and having different flow depth, velocity and different size surface material have been selected for study. The study shows that the velocity profile across the flow depth well follows the standard open channel velocity distribution. For those runs in which velocity profiles were measured at more than one locations shows very good matching of velocity profiles at different locations along the flow. This indicates a well developed steady uniform flow. The results of turbulence intensities correlate well with the findings of other researchers, and the effect of bed roughness is felt only in the near wall region. Dampening of the turbulence intensity with an increase in suspended sediment concentration and bottom roughness are also evident from the figures. The turbulent kinetic energy distribution obtained in this study shows a proper synchronization with the turbulence intensities. The Reynold shear stress distribution is also in well agreement with the previous findings. RSS gradually increases away from bed, attains a maximum value and again decreases towards the water surface. Self developed FORTRAN 95 code was used to decompose instantaneous velocity to study the dominating burst event. Out of the four events, ejection and sweeping was found to be dominant. The ejection contribution gradually increases from the free surface towards bed; attains a maximum value near the wall region and then decreases again towards bed. It was summarized that ejection and sweep may be mainly responsible for the sediment detachment and its transport.

Chapter 8

Conclusions

8.1 General

The primary objective of this study was to experimentally investigate the routing of suspended sediment through gravel bed channel. Numerous set of experiments were conducted in hydraulic laboratory of Indian Institute of Technology Roorkee, India. Three uniform gravels of varying sizes (5.2 mm, 2.7 mm and 1.9 mm) were used to form the bed of the channel. Very fine non cohesive sediment (silt) of median size 0.062 mm was used for the routing purpose. The runs were grouped under various series and each series were having different hydraulic conditions. The runs within each series were conducted at successive increasing concentration and maintaining same hydraulic condition. Experiments were conducted to analyse the velocity distribution, resistance to flow, infiltration of fines, bed load transport during sediment laden runs and entrainment of fine sediments deposited in the bed during passage of clear water. The turbulence characteristics of the flow were also investigated. The various measurements taken during the experimental runs were;

- Bed load transport due to flowing water containing suspended sediment.
- Average suspended sediment concentration (width integrating suspended sample)
- Depth wise suspended sediment concentration
- Measurement of velocity profile using Pitot tube
- Real time point velocity measurements using ADV

- Water surface profile
- Bed profile before and after each experimental run
- Proportion of fine sediment in different layers of bed by grab sampling method

A mathematical model was developed to compute the change in bed composition. Relationships were developed for the resistance to flow, change in Von Karman constant with varying suspended sediment concentration, bed load transport rate. Apart from these, turbulence analysis of the flow has also been carried out. Some general conclusions that have been drawn from the study are;

8.2 General Conclusions

- The fine sediments (silt) were found to infiltrate into the pores of gravel bed during its routing. Silt infiltrated down to the bottom of the gravel bed in case of bed composed of larger gravel sizes (5.2 mm and 2.7 mm). But while passing through smaller size gravel (1.9 mm), silt could only manage to infiltrate slightly below the top surface.
- At any particular concentration, the infiltration of fine sediment into the bed continued till equilibrium was reached. The equilibrium was supposed to reach when the rate of entrainment of fines became equal to the rate of deposition. The deposition of fines started in bottom up direction.
- The proportion of fines in each layer of bed increased with an increase of fine sediment concentration in flow.
- The bed level before and after the run remained practically same. No undulations, crests and troughs were observed.
- The resistance to flow was found to be affected by the presence of suspended sediment. The existing relations of resistance didn't validate accurately the present study data.
- The bed load transport was also found to be affected by the presence of suspended load.

Some specific conclusions drawn from the study are;

8.3 Specific Conclusions

8.3.1 Resistance to flow

The vertical velocity distributions have been checked for variation of Von Karman constant "κ". Considering the fact that increased sediment concentration at the bottom of flow may change the velocity distribution, logarithmic velocity distribution was plotted for all runs. It was found that Von Karman constant gradually decreased with the increasing suspended sediment concentration. A relationship to estimate "κ" with changing concentration was derived and is given in equation (4.1) . The chances of further decrease in "κ" value with further increase in concentration may be investigated.

Arora et al. (1986) has proposed a criterion for prediction of friction factor for the case of flow carrying suspended sediment. The same criterion didn't hold good for the present study data. For alluvial channel, it was observed that friction factor decreases with the increasing concentration. Based on the present study data and some previous data, a new friction factor prediction equation was derived and is given in equation (4.9) . About 86% of the present study data lie within the error band of $\pm 10\%$ with the derived friction factor relation.

8.3.2 Analysis of the Fines Infiltration an Entrainment

In all the runs with bed composed of large size gravel (5.2 mm and 2.7 mm), the fine sediments infiltrated down to the bottom of the bed. It was observed that fine sediment deposited per unit depth was more at the bottom of the bed and decreased as one moves up. The proportion of fines deposition gradually decreased towards the top surface but the difference was just marginal. Whereas the deposition phenomena in bed composed of small size gravel (1.9 mm) was quite different. The fines managed to filtrate only half way down the gravel bed. Contrary to large size gravel beds, the fines proportion in the bed composed of 1.9 mm was gradually increasing towards top surface and hence maximum fines were deposited on the top layer of bed. The entrainment of the fine sediments by the clear water, deposited during the routing of sediment laden flow was quite similar in all the experimental runs conducted with all the three gravels. At very low clear water discharge (below incipient condition), the clear water only washed the fines attached to the gravel surface. At progressively higher discharge, the clear water was

able to entrain deeper and deeper depth of fines. Along the channel, it was observed that fines proportion in the gravel bed gradually decreased towards downstream. However, the difference was just marginal.

A one dimensional numerical model based on the sediment and flow continuity and flow momentum equations has been developed for studying the process of routing of wash material through a coarse bed stream. The continuity equation (5.16) for the process of routing of fine sediments through coarse bed stream is derived. The governing equations used in the model are explained through equations (5.16) to (5.18) . A predictor and corrector based finite difference numerical scheme of MacCormack (1969) was utilized along with initial and boundary conditions in the solution. A computer program was developed in FORTRAN 95 to solve the governing equations. The proposed model was capable of satisfactorily predicting the change in bed composition with time and distance. The model accurately predicted the change in the porosity of the bed. The computed values of porosity resembled well with the corresponding observed porosity. The computed values of porosity fell within the range of ±7% from the observed porosity value. The model predicted that at a particular section of gravel bed, the porosity of bed decreased with time and with increasing suspended sediment concentration in flow. At equilibrium condition, at a particular section, the porosity became almost constant.

8.3.3 Bed load transport

The transport of bed material is found to increase with the increasing suspended sediment concentration. Though fines were deposited in the pores of gravel bed, it was supposed that the new properties of the bed material remained same as that of parent bed material. Some of the existing bed load transport relations (Meyer-Peter and Müller 1948; Misri et al. 1984 and Patel and Ranga Raju 1996) were tested for their applicability for the present data. None of those selected relations estimated bed load satisfactorily in its original form. Since the relationships were derived for relatively clear water flow, the estimations of bed load transport by the above mentioned methods were not very accurate for the present data. The modified flow velocity obtained from the modified friction factor (friction factor predictor equation 4.9) was used in the same relations tested earlier. The combination of the modified flow velocity with Misri et al. (1984) bed load transport relation resulted in satisfactory results with just 10% data falling beyond the error band of $\pm 30\%$.

8.4 Turbulence Analysis

The turbulence characteristics of flow over mobile rough bed were experimentally investigated in this study. Three dimensional instantaneous flow velocity components were measured at various points along the flow using ADV. The real time velocities were then analyzed to understand the various turbulence characteristics.

The velocity profiles drawn from the data were quite similar to the standard velocity distribution profile. Close observation of the plots showed that there was not much variation in the velocity profile taken at various longitudinal locations. This indicated a steady and uniform flow in the study reach of the flume. Plots that show the velocity distribution at particular location with increasing concentration showed that as the concentration of fines increased, average flow velocity has also marginally increased. In Chapter 4, it has been mentioned that flow velocity increased due to decreased friction factor in the presence of increasing concentration. This has been supported by Figures 7.5 and 7.6 .

The findings of turbulence intensities (TI) correlated reasonably well with the findings of previous results (Nezu and Nakagawa 1993). The maximum value of turbulence intensities was observed on an average in wall region i.e. $z/h \leq 0.2$. Very close to the bed, the TI was observed to decrease. The rough element present on the bed may be supposed to be responsible for reduction in TI value. It was observed that peak turbulence intensity decreased with an increase in bed roughness. The ratios of TI_v/TI_u and TI_w/TI_u have been observed to be slightly smaller than the previously observed values (Nezu and Nakagawa 1993; Song and Chiew 2001).

The turbulent kinetic energy distributions synchronized with the distribution of turbulence intensities. Reynold stress across the flow depth was also quantified. Reynold stress attained maximum value in the near wall region and then decreased towards bed.

Ejection and sweep events dominated the flow structure and they extended over the whole depth. In the middle part of flow depth, the ratio of contributions of sweep to ejection was observed to be about 0.8.

Bibliography

[1] Adams, J. N., Beschta, R. L. 1980. Gravel bed composition in Oregon coastal streams. Canadian Journal of Fisheries and Aquatic Science. 37(10), 1514-1521.

[2] Alabaster, J.S., Llyod, R.L. 1981. Water quality criteria for fresh water. Butterworth, London, pp. 297.

[3] Aldridge, D.W., Payne, B.S., Miller, A.C., 1987. The effects of intermittent exposure to suspended solids and turbulence on three species of fresh water mussel. Environmental Pollution. 45(1), 17-28.

[4] Ali, K.H.M., Lim, S.Y. 1986. Local scour caused by submerged wall jets. Proceedings of Institution of Civil engineers, Part 2, 81(4),607-645.

[5] Antonia, R.A., Krogstad, P. 2001. Turbulent structure in boundary layers over different types of surface roughness. Fluid Dynamics Research, 28(2), 139-157.

[6] Arora, A.K., Ranga Raju, K.G., Garde, R.J. 1986. Resistance to flow and velocity distribution in rigid boundary channels carrying sediment-laden flow. Water Resources Research, 22(6), 943-951.

[7] Ashida, K. Michue, M. 1971. An investigation of river bed degradation downstream of dam. Proceedings of 14th congress of IAHR, 3, 247-256.

[8] Balachandra R., Bhuiyan F. 2007. Higher-order moments of velocity fluctuations in an open-channel flow with large bottom roughness. Journal of Hydraulic Engineering, ASCE, 133(1),77-87.

[9] Balachandra R., Reddy, P. 2013. Scour caused by wall jets, sediment transport processes and their modelling applications. Dr. Andrew Manning (Ed.), ISBN: 978-953-51-1039-2.

[10] Barenblatt, G.I. 1996. Scaling, self-similarity and intermediate asymptotics. Cambridge University Press, London, UK.

[11] Barton, B. A. 1977. Short-term effects of highway construction on the limnology of a small stream in southern Ontario. Freshwater Biology, 7(2), 99-108.

[12] Barton, J. R., Lin, Pin-Nam 1955. A study of the sediment transport in alluvial channels. Civil Engineering Department, Colorado State University, Fort Collins, Colorado., pp.43.

[13] Bash J., Berman, C., Bolton, S. 2001. Effects of turbidity and suspended solids on salmonids. Research Project T1803, Task 42, Center for Streamside Studies, University of Washington, Seattle, WA.

[14] Bathurst, J. C. 2002. At-a-site variation and minimum flow resistance for mountain rivers. Journal of Hydrology, 269 (12), 1126.

[15] Bathurst, J.C. 2007. Effect of coarse surface layer on bed-load transport. Journal of Hydraulic Engineering, ASCE, 133(11), 1192-1205.

[16] Baxter, C.V., Hauer, F.R. 2000. Geomorphology, hyporheic exchange, and selection of spawning habitat by bull trout (Salvelinus confuentus). Canadian Journal of Fisheries and Aquatic Sciences. 57(7), 1470-1481.

[17] Berkman, H. E., Rabeni, C. F. 1987. Effects of siltation on stream fish communities. Environmental Biology of Fishes, 18(4), 285-294.

[18] Beschta, R.L., Jackson, W.L. 1979. The intrusion of fine sediments into a stable gravel bed. Journal of Fishery Research Board Canada, 36(2), 204-210.

[19] Birkinshaw, S. J., Bathurst, J. C., Iroum, A., Palacios, H. 2011. The effect of forest cover on peak flow and sediment dischargean integrated field and modelling study in centralsouthern Chile. Hydrological Processes, 25(8): 12841297

[20] Bogard, D.G., Tiderman, W.G. 1986. Burst detection with single point velocity measurement. Journal of Fluid Mechanics, 162, 389-413.

[21] Borah, D.K., Alonso, C.V., Prased, S.N. 1982. Routing of graded sediment in streams: Formulation. Journal of Hydraulic Division, ASCE,108(12), 1486-1503.

[22] Bridge, J.S., Bennet, S.J. 1992. A model for the entrainment of transport of sediment grains of mixed sizes, shapes and densities. Water Resources Researches, 28(2), 337-363.

[23] Brookes, A. 1986. Response of aquatic vegetation to sedimentation downstream from river channelization works in England and Wales. Biological Conservation, 38, 352-367.

[24] Buckley, A.B. 1922. The influence of silt on the velocity of water flowing in open channels. Minutes of Proceedings, Institution of Civil Engineers 216(1923), 183-211.

[25] Cardoso, A. H., Graf, W. H., Gust, G. 1989. Uniform flow in a smooth open channel. Journal of Hydraulic Research, IAHR, 27(5), 603-616.

[26] Carling, P. A. 1984. Deposition of Fine and Coarse Sand in an Open- Work Gravel Bed. Canadian Journal of Fisheries Aquatic Science, 41(2), 263-270.

[27] Carling, P. A., McCahon, C. P. 1987. Natural siltation of brown trout (Salmo trutta L.) spawning gravels during low-flow conditions. Pp. 229-244 in J. F. Craig and J. B. Kemper (eds.), Regulated streams: Advances in ecology. Plenum Press, New York.

[28] Carollo, F.G., Ferro, V., Termini, D. 2005. Analysisng turbulence intensity in gravel bed channels. Journal of Hydraulic Engineering, ASCE, 131(12), 1050-1061.

[29] Cellino, M. and Graf, W.H. 1999. Sediment laden flow in open channels under non capacity and capacity conditions. Journal of Hydraulic Engineering, ASCE, 125(5), 455-462.

[30] Chapman, D. W. 1988. Critical review of variables used to define effects of fines in redds of large salmonids. Transactions of the American Fisheries Society. 117(1), 1-21.

[31] Cioffi, F., Gallerano, F. 1991. Velocity and concentration profiles of solid particles in a channel with movable and erodible bed. Journal of Hydraulic Research, IAHR, 29(3), 387-401.

[32] Cline, L.D., Short, R.A., Ward, J.V. 1982. The influence of highway construction on macriinvertebrates and epilithic algae og a high mountain stream. Hydrobiologia, 96(2), 149-159.

[33] Colby, B.R. 1964. Discharge of sands and mean velocity relationship in sand bed streams. Professional paper no. 462-A, United States Geological Survey, Washington, D.C.

[34] Coleman, N.L. 1981. Velocity profiles with suspended sediment. Journal of Hydraulic Research, IAHR, 19(3), 211-229.

[35] Coleman, N. L. 1986. Effect of Suspended Sediment on Open Channel Velocity Distribution. Water Resources Research, 22(10), 1377-1384.

[36] Coleman, N. L., Alonso, C. V. 1983. Two-dimensional channel flow over rough surfaces. Journal of Hydraulic Engineering, 109(2), 175-188.

[37] Cordone, A.J., Kelly, D.W. 1961. The influence of inorganic sediment on the aquatic life of stream. California Fish and Game. 47, 189-228.

[38] Correia, L.R.P. 1992. Numerical modeling of unsteady channel flow over mobile boundary. PhD Thesis, EPFL, Lausanne, Switzerland.

[39] Culp, J.M., Wrona, F.J., Davies, R.W. 1985. Response of stream benthos and drift to fine sediment depositionversus transport. Canadian Journal of Zoology. 64(6), 1345-1351.

[40] Davies-Colley, R.J., Hickey, C.W., Quinn, J.M., Ryan, P.A. 1992. Effects of clay discharges on streams 1. Optical properties and epilithon. Hydrobiologia. 248(3), 215-234.

[41] Davies-Colley, R. J., Smith, D. G. 2001. Turbidity, suspended sediment and water clarity. A review. Journal of the American Water Resources Association 37(5), 1-17.

[42] Dey, S., Raikar, R.V. 2007. Characteristics of loose rough boundary streams at near threshold. Journal of Hydraulic Engineering, ASCE, 133(3), 288-304.

[43] Dhamotharan, S., Wood, A., Parker, G., Stefan, H. 1980. Bed load transport in a model gravel stream. Project Report No. 190. St. Anthony Falls Hydraulic Laboratory, University of Minnesota.

[44] Diplas, P. 1994. Modeling of fines and coarse sediment interaction over alternate bars. Journal of Hydrology, 159(1-4), 335-351.

[45] Diplas, P., Parker, G. 1985. Pollution of gravel spawning grounds due to fine sediment. Project Report, No. 240, St. Anthony Falls Laboratory, University of Minnesota, Minneapolis, Minnesota.

[46] Diplas, P., Parker, G. 1992. Deposition and removal of fines in gravel bedstreams. Dynamics of gravel bed rivers, John Wiley and Sons Ltd, 313-329.

[47] Drake, T.G., Shreve, R.L., Dietrich, W.E., Whiting, P.J., Leopold, L.B. 1988. Bed load transport of fine gravel observed by motion picture photography. Journal of Fluid Mechanics, 192, 193-217.

[48] Egiazaroff, I.V. 1965. Calculation of nonuniform sediment concentration. Journal of Hydraulic Division, ASCE, 91(4), 225-247.

[49] Einstein, H. A. 1950. The Bed-Load Function for Sediment Transport Channel Flows. USDA, Tech. Bull. No. 1026, Washington D.C.

[50] Einstein, H.A. 1968. Deposition of suspended particles in a gravel bed. Journal of Hydraulic Division, 94(5), 1197-1205.

[51] Einstein, H. A., Anderson, A. G., Johnson, J.W. 1940. Distinction between bed load and suspended load in natural streams. Transcation of American Geophysical Union, 21(2), 628-633.

[52] Einstein, H.A., Chien, N. 1955. Effects of heavy sediment concentration near the bed on the velocity and sediment distribution. Institute of Engineering Research, University of California, Berkeley, California, USA, 33(2).

[53] Elata, C., Ippen, A.T. 1961. Dynamics of Open Channel Flow with Suspensions of Neutrally Buoyant Particles. Technical Report No. 45, MIT Hydro- dynamics, Massachusetts, US.

[54] Erman, D.C., Ligon, F.K. 1988. Effects of discharge fluctuation and addition of fine sediment on stream fish and macroinvertebrates below water filtration facility. Environmental Management, 12(1), 85-97.

[55] Frostick, L. E., Lucas, P. M., Reid, I. 1984. The infiltration of fine matrices into coarse-grained alluvial sediments and its implications for stratigraphical interpretation. Journal of Geological Society London. 141(6), 955-965.

[56] Gammon, J. R. 1970. The effect of inorganic sediment on stream biota. Environmental Protection Agency, Water Pollution Control Research, Series, 18050 DWC 12/70. USGPO, Washington, DC.

[57] Garcia, C.M., Cantero, M.I. Nino, Y. Garcia, M.H. 2005. Turbulence measurement with acoustic Doppler velocimeter. Journal of Hydraulic Engineering, ASCE, 131(12), 1062-1073.

[58] Garde, R. J., Ranga Raju, K. G. 1985. Mechanics of sediment transportation and alluvial stream problems, Second Edition, Wiley Eastern Limited, New Delhi, India.

[59] Goel, A. 2008. Estimation of Scour Downstream of Spillways Using SVM Modeling. Proceedings of the World Congress on Engineering and Computer Science, USA, October 22 - 24.

[60] Goel, A., Pal, M. 2009. Application of support vector machines in scour prediction on grade-control structures. Engineering Applications of Artificial Intelligence 22(2), 216-223.

[61] Graham, A. A. 1990. Siltation of stone surface periphyton in rivers by clay sized particles from low concentration in suspension. Hydrobiologia, 199(2), 107-115.

[62] Grass, A. J. 1971. Structural Features of Turbulent Flow over Smooth and Rough Boundaries. Journal of Fluid Mechanics, 50(2),223-256.

[63] Greig, S. M., Sear, D. A., Carling, P.A. 2005. The impact of fine sediment accumulation on the survival of incubating salmon progeny: implications for sediment management. Science of the Total Environment. 344(1-3), 241-258.

[64] Guo, J. 1998. Turbulent velocity profiles in clear water and sediment-laden flows. Ph.D. dissertation, Colorado State University, Fort Collins.

[65] Guo, J., Julien, P. Y. 2001. Turbulent velocity profiles in sediment laden flows. Journal of Hydraulic Research, IAHR, 39(1), 11-23.

[66] Harrod, T. R., Theurer, F. D., 2002. Sediment. In: Haygarth, P.M., Jarvis, S.C. (Eds.), Agriculture, Hydrology and Water Quality. CABI, Wallingford, pp. 502.

[67] Hayashi, T., Ozaki, S., Ichibasi, T. 1980. Study on bed load transport of sediment mixture. Proceedings Of 24th Congress on Hydraulics, 35-43.

[68] Holtorff, G. 1985. The Role of the Karman Number in Suspended Sediment Transport. In: Proceedings of Euromech 192: Transport of Suspended Solids in Open Channel, Neubiberg, Germany, 23-28.

[69] Huang, X., Garcia, H. 2000. Pollution of gravel spawning ground by deposition of suspended sediment. Journal of Environmental Engineering, ASCE, 126(10), 963-967.

[70] Hynes, H. B. N. 1970. The Ecology of Running Waters. Liverpool University Press, Liverpool.

[71] IIHR and U.S. Govt. 1957. A study of measurement and analysis of sediment loads in streams: some fundamental of particle size analysis. Report No. 12

[72] Imamoto, H., Asano, T., Ishigaki, T. 1977. Experimental investigation of a free surface shear flow with suspended sand grains. In: Proceedings of 17th Congress, Inter- national Association for Hydraulic Research, 1, 105-112.

[73] Ippen, A.T. 1971. A new look at sedimentation in turbulent streams. Journal of Boston Society of Civil Engineers, 58(3), 131-163.

[74] Jeffreys, H. 1929. On the transport of sediment in stream. Proceedings of Cambridge Philosophical Society, 25, 3.‘

[75] Karim, F. 1998. Bed material discharge prediction for nonuniform bed sediment. Journal of Hydraulic Engineering, ASCE, 124(6), 597-604.

[76] Keulegan, G. H. 1938. Laws of turbulent flow in open channels. NBS Vol. 21, U.S. Dept. of Commerce, Washington, D.C.

[77] Khullar, N. K. 2002. Effect of wash load on transport of uniform and nonuniform sediments. Ph.D. thesis, Indian Institute of Technology Roorkee, India.

[78] Khullar, N.K., Kothyari, U. C., Ranga Raju, K. G. 2007. Bed load transport in the presence of wash load transport. ISH Journal Hydraulic Engineering, 13(1), 106-122.

[79] Khullar, N.K., Kothyari, U. C., Ranga Raju, K. G. 2010. Effect of wash load on flow resistance. Journal of Hydraulic Research, IAHR, 45(4), 497-504.

[80] Kikkawa, H., Fukuoka, S. 1969. The characteristics of flow with wash load. In: Proceeding of the 13th Congress, IAHR, Ecole Polytechnique Federale, Lausanne, Switzerland, 2, 233-240.

[81] Kirkoz, S. 1989. Turbulent velocity profiles for smooth and rough open-channel flow. Journal of Hydraulic Engineering, ASCE, 115(11), 1543-1561.

[82] Kim, H.T., Kline, S.J., Reynolds, W.C. 1971. The production of turbulence near a smooth wall in turbulent boundary layer. Journal of Fluid Mechanics, 50(1), 133-160.

[83] Kironoto, B. A., Graf, W.H. 1994. Turbulence characteristics in rough non-uniform open- channel flow. In: Proceedings of Institution of Civil Engineers, Water, Maritime & Energy. 112, 336-348.

[84] Kondolf , G. M. 1997. Hungry water: effects of dams and gravel mining on river channels. Environmental Management, 21(4), 533-551.

[85] Kothyari, U. C., Jain, R. K. 2010. Erosion characteristics of cohesive sediment mixtures. River Flow, 815-820.

[86] Kothyari, U. C., Kumar, A., Jain, R. K. 2014. Influence of cohesion on river bed scour in wake region of piers. Journal of Hydraulic Engineering, ASCE, 140(1), 1-13.

[87] Kraus, N.C., Lohrmann, A., Cabrea, R. 1994. New acoustic meter for measuring 3D laboratory flows. Journal of Hydraulic Engineering, ASCE, 120(3), 406-412.

[88] Kumar, A., Jain, R.K., Kothyari, U.C. 2011. Flow characteristics in wake zone of a pier founded in clay-sand-gravel mixture. 34th IAHR World Congress, Brisbane, Australia 26th June to 1st July.

[89] Kumar, P. 1988. Mathematical modeling of transient bed profiles in nonuniform sediment. M.E. Thesis, Department of Civil Engineering, University of Roorkee, India.

[90] Lane, E. W. 1947. Report of the subcommittee on sediment terminology. Transaction of American Geophysical Union, 28.

[91] Langer, O. E. 1980. Effects of sedimentation on salmonid stream life. In: Weagle, K. (Ed.), Report on the Technical Workshop on Suspended Solids and the Aquatic Environment. Contract No. OH-80-019, Department of Indian Affairs and Northern Development, Whitehorse, Yukon Territory. 21

[92] Lau, Y. L. 1983. Suspended sediment effect on flow resistance. Journal of Hydraulic Engineering, ASCE, 109(5), 757-763.

[93] Laursen, E.M. 1958. Total sediment load of streams. Journal of Hydraulic Division, ASCE, 84(1), 1-36.

[94] Lemly, A. D. 1982. Modification of benthic insects communities in polluted stream: Combined effects of sedimentation and nutrient enrichment. Hydrobiologia, 87(3), 229-245.

[95] Levasseur, M., Bergeron, N.E., Lapointe, M.F., Berube F. 2006. Effects of silt and very fine sand dynamics in Atlantic salmon (Salmo salar) redds on embryo hatching success. Canadian Journal of Fisheries and Aquatic Sciences, 63(7), 1450-1459.

[96] Lewis, K. 1973a. The effect of suspended coal particles on the life forms of the aquatic moss Eurhynchium riparicides (hedw.). I. The gametophyte plan. Fresh Water Biology, 3(3), 251-257.

[97] Lewis, K. 1973b. The effect of suspended coal particles on the life forms of the aquatic moss Eurhynchium riparicides (hedw.). II. The effect of spore germination and generation of apical tips. Fresh Water Biology, 3(4), 391-395.

[98] Li, Y. T. 1987. Initial study of the bed material gradation under deposition-erosion equilibrium. Journal of Sediment Research, 1, 82-87.

[99] Li, Y.T., Wang, F., Tang, J.W., Zhu, L.L. 2013. Mechanism and prediction of bank failure. Advances in River Sediment Research- Fukuoka et al. (eds.)

[100] Liriano, S.L. Day, R.A. 2000. Structures of turbulent flow in scour holes downstream of submerged jets, in stochastic hydraulics. In: Wang, and Hu (eds.), Balkema, Rotterdam.

[101] Lisle, T. 1980. Sedimentation of Spawning Areas during Storm Flows, Jacoby Creek, North Coastal California. Presented at the fall meeting of the American Geophysical Union, San Francisco, Dec.

[102] Lu, S.S., Willmarth, W.W. 1973. Measurements of structure of the Reynolds stress in a turbulent boundary layer. Journal of Fluid Mechanics, 60(3), 481-511.

[103] Lyn, D. A. 1992. Turbulence Characteristics of Sediment-Laden Flows in Open Channels. Journal of Hydraulic Research, IAHR, 118(7), 971-988.

[104] MacCormack, R.W. 1969. The effect of viscosity in hypervelocity impact cratering. paper 69-354, American Institute of Aeronautics, Cincinnati, Ohio.

[105] McNeil, W. J., Ahnell, W. H. 1964. Success of pink salmon spawning relative to size of spawning bed material. US Fish and Wildlife Service. Special Scientific Report, Fisheries 469: Washington, DC.

[106] Meyer-Peter, E., Müller, R. 1948. Formulas for bedload transport. In Proceedings 2nd Meeting International Association of Hydraulic Research Stockholm, 39-64.

[107] Milhous, R. T. 1973. Sediment transport in a gravel bottomed stream. Ph.D. thesis, Oregon State University, Corvallis, Oregon, USA.

[108] Misri, R. L., Garde, R. J., Ranga Raju, K. G. 1984. Bed load transport of coarse nonuniform sediment. Journal of Hydraulic Engineering, ASCE, 110(3), 312-328.

[109] Mittal, M.K., Porey, P.D., Ranga Raju, K.G. 1990. Bed load transport of non uniform sediment. Proceedings of the Euromech 262- Colloquium on sand transport in river, estuaries and sea, Wallingford UK.

[110] Mohapatra, P., Bhallamudi, S. 1994. Bed-Level Variation in Channel Expansions with Movable Beds. Journal of Irrigation and Drainage Engineering, ASCE, 120(6), 11141121.

[111] Mohnakrishnan, A. 2001. Reservoir sedimentation. Seminar on Reservoir sedimentation, Ooty, TamilNadu, India.

[112] Muste, M., Patel, V. C. 1997. Velocity profiles for particles and liquid in open-channel flow with suspended sediment. Journal of Hydraulic Engineering, ASCE, 123(9), 742-751.

[113] Nakagawa, H., Tsujimoto, T. 1980. Sand bed instability due to bed load motion. Journal of Hydraulic Division, ASCE, 106(12), 2029-2051.

[114] Nezu, I., Nakagawa, H. 1993. Turbulence in Open Channel Flows. IAHR Monograph, Balkema, Rotterdam.

[115] Nezu, I., Rodi, W. 1986. Open-channel flow Measurements with a Laser-Doppler Anemometer. Journal of Hydraulic Engineering, ASCE, 112(5), 335-355.

[116] Newcombe, C. P., MacDonald, D. D. 1991. Effects of suspended sediments on aquatic ecosystems. North American Journal of Fisheries Management, 11(1), 72-82.

[117] Niekerk, A.V., Vogel, K.R., Slingerland, R.L., Bridge, J.S. 1992. Routing of heterogeneous sediment over mobile bed. Model development. Journal of Hydraulic Engineering, ASCE, 118(2), 246-262.

[118] Nikora, V., Goring, D. 2000. Flow turbulence over fixed and weakly mobile gravel beds. Journal of Hydraulic Engineering, ASCE. 126(9), 679-690.

[119] Olsson, T. I., Petersen, B. 1986. Effects of gravel size and peat material on embryo survival and alevin emergence of brown trout, Salmo trutta L. Hydrobiologia. 135, 9-14.

[120] Papanicolaous, A.N., Diplas, P., Balakrishnan, M., Dancey, C.L. 2001. The role of near bed turbulence structure in the inception of sediment motion. J. Eng. Mech., 127(3), 211-219.

[121] Parker, G. 1990. Surface based bed load transport relationships. Journal of Hydraulic Research, IAHR, 28(4), 417-436.

[122] Parker, G., Coleman, N. L. 1986. Simple model of sediment laden flows. Journal of Hydraulic Engineering, ASCE, 112(5), 356-375.

[123] Patel, P. L., Ranga Raju, K. G. 1996. Fractionwise calculation of bed load transport. Journal of Hydraulic Research, IAHR, 34(3), 363-379.

[124] Pullaiah, V. 1978. Transport of fine suspended sediment in smooth bed channels. Ph.D. Thesis, University of Roorkee, Roorkee, India.

[125] Quinn, J. M., Davies- Coley, R. J., Hickey, C. W., Vickers, M. L., Ryan, P. A. 1992. Effects of clay discharges on streams 2. Benthic invertebrates. Hydrobiologia, 248(3), 235-247.

[126] Rahuel, J.L., Holly, F.M., Chollet, J.P., Belleudy, P., Yang, G. 1989. Modeling of river bed evolution for bed load sediment mixtures. Journal of Hydraulic Engineering, ASCE, 115(11), 1521-1542.

[127] Ramesh, B. 2012. Near bed particle motion over transitionally rough bed using high speed imaging. PhD thesis, Department of Civil Eng. Indian Institute of Technology Roorkee, India.

[128] Reiser, D. W., White, R. G. 1990. Effects of stream flow reduction on Chinook salmon egg incubation and fry quality. Rivers. 1, 110-118.

[129] Reddy, H.A., Roussinova, V., Balachandar, R., Bolisetti, T. 2012. Higher-order moments of velocity fluctuations in an open channel flow with mobile bedforms. River Flow Murillo (Ed.)

[130] Richards, C., Bacon, K. L. 1994. Influence of fine sediment on macroibvertebrates colonization of surface and hyporheic stream substrate. Great Basin Naturalist, 54(2), 106-113.

[131] Rosenberg, D. M., Weins, A. P. 1978. Effects of sediment addition on macrobenthic invertebrates in a northern Canadian stream. Water Research, 12, 753-763.

[132] Ryan, P. A. 1991. Environmental effects of sediment on New Zealand streams: A review. New Zealand Journal of Marine and Freshwater Research. 25(2), 207-221.

[133] S. Murty Bhallamudi, Chaudhry, M.H. 1991. Numerical modeling of aggradation and degradation in alluvial channels. Journal of Hydraulic Engineering, ASCE, 117(9) 1145-1164.

[134] S. Murty Bhallamudi, Chaudhry, M.H. 1992. Computation of flows in open-channel transitions. Journal of Hydraulic Research, IAHR, 30(1), 77-93.

[135] Samaga, B.R., Ranga Raju, K.G., Garde, R.J. 1986. Bed load transport of sediment mixture. Journal of Hydraulic Engineering, ASCE, 112(11), 1003-1018.

[136] Samaiya, N.K. 2009. Effect of cohesive wash load on transport of nonuniform sediments. PhD thesis, Indian Institute of Technology Roorkee, India.

[137] Sarma , K. V. N., Lakshminarayana, P., Rao, N. S. L. 1983. Velocity distribution in smooth rectangular open channels. Journal of Hydraulic Engineering, ASCE, 109(2), 270-289.

[138] Sear, D. A. 1993. Fine sediment infiltration into gravel spawning beds within a regulated river experiencing floods: Ecological implications for salmonids. Regulated Rivers: Research and Management, 8(4), 373-390.

[139] Shen, H. W. 1970. Chapter II: Wash load and bed load. River mechechanics, H. W. Shen, ed., Vol. I, Fort Collins.

[140] Simons, D. B., Richardson, E. V., Haushid, W. L. 1963. Some effects of fine sediments on flow phenomenon. Water Supply Paper No.1498G, United States Geological Survey, Washington. D.C.

[141] Song, T., Chiew, Y.M. 2001. Turbulence measurement in nonuniform open channel flow using Acoustic Doppler Velocimeter (ADV). Journal of Engineering Mechanics, ASCE, 127(3), 219-233.

[142] Song, T. Graf, W.H., Lemmin, U. 1994. Uniform flow in open channels with movable gravel bed. Journal of Hydraulic Research, IAHR, 32(6), 861-876.

[143] Sutherland, A. J. 1967. Proposed mechanism of sediment entrainment by turbulent flows. Journal of Geophysical Research, 72(24), 6183-6194.

[144] Swamee, P.K., Ojha, C.S.P. 1991. Drag coefficient and fall velocity of nonspherical particles. Journal of Hydraulic Engineering, ASCE, 117(5), 660-667.

[145] Taggart, W.C., Yermoli, C.A., Montes, S., Ippen, A.T. 1972. Effects of sediment size and gradation on concentration profiles for turbulent flow. M.I.T. Report No. 152.

[146] Thomas, R. B. 1985. Estimating Total Suspended-Sediment Yield with Probability Sampling. Water Resources Research, 21(9), 1381-1388.

[147] Van Nieuwenhuyse, E. E., LaPerriere, J. D. 1986. Effects of placer gold mining on primary production in subarctic streams of Alaska. Journal of American Water Resources Association, 22(1), 91-99.

[148] Vanoni, V. A. 1946. Transportation of suspended sediment by water. Transaction, ASCE, Paper No. 2267, 67-133.

[149] Vanoni, V. A., Brooks, N. H. 1957. Laboratory Studies of the Roughness and Suspended Load of Alluvial Streams. Sedimentation Laboratory, California Institute of Technology, Report E-68, Pasadena, Calif.

[150] Vanoni, V. A., Nomicos, G. N. 1960. Resistance properties of sediment laden streams. Transcation ASCE, Paper No. 3055, 1140-1175.

[151] Verma, D. V. S., Goel, A. 2005. Scour downstream of a sluice gate. ISH Journal of Hydraulic Engineering, 11(3), 57-65.

[152] Vetter, M. 1986. Velocity distrubution and Von-Karman constant in Open-channel Flows with Sediment Transport. In: Proceedings, 3rd Int. Symp. River Sedimentation, Univ. Mississippi, 814- 823.

[153] Vorosmarty, C. J., Meybeck M., Fekete, B., Sharma, K., Green, P., Syvitski, J. P. M. 2003. Anthropogenic sediment retention: major global impacts from registered river impoundments. Global and Planetary Change. 39(1-2), 169-190.

[154] Voulgaris, G. Trowbridge, J.H. 1998. Evaluation of Acoustic Doppler Velocimeter (ADV) for turbulence measurement. Journal of Atmospheric and Oceanic Technology, 15, 272-289.

[155] Wan, Z. 1985. Bed material movement in hyperconcentrated flow. Journal of Hydraulic Engineering, ASCE, 111(6), 987-1002.

[156] Wiberg, P.L., Smith, J.D. 1987. Calculations of critical shear stress for motion of uniform and heterogeneous sediments. Water Resources Research, 23(8), 1471-1480.

[157] Woo, H.S., Julien, P.Y., Richardson, E.V. 1986. Wash load and fine sediment load. Journal of Hydraulic Engineering, ASCE, 112(6), 541-545.

[158] Woo, H.S., Julien, P.Y., Richardson, E.V. 1987. Transport of bed sediment in clay suspension. Journal of Hydraulic Engineering, ASCE, 113(8), 1061-1066.

[159] Wood, P.J., Armitage, P. D. 1997. Biological effects of fine sediment in the lotic environment. Environmental Management, 21(2), 203-217.

[160] Wooster, J. K., Dusterhoff, S. R., Cui, Y., Sklar, L. S., Dietrich, W. E., Malko, M. 2008. Sediment supply and relative size distribution effects on fine sediment infiltration into immobile gravels. Water Resources Research. 44(W03424), 1-18.

[161] Wu, W., Wang, S.Y., Jia, Y, 2000. Comparison of fractional sediment transport methods. Proceedings Of XXIX Congress of IAHR, Beijing, China, 336-342.

[162] Yano, K., Daido, A. 1964. Fundamental study on mudflow(i) to (ii). Bulletin Disaster Prevention Research Institute Kyoto, University, Kyoto, Japan.

Appendix A

Hydraulic Parameters of data collected during the present study

Table A.1: Appendix A

Series No.	Run No.	Q $[m^3/s]$	h $[m]$	U $[m/s]$	S	q_B $[N/m-s]$	C	T^0c	F_r
1L	1LC1	0.0252	0.089	0.7079	0.00844	0.06044	1	17.75	0.76
	1LW1	0.0253	0.089	0.7107	0.00844	0.06184	137	18	0.76
	1LW2	0.0254	0.087	0.7299	0.00844	0.06271	346	20.25	0.79
	1LW3	0.0253	0.087	0.7270	0.00844	0.07176	512	23	0.79
	1LW4	0.0259	0.089	0.7275	0.00844	0.07625	822	21	0.78
	1LW5	0.0259	0.089	0.7275	0.00844	0.08231	1352	22	0.78
	1LW6	0.0262	0.090	0.7278	0.00844	0.09451	2168	22	0.77
	1LW7	0.026	0.089	0.7303	0.00844	0.09738	3204	24	0.78
	1LW8	0.0257	0.089	0.7219	0.00844	0.08657	4158	26	0.77
	1LW9	0.0262	0.088	0.7443	0.00844	0.09939	4745	28	0.80
	1LW10	0.026	0.087	0.7471	0.00844	0.10644	6312	27	0.81
	1LW11	0.0261	0.087	0.7500	0.00844	0.11742	8384	29	0.81
	1LE1	0.0121	0.079	0.3829	0.00844	-	10	28	0.43
	1LE2	0.0143	0.048	0.7448	0.00844	0.08056	48	28	1.09
	1LE3	0.0218	0.070	0.7786	0.00844	0.12878	39	28	0.94
1S	1SC1	0.0235	0.093	0.6317	0.004	0.09748	1	30	0.66
	1SW1	0.0239	0.094	0.6356	0.004	0.10363	297	32	0.66
	1SW2	0.0235	0.092	0.6386	0.004	0.10975	446	30	0.67
	1SW3	0.0233	0.091	0.6401	0.004	0.11581	833	31	0.68
	1SW4	0.0236	0.092	0.6413	0.004	0.11486	2173	32	0.68
	1SW5	0.0232	0.09	0.6444	0.004	0.12447	3454	29	0.69
	1SW6	0.0234	0.09	0.6500	0.004	0.18006	4611	30	0.69
	1SW7	0.0234	0.089	0.6573	0.004	0.21373	5839	30	0.70
	1SW8	0.0234	0.088	0.6648	0.004	0.26912	6953	30	0.72
	1SW9	0.0235	0.088	0.6676	0.004	0.29815	7065	30	0.72
	1SE1	0.0113	0.052	0.5433	0.004	0.01897	12	30	0.76
	1SE2	0.0217	0.08	0.6781	0.004	0.19142	15	30	0.77
	1SE3	0.0267	0.1	0.6675	0.004	0.17052	11	30	0.67
	1SE4	0.0272	0.095	0.7158	0.004	0.28363	17	30	0.74

Table A.2: Appendix A

Series No.	Run No.	Q $[m^3/s]$	h $[m]$	U $[m/s]$	S	q_B $[N/m-s]$	C	T^0c	F_r
1M	1MC1	0.021	0.082	0.6402	0.00517	0.08937	1	30	0.71
	1MW1	0.0207	0.08	0.6469	0.00517	0.10026	104	30	0.73
	1MW2	0.0209	0.077	0.6786	0.00517	0.10109	395	30	0.78
	1MW3	0.021	0.078	0.6731	0.00517	0.1094	520	30	0.77
	1MW4	0.0211	0.079	0.6677	0.00517	0.10305	989	30	0.76
	1MW5	0.0214	0.08	0.6688	0.00517	0.11529	1570	30	0.75
	1MW6	0.0212	0.079	0.6709	0.00517	0.13617	2594	30	0.76
	1MW7	0.0213	0.078	0.6827	0.00517	0.1525	3740	30	0.78
	1MW8	0.0213	0.08	0.6656	0.00517	0.14361	6184	30	0.75
	1ME1	0.0139	0.057	0.6096	0.00517	0.0294	26	30	0.82
	1ME2	0.0199	0.069	0.7210	0.00517	0.18595	31	30	0.88
	1ME3	0.0308	0.092	0.8370	0.00517	0.60131	25	30	0.88
	1ME4	0.0337	0.093	0.9059	0.00517	1.00033	17	30	0.95
2L	2LC1	0.0218	0.075	0.7267	0.009956	0.12726	1	31	0.85
	2LW1	0.0216	0.073	0.7397	0.009956	0.10336	118	31	0.87
	2LW2	0.0221	0.076	0.7270	0.009956	0.09551	378	31	0.84
	2LW3	0.0217	0.074	0.7331	0.009956	0.1004	500	31	0.86
	2LW4	0.0214	0.075	0.713333	0.009956	0.08631	1028	32	0.83
	2LW5	0.0219	0.074	0.739865	0.009956	0.11073	1986	32	0.87
	2LW6	0.0216	0.071	0.760563	0.009956	0.16351	3265	32	0.91
	2LW7	0.0219	0.071	0.771127	0.009956	0.17905	4555	32	0.92
	2LW8	0.022	0.074	0.743243	0.009956	0.14028	6606	32	0.87
	2LW9	0.0221	0.076	0.726974	0.009956	0.13803	8400	32	0.84
	2LW10	0.0221	0.072	0.767361	0.009956	0.21069	9917	31	0.91
	2LE1	0.0156	0.051	0.764706	0.009956	0.13091	14	30	1.08
	2LE2	0.0233	0.065	0.896154	0.009956	0.65096	15	25	1.12
	2LE3	0.0285	0.078	0.913462	0.009956	0.70473	18	25	1.04
	2LE4	0.0324	0.086	0.94186	0.009956	0.98061	12	23	1.03

Table A.3: Appendix A

Series No.	Run No.	Q $[m^3/s]$	h $[m]$	U $[m/s]$	S	q_B $[N/m-s]$	C	T^0c	F_r
2M	2MC1	0.0198	0.075	0.66	0.007624	0.17143	1	26	0.77
	2MW1	0.0198	0.077	0.642857	0.007624	0.15084	201	26	0.74
	2MW2	0.0198	0.077	0.642857	0.007624	0.16233	337	24	0.74
	2MW3	0.0201	0.074	0.679054	0.007624	0.18108	516	25	0.80
	2MW4	0.0200	0.073	0.684932	0.007624	0.21011	1020	24	0.81
	2MW5	0.0200	0.073	0.684932	0.007624	0.21062	1729	25	0.81
	2MW6	0.0200	0.074	0.675676	0.007624	0.22355	2500	25	0.79
	2MW7	0.0200	0.074	0.675676	0.007624	0.2423	4067	23	0.79
	2MW8	0.0198	0.071	0.697183	0.007624	0.30102	5892	24	0.84
	2MW9	0.0201	0.071	0.707746	0.007624	0.37872	8775	24	0.85
	2ME1	0.0098	0.043	0.569767	0.007624	0.03621	25	18	0.88
	2ME2	0.0193	0.061	0.790984	0.007624	0.6581	21	18	1.02
	2ME3	0.0228	0.070	0.814286	0.007624	0.82145	17	17	0.98
	2ME4	0.0253	0.075	0.843333	0.007624	0.80054	12	17	0.98
2S	2SC1	0.0174	0.074	0.587838	0.006273	0.12052	1	21	0.69
	2SW1	0.0176	0.072	0.611111	0.006273	0.15956	251	21	0.73
	2SW2	0.0174	0.074	0.587838	0.006273	0.11076	485	22	0.69
	2SW3	0.0174	0.075	0.58	0.006273	0.15057	1331	22	0.68
	2SW4	0.0176	0.072	0.611111	0.006273	0.18327	2150	22	0.73
	2SW5	0.0176	0.074	0.594595	0.006273	0.16683	3381	22	0.70
	2SW6	0.0177	0.074	0.597973	0.006273	0.18149	4608	22	0.70
	2SW7	0.0176	0.074	0.594595	0.006273	0.20144	5706	21	0.70
	2SW8	0.0177	0.074	0.597973	0.006273	0.21375	6291	21	0.70
	2SE1	0.0084	0.04	0.525	0.006273	0.03511	31	18	0.84
	2SE2	0.017	0.061	0.696721	0.006273	0.42319	22	15	0.90
	2SE3	0.0234	0.075	0.78	0.006273	0.78012	17	15	0.91
	2SE4	0.0268	0.083	0.807229	0.006273	0.95024	11	15	0.89

Table A.4: Appendix A

Series No.	Run No.	Q $[m^3/s]$	h $[m]$	U $[m/s]$	S	q_B $[N/m-s]$	C	T^0c	F_r
3M	3MC1	0.0179	0.074	0.60473	0.007037	0.06043	1	20	0.71
	3MW1	0.0179	0.075	0.596667	0.007037	0.06231	85	20	0.70
	3MW2	0.0179	0.074	0.60473	0.007037	0.07087	120	19	0.71
	3MW3	0.018	0.074	0.608108	0.007037	0.08163	168	20	0.71
	3MW4	0.018	0.074	0.608108	0.007037	0.08854	431	20	0.71
	3MW5	0.0179	0.074	0.60473	0.007037	0.0815	823	20	0.71
	3MW6	0.018	0.075	0.6	0.007037	0.08585	2141	20	0.70
	3MW7	0.0181	0.074	0.611486	0.007037	0.10034	2186	19	0.72
	3MW8	0.018	0.074	0.608108	0.007037	0.11249	4217	20	0.71
	3MW9	0.0181	0.075	0.603333	0.007037	0.12966	7986	20	0.70
	3MW10	0.0181	0.075	0.603333	0.007037	0.14879	10302	20	0.70
	3ME1	0.0077	0.043	0.447674	0.007037	0.002003	1	15	0.69
	3ME2	0.0109	0.055	0.495455	0.007037	0.00522	28	16	0.67
	3ME3	0.0148	0.07	0.528571	0.007037	0.01041	12	14	0.64
	3ME4	0.0167	0.075	0.556667	0.007037	0.02275	8	14	0.65

Appendix B

Variation of proportion of fine sediment within the bed layer along the length of channel

Table B.1: Appendix B

Run No.	Distance from u/s end of channel (m) / C (ppm)	3.0	6.0	9.0	Average %age of fine sediment in bed layers	STDEV of %age of fine sediment in bed layers	AVEDEV of %age of fine sediment in bed layers
1LW1	137	1.42	1.73	1.62	1.59	0.16	0.11
1LW2	346	3.33	3.24	3.3	3.29	0.05	0.03
1LW3	512	5.44	5.35	5.22	5.34	0.11	0.08
1LW4	822	8.52	7.56	7.77	7.95	0.50	0.38
1LW5	1352	13.15	12.75	12.71	12.87	0.24	0.19
1LW6	2168	15.82	15	14.87	15.23	0.52	0.39
1LW7	3204	17.03	16.21	16.93	16.72	0.45	0.34
1LW8	4158	18.46	17.89	18.31	18.22	0.30	0.22
1LW9	4745	19.95	18.87	18.43	19.08	0.78	0.58
1LW10	6312	22.27	21.26	19.98	21.17	1.15	0.79
1LW11	8384	23.01	23.13	23.08	23.07	0.06	0.04
1SW1	297	3.04	2.84	2.56	2.81	0.24	0.17
1SW2	446	4.65	5.24	4.05	4.65	0.60	0.40
1SW3	833	5.02	6.19	4.54	5.25	0.85	0.63
1SW4	2173	6.99	6.47	5.54	6.33	0.73	0.53
1SW5	3454	8.05	7.44	6.53	7.34	0.76	0.54
1SW6	4611	8.48	8.14	7.08	7.90	0.73	0.55
1SW7	5893	9.23	7.59	6.81	7.88	1.24	0.90
1SW8	6953	9.7	10.52	9.13	9.78	0.70	0.49
1SW9	7065	10.92	10.59	9.91	10.47	0.52	0.38
1MW1	104	1.49	1.50	1.41	1.47	0.05	0.04
1MW2	395	3.61	3.34	3.38	3.44	0.15	0.11
1MW3	520	4.90	4.81	4.60	4.77	0.15	0.11
1MW4	989	7.62	7.47	7.39	7.49	0.12	0.08
1MW5	1570	11.71	12.32	12.29	12.11	0.34	0.26
1MW6	2594	16.58	16.42	15.35	16.12	0.67	0.51
1MW7	3740	18.40	17.93	17.19	17.84	0.61	0.43
1MW8	6184	19.30	18.73	18.49	18.84	0.42	0.31

Table B.2: Appendix B

Run No.	Distance from u/s end of channel (m) / C (ppm)	3.0	6.0	9.0	Average %age of fine sediment in bed layers	STDEV of %age of fine sediment in bed layers	AVEDEV of %age of fine sediment in bed layers
2LW1	118	1.38	1.38	1.32	1.36	0.03	0.03
2LW2	378	3.3	3.27	3.24	3.27	0.03	0.02
2LW3	500	5.97	5.81	5.65	5.81	0.16	0.11
2LW4	1028	9.63	9.42	9.19	9.41	0.22	0.15
2LW5	1986	16.09	15.92	15.7	15.90	0.20	0.14
2LW6	3265	18.86	17.96	17.69	18.17	0.61	0.46
2LW7	4555	21.21	20.78	21.14	21.04	0.23	0.18
2LW8	6606	23.22	23.39	23.46	23.36	0.12	0.09
2LW9	8400	23.24	23.64	23.63	23.50	0.23	0.18
2LW10	9917	23.29	23.63	23.67	23.53	0.21	0.16
2MW1	201	1.71	1.61	1.64	1.65	0.05	0.04
2MW2	337	2.95	2.32	2.22	2.50	0.40	0.30
2MW3	516	4.68	4.48	4.40	4.52	0.14	0.11
2MW4	1020	7.80	7.73	7.53	7.69	0.14	0.10
2MW5	1729	11.89	11.57	11.49	11.65	0.21	0.16
2MW6	2500	16.02	15.99	15.87	15.96	0.08	0.06
2MW7	4067	19.50	19.35	18.80	19.22	0.37	0.28
2MW8	5892	20.43	19.81	19.55	19.93	0.45	0.33
2MW9	8775	20.44	20.15	20.32	20.30	0.15	0.10
2SW1	251	2.63	2.11	2.01	2.25	0.33	0.25
2SW2	485	3.92	3.78	3.63	3.78	0.15	0.10
2SW3	1331	4.80	4.27	4.30	4.46	0.30	0.23
2SW4	2150	6.18	6.08	6.00	6.09	0.09	0.06
2SW5	3381	6.93	7.01	6.90	6.95	0.06	0.04
2SW6	4608	7.84	7.49	7.29	7.54	0.28	0.20
2SW7	5706	9.01	8.81	8.73	8.85	0.14	0.11
2SW8	6291	9.71	9.68	9.57	9.65	0.07	0.06

Table B.3: Appendix B

Run No.	Distance from u/s end of channel (m) / C (ppm)	3.0	6.0	9.0	Average %age of fine sediment in bed layers	STDEV of %age of fine sediment in bed layers	AVEDEV of %age of fine sediment in bed layers
2LW1	118	1.38	1.38	1.32	1.36	0.03	0.03
2LW2	378	3.3	3.27	3.24	3.27	0.03	0.02
2LW3	500	5.97	5.81	5.65	5.81	0.16	0.11
2LW4	1028	9.63	9.42	9.19	9.41	0.22	0.15
2LW5	1986	16.09	15.92	15.7	15.90	0.20	0.14
2LW6	3265	18.86	17.96	17.69	18.17	0.61	0.46
2LW7	4555	21.21	20.78	21.14	21.04	0.23	0.18
2LW8	6606	23.22	23.39	23.46	23.36	0.12	0.09
2LW9	8400	23.24	23.64	23.63	23.50	0.23	0.18
2LW10	9917	23.29	23.63	23.67	23.53	0.21	0.16
2MW1	201	1.71	1.61	1.64	1.65	0.05	0.04
2MW2	337	2.95	2.32	2.22	2.50	0.40	0.30
2MW3	516	4.68	4.48	4.40	4.52	0.14	0.11
2MW4	1020	7.80	7.73	7.53	7.69	0.14	0.10
2MW5	1729	11.89	11.57	11.49	11.65	0.21	0.16
2MW6	2500	16.02	15.99	15.87	15.96	0.08	0.06
2MW7	4067	19.50	19.35	18.80	19.22	0.37	0.28
2MW8	5892	20.43	19.81	19.55	19.93	0.45	0.33
2MW9	8775	20.44	20.15	20.32	20.30	0.15	0.10
2SW1	251	2.63	2.11	2.01	2.25	0.33	0.25
2SW2	485	3.92	3.78	3.63	3.78	0.15	0.10
2SW3	1331	4.80	4.27	4.30	4.46	0.30	0.23
2SW4	2150	6.18	6.08	6.00	6.09	0.09	0.06
2SW5	3381	6.93	7.01	6.90	6.95	0.06	0.04
2SW6	4608	7.84	7.49	7.29	7.54	0.28	0.20
2SW7	5706	9.01	8.81	8.73	8.85	0.14	0.11
2SW8	6291	9.71	9.68	9.57	9.65	0.07	0.06